

ANL-87-15 ANNEX
RETURN TO 401 LIBRARY
FS

LIBRARY REC'D: SEP 15 1989
CIRC TO:

Annex to GeV Advanced Photon Source Conceptual Design Report

Advanced Photon Source



ARGONNE NATIONAL LABORATORY
9700 South Cass Avenue, Argonne, Illinois 60439

ANL-87-15 Annex

ANNEX TO
7-GeV ADVANCED PHOTON SOURCE
CONCEPTUAL DESIGN REPORT

May 1988

work sponsored by

U.S. DEPARTMENT OF ENERGY
Office of Energy Research

TABLE OF CONTENTS

	Page
CHAPTER I: BACKGROUND AND OVERVIEW	
SUMMARY	I-1
CHAPTER II: STORAGE RING	
1 MAGNET LATTICE	II.1-1
1.2 Choice of Lattice	II.1-1
1.4.4 Multipole Imperfections	II.1-1
1.10 Injection	II.1-4
4 MAGNET SYSTEM	II.4-1
4.7.1 Septum Magnets	II.4-1
4.7.2 Storage-Ring Injection Bumper	II.4-1
4.10.3 Remote Vertical Positioner for the Storage- Ring Quadrupoles	II.4-1
5 POWER SUPPLIES	II.5-1
5.6.2 Storage-Ring Injection Bumper Power Supply	II.5-1
6 VACUUM SYSTEM	II.6-1
6.3.1 Vacuum Chamber	II.6-1
6.6 Vacuum Chamber Thermal Protection	II.6-3
9 INSERTION DEVICES	II.9-1
9.12 Improvement of Insertion-Device Design	II.9-1
9.12.1 Pure CSEM Undulator and Its Tunability	II.9-1
9.12.2 Relaxation of the Minimum-Gap Requirement through New Undulator Configurations	II.9-6
9.12.3 Straight-Section Vacuum Chamber Design	II.9-6
9.17 References	II.9-8
10 INJECTION SYSTEM	II.10-1
10.1 Introduction - The Positron Injection Process	II.10-1
10.2 Linac	II.10-2
10.2.1 Introduction	II.10-2
10.2.2 Linac Injection System	II.10-2
10.2.3 Linac Accelerating Sections	II.10-5
10.2.4 Linac Klystron and Modulators	II.10-5
10.2.7 Positron Production	II.10-5
10.2.10 The Energy Compression System (Debuncher)	II.10-5

TABLE OF CONTENTS (Cont'd)

	Page
10.2A Positron Accumulator Ring (PAR)	II.10-9
10.2A.1 Introduction	II.10-9
10.2A.2 Lattice	II.10-10
10.2A.3 RF Capture and Bunch-Length Damping	II.10-10
10.2A.4 Injection	II.10-15
10.2A.5 Extraction	II.10-20
10.2A.6 Injection/Extraction Septum Magnet	II.10-20
10.2A.7 Orbit Corrections	II.10-22
10.2A.8 Stored Beam Current	II.10-22
10.2A.9 Magnets, Supports, and Power Supplies	II.10-23
10.2A.9.1 Magnets	II.10-23
10.2A.9.2 Magnet Supports	II.10-27
10.2A.9.3 Power Supplies	II.10-31
10.2A.10 PAR Vacuum System	II.10-35
10.2A.10.1 Vacuum Chamber	II.10-35
10.2A.10.2 Pumping	II.10-35
10.2A.10.3 System Monitoring	II.10-37
10.2A.11 PAR RF Systems	II.10-37
10.2A.11.1 Introduction	II.10-37
10.2A.11.2 First-Harmonic (9.8-MHz) Cavity	II.10-37
10.2A.11.3 Twelfth-Harmonic (118-MHz) Cavity	II.10-39
10.2A.11.4 Synchronization and Frequency Control	II.10-41
10.3 Injector Synchrotron	II.10-45
10.3.1 Introduction	II.10-45
10.3.3 Injector Synchrotron Performance	II.10-45
10.3.4.3 Injector Synchrotron Ring Magnet Power Supplies	II.10-45
10.3.6 Injector Synchrotron RF System	II.10-50
10.3.6.1 Introduction	II.10-50
10.3.6.2 Deleted	II.10-50
10.3.6.3 Deleted	II.10-50
10.3.6.4 353-MHz RF Cavity	II.10-50
10.4 Transport and Injection into Injector Synchrotron	II.10-51
10.4.1 Transport Lines from Linac to PAR to Injector Synchrotron	II.10-51
10.4.2 Injection Geometry and Procedure	II.10-54
10.4.3 Injection Septum Magnet	II.10-54
10.4.4 Injection Kicker Magnet	II.10-54
10.5.1 Extraction Procedure and Geometry	II.10-54
10.5.3 Septum Magnet	II.10-58
10.7 Injection Control System	II.10-58

TABLE OF CONTENTS (Cont'd)

	Page
CHAPTER III: EXPERIMENTAL FACILITIES	
2 FRONT-END OF A BEAM LINE	III.2-1
2.6 Front-End	III.2-1
2.7 Liquid-Gallium-Cooled X-Ray Optics	III.2-1
3 DESCRIPTION OF BEAM LINES	III.3-1
3.5 Preliminary Plans for the Beam Line "Trust Fund"	III.3-1
3.6 References	III.3-3
CHAPTER IV: CONVENTIONAL FACILITIES	
1 OVERVIEW	IV.1-1
1.1 Objective of the Facilities' Construction	IV.1-1
1.2 Organization and Layout of Facility Components	IV.1-4
2 TECHNICAL AND LEGAL DETERMINANTS	IV.2-1
2.1 Siting Constraints	IV.2-1
2.2 Geotechnical Evaluation	IV.2-3
2.2.1 Geology	IV.2-3
2.3 Shielding Requirements	IV.2-4
2.3.1 Introduction	IV.2-4
2.3.2 Shielding Design Objectives	IV.2-4
2.3.3 Access Objectives	IV.2-5
2.3.4 Shielding Approach	IV.2-6
2.3.5 Recommended Shielding	IV.2-6
2.3.5.1 Linac System	IV.2-6
2.3.5.1A Positron Accumulator Ring (PAR)	IV.2-6
2.3.5.2 Injector Synchrotron	IV.2-7
2.3.5.3 Storage Ring	IV.2-7
2.4 Alignment	IV.2-8
2.4.4 Storage-Ring Alignment	IV.2-8
2.4.5 Injector Synchrotron Alignment	IV.2-8
2.5 Vibration Control	IV.2-10
2.5.3.1 Measurement Program	IV.2-10
2.5.3.2 Modeling/Analysis Program	IV.2-11
2.6 Life Safety Provisions	IV.2-11
2.9 Environmental Compliance	IV.2-12
2.9.1 Approach to Environmental Compliance	IV.2-12
2.10 References	IV.2-12

TABLE OF CONTENTS (Cont'd)

	Page
3 BUILDING SYSTEMS DESCRIPTION	IV.3-1
3.1 Machine Support	IV.3-1
3.1.1 Introduction	IV.3-1
3.1.2 Linac Building	IV.3-3
3.1.2.1 Architecture	IV.3-4
3.1.2.2 Structure	IV.3-4
3.1.2.3 Heating, Ventilation, and Air-Conditioning (HVAC)	IV.3-6
3.1.2.5 Electrical Power	IV.3-6
3.1.3 Synchrotron Injection Building	IV.3-7
3.1.3.1 Architecture	IV.3-7
3.1.3.5 Electrical Power	IV.3-9
3.1.4 Synchrotron Enclosure	IV.3-10
3.1.4.1 Architecture	IV.3-10
3.1.5 Synchrotron Extraction Building	IV.3-10
3.1.5.1 Architecture	IV.3-10
3.1.6 Storage-Ring Enclosure	IV.3-12
3.1.6.1 Architecture	IV.3-12
3.1.6.2 Structure	IV.3-16
3.1.7 RF/Power Buildings (East and West)	IV.3-16
3.2 Experiment Support	IV.3-17
3.2.1 Introduction	IV.3-17
3.2.2 Experiment Hall	IV.3-19
3.2.2.1 Architecture	IV.3-20
3.2.2.2 Structure	IV.3-20
3.2.2.4 Plumbing/Process Piping/Fire Protection	IV.3-21
3.2.3 Laboratory/Office Modules	IV.3-23
3.2.3.1 Architecture	IV.3-25
3.2.3.3 Heating, Ventilation, and Air-Conditioning	IV.3-25
3.2.4 Central Laboratory/Office Building -- Support Wing	IV.3-26
3.2.4.1 Architecture	IV.3-26
3.2.4.3 Heating, Ventilation, and Air-Conditioning	IV.3-30
3.2.5 Central Laboratory/Office Building -- Office Wing	IV.3-30
3.2.5.1 Architecture	IV.3-31
3.2.6 Central Laboratory/Office Building -- Multi-Function Meeting Facility Wing	IV.3-36
3.2.6.1 Architecture	IV.3-36
3.2.6.2 Structure	IV.3-38
3.2.6.3 Heating, Ventilation, and Air-Conditioning	IV.3-38
3.2.6.5 Electrical Power	IV.3-38
3.3 Utilities and Sitework	IV.3-39
3.3.5.2 Control Tunnel	IV.3-39

LIST OF FIGURES

		Page
I.1.3-1	Layout of the Advanced Photon Source	I-3
II.1.4-17	Dynamic aperture for the APS lattice with multipole field coefficients in the quadrupole magnets given in Table II.1.4-4. The data points represent the average and rms spread of the dynamic aperture for 11 Monte Carlo calculations. The solid curve presents the dynamic aperture for the perfect lattice	II.1-3
II.4.10-3	End view of remote vertical positioner for the storage ring quadrupole magnet	II.4-2
II.6.3-4	Vacuum chamber for storage-ring quadrupole magnet (arrows indicate machined areas to allow vertical adjustment)	II.6-2
II.6.6-1	The vertical vacuum chamber height as a function of distance along the undulator photon beam. The height is shown for horizontal closed-orbit divergence angles of +1, 0, and -1 mrad. The figure shows that a vertical angle of 0.45 mrad or greater causes illumination of the vacuum chamber slot	II.6-4
II.6.6-2	Vertical closed-orbit distortions in the 40 ID sections resulting from a single correction magnet changing its value by 0.25 mrad. The results are shown for four different correction magnets: (a) W1, (b) S1, (c) S2, and (d) SD. The dashed lines show the distortion necessary to illuminate the vacuum chamber slot with undulator beam, and the solid lines show the undulator vacuum chamber physical aperture for the circulating positron beam	II.6-5
II.9.12-1	Tunability of undulators of different periods with pure CSEM configuration using Nd-Fe-B magnets. None of the undulators provide the first-harmonic tunability from 4.7 to 14 keV recommended in Ref. 4. The limits of tunability are defined by the minimum gap (1.0 or 1.4 cm) and the maximum gap (0.8 x period)	II.9-3

LIST OF FIGURES (Cont'd)

		Page
II.9.12-2	Tunability of hybrid undulator using Nd-Fe-B magnets. The undulator with about 3.1-cm period provides the tunability range recommended in Ref. 4	II.9-4
II.9.12-3	Laterally compensated hybrid geometry and wedge pole hybrid geometry for undulators	II.9-7
II.9.12-4	A cross section of the ID vacuum chamber and its support	II.9-9
II.10.2-1	Schematic diagram of the electron and positron linacs showing the rf power distribution	II.10-3
II.10.2-2	Energy compression system layout	II.10-6
II.10.2-3	Longitudinal phase-space ellipses in the energy compression system	II.10-8
II.10.2A-1	Positron accumulator ring layout	II.10-11
II.10.2A-2	Lattice and dispersion functions for one-half of a period for the PAR	II.10-13
II.10.2A-3	Phase space of the injected pulse ($\frac{\Delta E}{E} = \pm 1\%$, 30 ns) fitting within a 40-kV, first-harmonic PAR-rf-bucket. Also shown is the rf bucket that contains at least 95% of the injected pulse	II.10-16
II.10.2A-4	The $\sqrt{6}$ σ contour bunch in the combined first-harmonic and twelfth-harmonic rf bucket at the time of the twelfth-harmonic turn-on. Also shown is the bucket area available for the first-harmonic damped beam.....	II.10-17
II.10.2A-5	$\sqrt{6}$ σ bunch from the PAR in a 100-kV, 353-MHz injector synchrotron bucket. Also shown is the bucket area for $\sqrt{6}$ σ injected beam	II.10-18
II.10.2A-6	Horizontal phase space at the injection septum magnet	II.10-19
II.10.2A-7	Bumped orbit and injected and extracted beams.....	II.10-21
II.10.2A-8	Top and end views of the PAR dipole magnet.....	II.10-24

LIST OF FIGURES (Cont'd)

		Page
II.10.2A-9	End view of the PAR quadrupole magnet	II.10-25
II.10.2A-10	End view of the PAR multipole magnet	II.10-26
II.10.2A-11	Cross section of the PAR kicker/bumper magnet	II.10-30
II.10.2A-12	Dipole power supply for PAR	II.10-34
II.10.2A-13	Power supply for kicker/bumper system	II.10.36
II.10.2A-14	Schematic of first-harmonic (9.8-MHz) cavity, half section	II.10-38
II.10.2A-15	9.8-MHz rf system block diagram showing program generator	II.10-40
II.10.2A-16	Schematic of twelfth-harmonic (118-MHz) cavity	II.10-42
II.10.2A-17	Twelfth-harmonic (118-MHz) rf system block diagram	II.10-43
II.10.2A-18	PAR rf systems showing synchronization scheme	II.10-44
II.10.3-1	Physical layout of the injector synchrotron	II.10-46
II.10.3-9	Current and voltage shapes and block diagram of the dipole ring magnet power supply for the injector synchrotron	II.10-48
II.10.4-1	Layout of the linac-to-PAR-to-injector-synchrotron transport line	II.10-52
II.10.4-2	Beta and dispersion functions for the linac-to-PAR transport line	II.10-53
II.10.4-3	Beta and dispersion functions for the PAR-injector-synchrotron transport line	II.10-55
II.10.4-4	Beam trajectory and $4\text{-}\sigma$ envelope for the injected and undamped beams in the injection region of the injector synchrotron. The 2-mm injection septum is 21 mm from the unperturbed orbit	II.10-56

LIST OF FIGURES (Cont'd)

		Page
III.2.7-1	Increase in the surface temperature along the x-direction for various silicon crystal cooling schemes with the CHESS wiggler operated at 46 mA of stored current at 5.4 GeV. (a) Si crystal mounted on a copper block, which is cooled with water. (b) Si crystal with channels carrying water and (c) liquid gallium. (d) Si crystal with optimized location of channels cooled with liquid gallium	III.2-3
III.2.7-2	Rocking curves at 20 keV for various cooling geometries described in the caption for Figure III.2.7-1	III.2-4
IV.1.1-1	Project site isometric	IV.1-2
IV.1.1-2	Argonne campus plan	IV.1-5
IV.1.1-3	Project area plan	IV.1-6
IV.1.2-1	Project site plan	IV.1-7
IV.2.4-2	Position of control points in one cell of the storage-ring lattice	IV.2-9
IV.3.1-1	Infield isometric projection	IV.3-2
IV.3.1-2	Linac building	IV.3-5
IV.3.1-3	Synchrotron injection building	IV.3-8
IV.3.1-4	Synchrotron extraction building	IV.3-11
IV.3.1-5	Experiment hall segment	IV.3-13
IV.3.1-6	Ratchet-wall dimension details	IV.3-14
IV.3.1-7	Cross section through storage-ring enclosure	IV.3-15
IV.3.1-8	Typical rf building	IV.3-18
IV.3.2-1	Experiment hall cross section	IV.3-21

LIST OF FIGURES (Cont'd)

		Page
IV.3.2-2	Typical laboratory/office module	IV.3-24
IV.3.2-3	Support wing, central laboratory/office building ground floor plan	IV.3-27
IV.3.2-4	Support wing, central laboratory/office building mechanical-equipment penthouse plan	IV.3-28
IV.3.2-5	Support wing, central laboratory/office building sections	IV.3-29
IV.3.2-6	Office wing, central laboratory/office building ground floor plan	IV.3-32
IV.3.2-7	Office wing, central laboratory/office building service level plan	IV.3-33
IV.3.2-8	Office wing, central laboratory/office building sections	IV.3-34
IV.3.2-9	Office wing, central laboratory/office building fourth-floor plan	IV.3-35
IV.3.2-10	Multi-function meeting facility wing, central laboratory/office building	IV.3-37
IV.3.3-1	Utility area plan	IV.3-40

LIST OF TABLES

II.1.4-4	Multipole Coefficients b_n and a_n for Systematic and Random Imperfections Used for APS Quadrupole Obtained by Scaling the FNAL Measured Quadrupole Coefficients to a 4-cm Aperture.	II.1-2
II.9.12-1	A Comparison of the Characteristics of a Pure CSEM Configuration and a Hybrid Configuration	II.9-5
II.10.2-1	Nominal Linac Parameters	II.10-4
II.10.2-3	Parameters for Energy Compression System Magnets	II.10-7

LIST OF TABLES (Cont'd)

		Page
II.10.2A-1	PAR Lattice Components for One-Fourth Machine	II.10-12
II.10.2A-2	Parameters for the Positron Accumulator Ring	II.10-14
II.10.2A-3	Field Qualities of PAR Magnets	II.10-27
II.10.2A-4	Parameters for Principal PAR Magnets	II.10-28
II.10.2A-5	Parameters for PAR Septum Magnet	II.10-29
II.10.2A-6	Design Parameters for Kicker/Bumper Magnets	II.10-31
II.10.2A-7	Magnet Power Supplies for PAR	II.10-33
II.10.2A-8	PAR Cavity Parameters	II.10-39
II.10.3-2	Injector Synchrotron Parameters	II.10-47
II.10.3-5	Magnet Power Supplies for Injector Synchrotron	II.10-49
II.10.3-8	Parameters for the Five-Cell, $\lambda/2$, 353-MHz Cavity	II.10-51
II.10.4-1	Parameters for Magnets in Transport Line between Linac and Synchrotron	II.10-57
III.3.5-1	Distribution Plans for the "Trust Fund" to Develop Experimental Facilities	III.3-2
IV.1.2-1	Building Dimensions	IV.1-9

I. 1 BACKGROUND AND OVERVIEW

SUMMARY

The Annex to the 7-GeV Advanced Photon Source Conceptual Design Report updates the Conceptual Design Report of 1987* (CDR-87) to include the results of further optimization and changes of the design during the past year.

This Annex contains four types of material, as follows:

- New sections are sections that do not exist in CDR-87.
- Additional materials are materials added to existing sections to supplement information presented in CDR-87.
- Replacement sections are to be substituted for corresponding sections in CDR-87.
- Revised sections incorporate changes made to corresponding sections in CDR-87. The bulk of the information presented in the original sections remains unchanged.

The type of material presented in a given section of the Annex is indicated in the section heading. Tables and figures included in the Annex represent changes from the corresponding elements in CDR-87. Those sections of CDR-87 that remain unchanged do not appear in the Annex. The numbering of sections, tables, and figures corresponds to that used in CDR-87.

The design changes can be summarized as affecting three areas: the accelerator system, conventional facilities, and experimental systems. Most of the changes in the accelerator system result from inclusion of a positron accumulator ring (PAR), which was added, at the suggestion of the 1987 DOE Review Committee, to speed up the filling rate of the storage ring. The addition of the PAR necessitates many minor changes in the linac system, the injector synchrotron, and the low-energy beam transport lines.

Inclusion of the PAR also requires some changes in the design of the conventional facilities. However, more significant changes in the conventional facilities result from further optimization of their design on the basis of input from the APS Users Organization. In place of the modularized users' laboratory/office building design shown

*7-GeV Advanced Photon Source Conceptual Design Report, Argonne National Laboratory Report ANL-87-15 (April 1987).

I. 1 BACKGROUND AND OVERVIEW

in CDR-87, a contiguous configuration of modules extending around the outer periphery of the experimental area is proposed. In the new configuration, if all eight modules are built, each beam line will have four offices and one laboratory; the project plan calls for building four modules initially. This change in users' laboratory/office buildings reduces the number of laboratories required for users in the central laboratory/office building. This is discussed in detail in Chapter IV. A new layout of the buildings is shown in Fig. I.1.3-1.

With respect to the experimental systems, additional material is added to the beam-line and insertion-device sections. This includes a new evaluation of hybrid vs. non-hybrid undulators, a newer configuration of magnets in hybrid undulators to increase the minimum gap, and the results of an experiment using a liquid-gallium pump constructed to cool the first optical element.

I. 1 BACKGROUND AND OVERVIEW

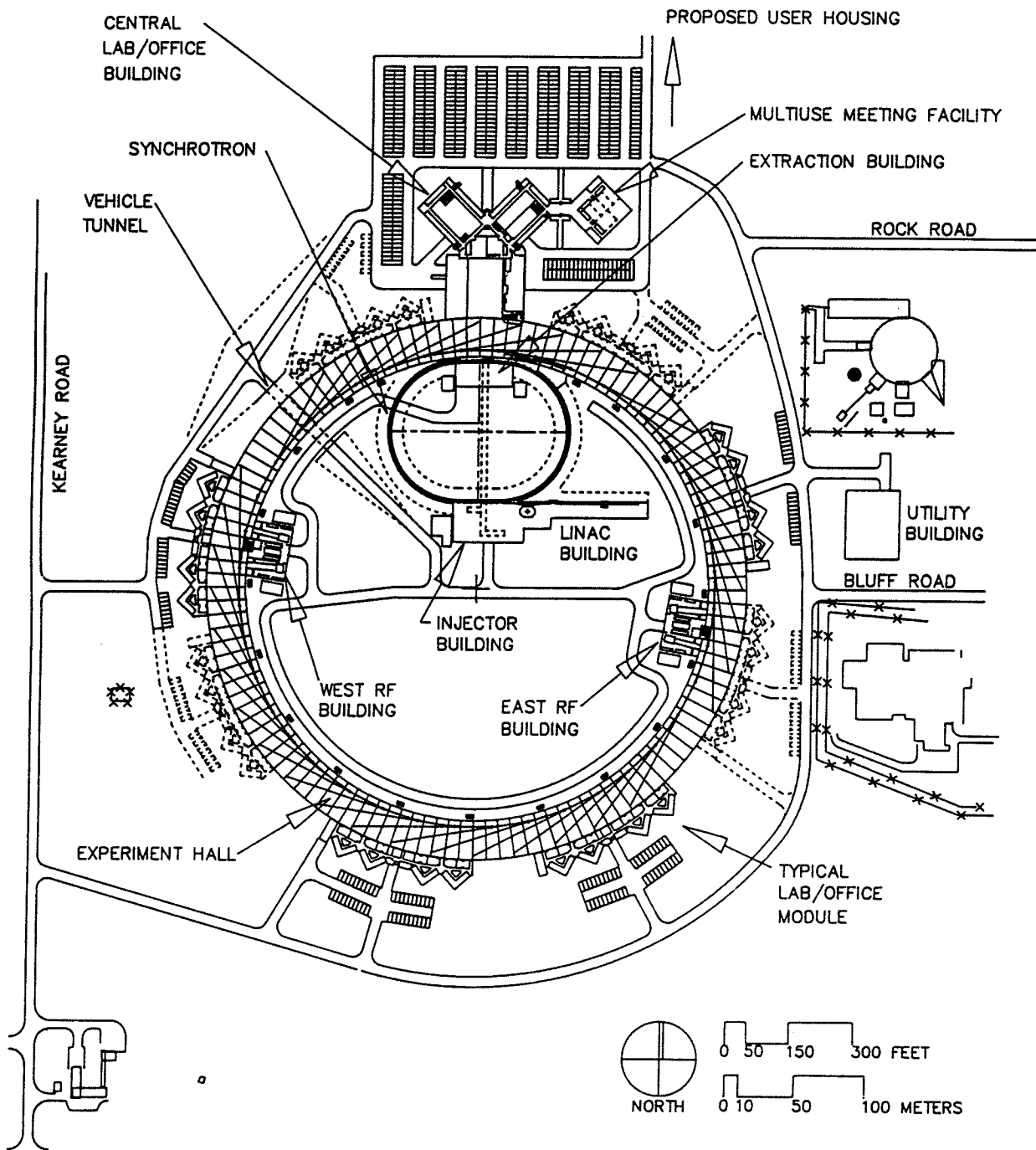


Figure I.1.3-1
Layout of the Advanced Photon Source.

I. 1 BACKGROUND AND OVERVIEW

II. 1. MAGNET LATTICE

1.2 Choice of Lattice [Additional Material]

In May 1987, the APS Accelerator Advisory Committee reviewed the lattice designs described in this section. The committee agreed with the interim conclusions. Further project effort on the lattice will be concentrated on the Chasman-Green type.

1.4.4 Multipole Imperfections [Additional Material]

In this section, results of dynamic aperture studies using additional quadrupole field tolerances are presented. The relative magnitudes of the quadrupole-magnet harmonic coefficients have been scaled from measured harmonic coefficients obtained from a large number of quadrupole magnets constructed for the Antiproton Source at FNAL. This scaling was done by setting the relative field errors to be equal at their respective pole apertures. The multipole coefficients, scaled to the APS aperture radius of 4 cm, are listed in Table II.1.4-4.

The dynamic aperture for the lattice with the multipole coefficients of the quadrupoles given by Table II.1.4-4 is presented in Fig. II.1.4-17. The reduction of the dynamic aperture is approximately 15%. The dynamic aperture has also been studied with the systematic imperfections increased by a factor of two over those listed in Table II.1.4-4. No additional reduction in the dynamic aperture below that presented in Fig. II.1.4-17 occurs in this case. Further calculations are planned to determine where the systematic imperfections and random imperfections become significant.

The tolerances in Table II.1.4-4 can be achieved provided similar care is taken with the construction of APS quadrupoles as was taken for the FNAL quadrupoles. Recent calculations have been performed to study the effects of construction procedures on these multipole coefficients. A lamination stacking accuracy of ± 0.05 mm is tolerable.

II. 1. MAGNET LATTICE

Table II.1.4-4 [Additional Material]

Multipole Coefficients b_n and a_n for Systematic and Random Imperfections Used for APS Quadrupole Obtained by Scaling the FNAL Measured Quadrupole Coefficients to a 4-cm Aperture.

n	b_n [$\text{cm}^{-(n)}$]	a_n [$\text{cm}^{-(n)}$]
1	1.0	0.0
2	$(-1.9 \pm 5.4) \times 10^{-5}$	$(-5.0 \pm 11.2) \times 10^{-5}$
3	$(-2.8 \pm 1.1) \times 10^{-5}$	$(-2.3 \pm 3.3) \times 10^{-6}$
4	$(-2.8 \pm 6.20) \times 10^{-7}$	$(5.5 \pm 7.2) \times 10^{-7}$
5	$(-1.4 \pm 0.3) \times 10^{-6}$	$(0.2 \pm 1.0) \times 10^{-7}$
9	$(6.9 \pm 0.3) \times 10^{-9}$	$(-1.4 \pm 2.8) \times 10^{-10}$

II. 1. MAGNET LATTICE

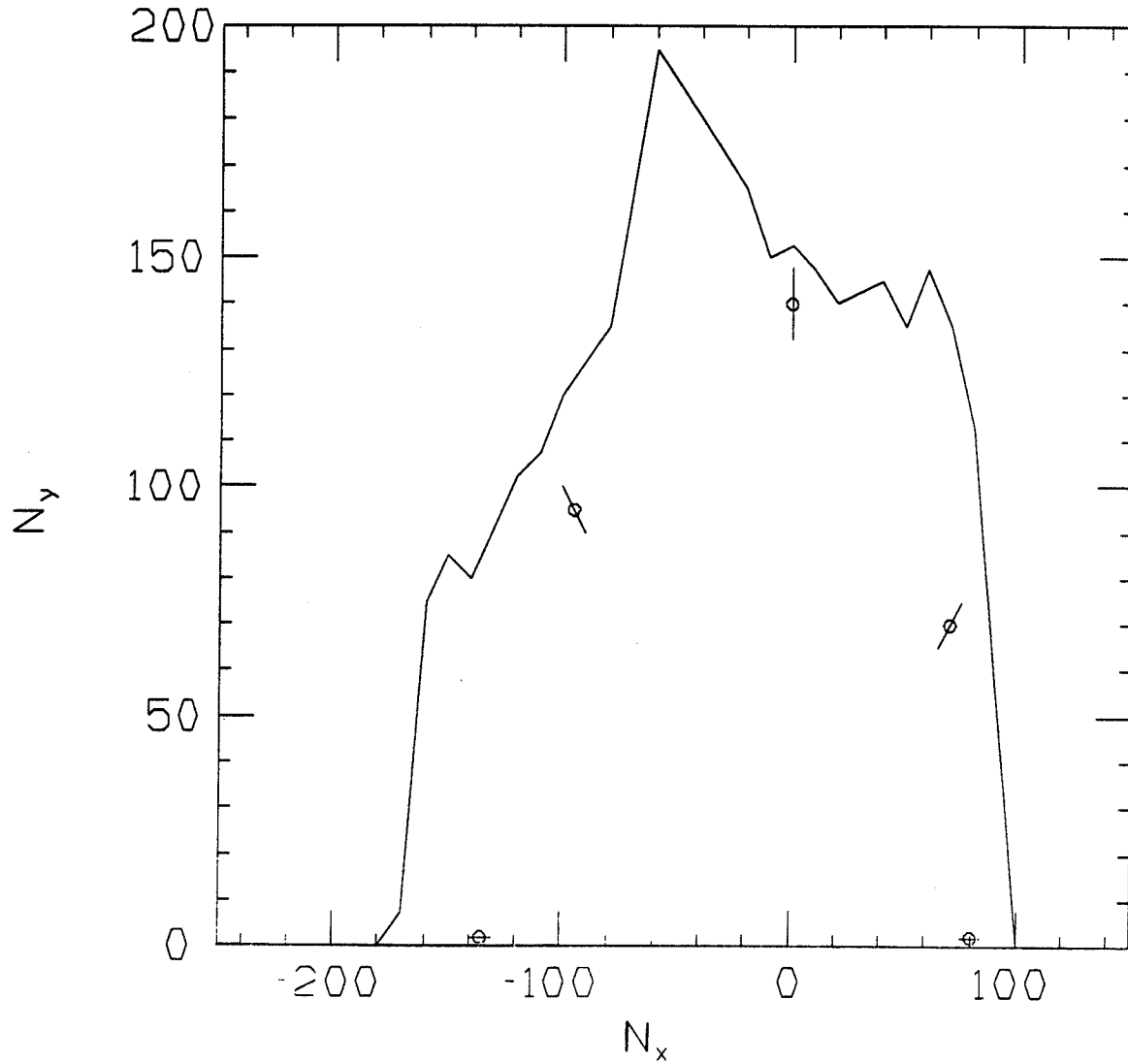


Figure II.1.4-17

Dynamic aperture for the APS lattice with multipole field coefficients in the quadrupole magnets given in Table II.1.4-4. The data points represent the average and rms spread of the dynamic aperture for 11 Monte Carlo calculations. The solid curve presents the dynamic aperture for the perfect lattice.

II. 1. MAGNET LATTICE

1.10 Injection [Revision]

With the PAR, single bunches are extracted from the injector synchrotron and injected into the storage ring at a 2-Hz rate (see Sec. II.10.1), instead of at an 8-Hz rate. Otherwise, there is no change in the injection process to the storage ring.

II. 4. MAGNET SYSTEM

4.7.1 Septum Magnets [Revision]

The repetition rate has been changed from 8 pps to 2 pps due to inclusion of the PAR. The design of the magnet is unchanged.

4.7.2 Storage-Ring Injection Bumper [Revision]

The repetition rate has been changed from 8 pps to 2 pps due to inclusion of the PAR. The design of the magnet is unchanged.

4.10.3 Remote Vertical Positioner for the Storage-Ring Quadrupoles [New Section]

Vertical adjustments for four 0.5-m-long quadrupoles in each sector are provided by means of remotely controlled jack systems. A jack system consists of three ball screw jacks, each independently powered with a directly coupled stepping motor. The vertical position of each jack is independently monitored by an inductive proximity sensor with a total working range of 3 mm. The total range of vertical motion is ± 1 mm, and the vertical displacement for each step of the drive motors is $1.27 \mu\text{m}$. The three drive motors are controlled by a local microprocessor so that all three, for a given magnet, are moved together to within ± 1 step. The components of this system are shown in Fig. II.4.10-3, along with some parts of the magnet and primary support structure.

II. 4. MAGNET SYSTEM

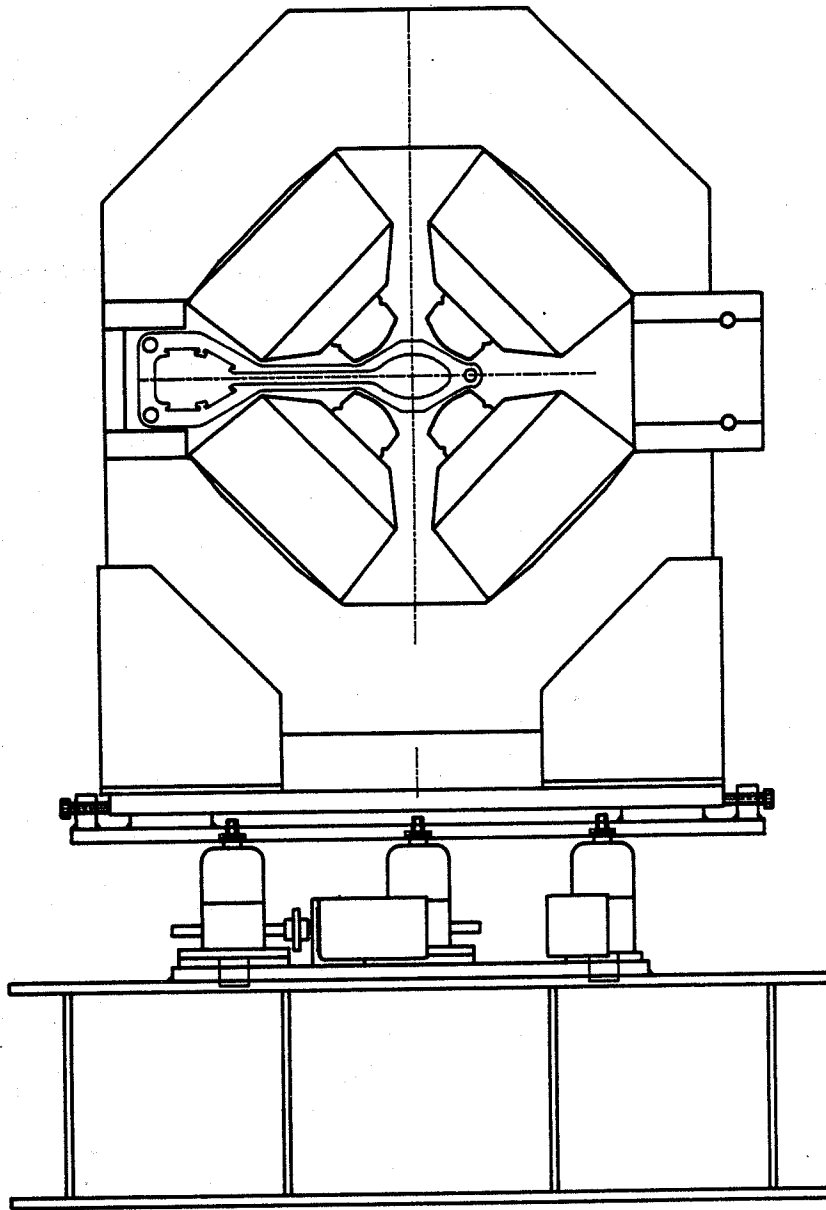


Figure II.4.10-3
End view of remote vertical positioner for the storage-ring quadrupole magnet.

II. 5. POWER SUPPLIES

5.6.2 Storage-Ring Injection Bumper Power Supply [Revision]

The storage-ring injection bumper power supply repetition rate is changed from 60 Hz to 2 Hz.

II. 5. POWER SUPPLIES

II. 6. VACUUM SYSTEM

6.3.1 Vacuum Chamber [Additional Material]

The portion of the fixed vacuum chamber within the vertically adjustable quadrupoles (see Sec. II.4.10.3) is further machined to provide clearance between the chamber and pole tips. Figure II.6.3-4 shows four areas machined to a depth of 1 mm on the chamber section. Tests were performed under vacuum at 150°C on chamber sections containing machined areas with depths greater than 1 mm. These tests demonstrate that the chambers still have adequate yield strength with a safety factor of approximately 2.5, in spite of the 1-mm-deep grooves.

II. 6. VACUUM SYSTEM

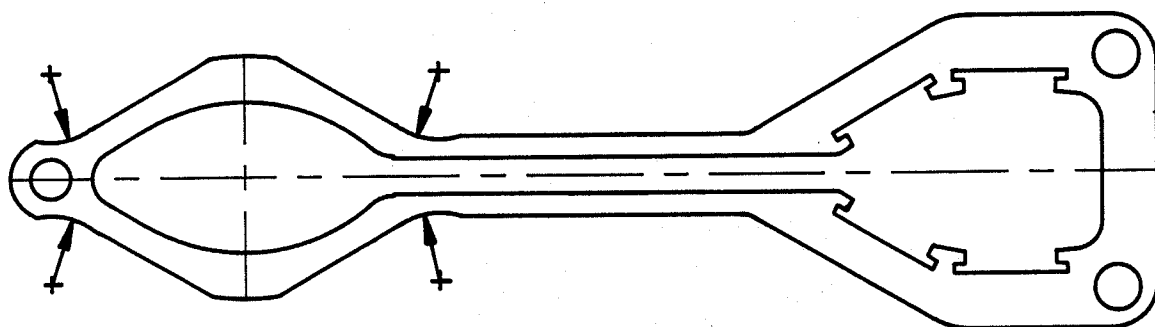


Figure II.6.3-4
Vacuum chamber for storage-ring quadrupole magnet (arrows indicate machined areas to allow vertical adjustment).

II. 6. VACUUM SYSTEM

6.6 Vacuum Chamber Thermal Protection [New Section]

High brilliance undulator beams present a potential thermal risk to the structural integrity of the ring vacuum chamber. (See Fig. II.6.6-1, which shows the vertical vacuum chamber height as a function of distance along the beam line). If the mis-steered photon beam is to be prevented from striking the downstream edge of the vacuum chamber slot, the vertical angle of mis-steering must be no larger than 0.45 mrad. Such a large mis-steering of the beam would be most likely to result if a single vertical closed-orbit correction magnet were to change the correction angle by more than 0.4 mrad.

To eliminate this potential risk during times of high circulating-beam current, the raw dc voltage of the vertical correction-magnet power supplies is limited. This permits nominal operation at a maximum correction angle of 0.25 mrad and prevents exceeding the 0.4-mrad limit in the event of loss of regulation. This allows sufficient vertical correction angle to correct the closed orbit with 10^{-4} tolerance, as shown in Fig. II.1.4-16.

Four quadrupoles per period (Q3 and Q4 in Fig. II.1.3-1) are provided with remotely controlled jacks for additional vertical steering. These jacks provide ± 1 mm of vertical motion, which yields ± 0.22 and ± 0.40 mrad of vertical steering from Q3 and Q4, respectively. Since these quadrupoles are close to the vertical orbit correction magnets, their steering will directly add to the corrector strength. The mechanical design of these jacks (see Sec. II.4.10.3) provides the ± 1 mm vertical motion with a resolution and reproducibility of better than ± 0.01 mm.

Figure II.6.6-2 shows the closed-orbit distortion in all 40 ID regions for four different corrector magnets tripping off when they are set at a maximum value of 0.25 mrad. It is shown that no single corrector tripping off produces a closed-orbit distortion sufficient to illuminate the vacuum chamber. During commissioning of each new undulator, the corrector limits may have to be removed to allow sufficient steering range. This commissioning would be performed at beam currents below 3 mA.

In addition to the passive protection system described above, there are several active systems protecting the vacuum chamber. These include beam position monitors, power supply limits, vacuum pressure limits, and external photon beam position monitors.

II. 6. VACUUM SYSTEM

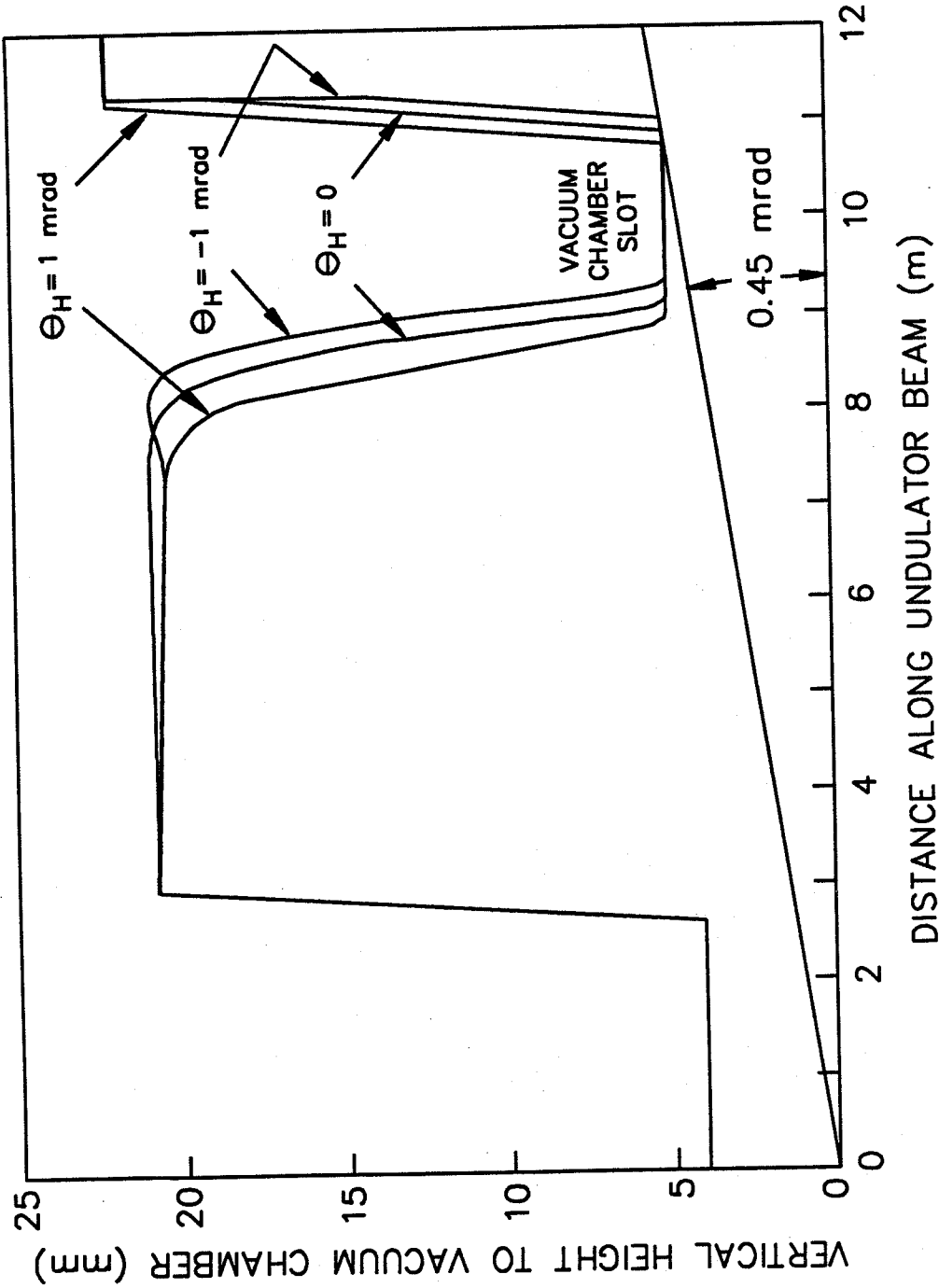


Figure II.6.6-1

The vertical vacuum chamber height is a function of distance along the undulator photon beam. The height is shown for horizontal closed-orbit divergence angles of +1, 0, and -1 mrad. The figure shows that a vertical angle of 0.45 mrad or greater causes illumination of the vacuum chamber slot.

II. 6. VACUUM SYSTEM

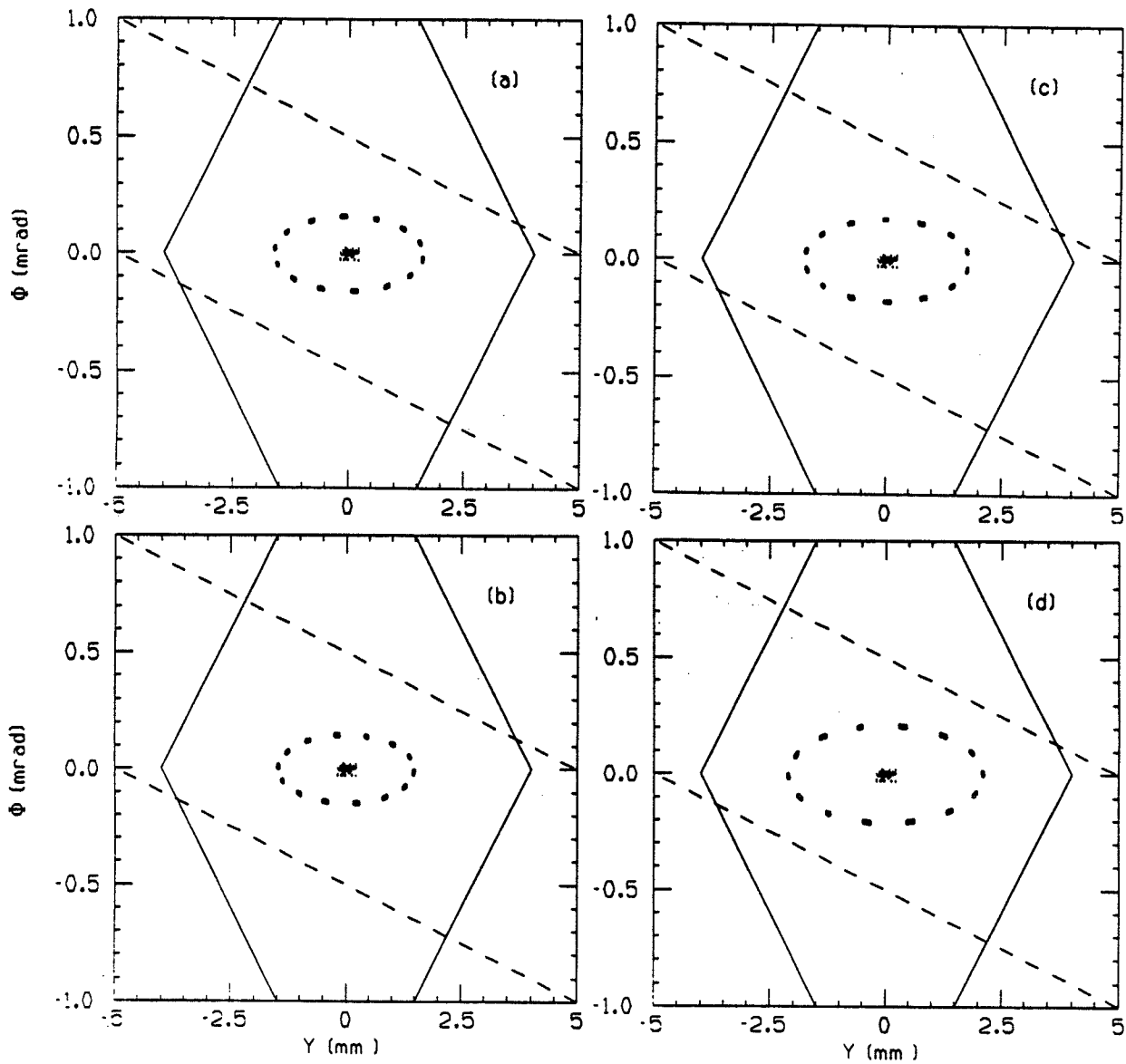


Figure II.6.6-2

Vertical closed-orbit distortions in the 40 ID sections resulting from a single correction magnet changing its value by 0.25 mrad. The results are shown for four different correction magnets: (a) W1, (b) S1, (c) S2, and (d) SD. The dashed lines show the distortion necessary to illuminate the vacuum chamber slot with undulator beam, and the solid lines show the undulator vacuum chamber physical aperture for the circulating positron beam.

II. 6. VACUUM SYSTEM

II. 9. INSERTION DEVICES

9.12 Improvement of Insertion-Device Design [New Section]

The design of hybrid-type undulators and wigglers suitable for the 7-GeV Advanced Photon Source has been discussed in previous sections. The characteristics of these and other special devices have been presented in the current version of the Users Guide.⁽¹⁸⁾ Prototype undulators of 2-m length with 3.3-cm and 7.5-cm periods have been designed. The 3.3-cm device has been constructed by Spectra Technology, Inc.⁽¹²⁾ and is being installed on the low-emittance CESR lattice. The design work on the 7.5-cm device has been completed. It is being procured and will be installed on the NSLS UV-ring in 1990.⁽¹⁹⁾

A study was undertaken to test the suitability of a pure Current Sheet Equivalent Material (CSEM) magnet configuration (non-hybrid) for undulators on the 7-GeV Advanced Photon Source. Though the cost is somewhat lower, such a configuration provides restricted tunability, compared with the hybrid configuration, in the hard x-ray range.

In order to relax the vertical minimum-aperture requirement (0.8 cm) on the undulator straight sections, new hybrid geometries have been investigated. The preliminary results are very encouraging, and a larger value for the minimum aperture is expected. Enlargement of the minimum aperture will improve the storage-ring operation.

The NeG-pump geometries for the straight-section vacuum chamber have been reevaluated, and a more suitable vacuum-chamber geometry has been designed.

9.12.1 Pure CSEM Undulator and Its Tunability [New Section]

The hybrid configuration for an undulator is widely accepted in both synchrotron and free-electron laser applications. The principal advantage of the hybrid configuration relative to the pure CSEM⁽²⁰⁾ geometry is the higher field strength that the former produces at small gaps. However, the pure CSEM geometry using Nd-Fe-B as magnet material produces as high a field as the hybrid configuration built using SmCo₅. Hence, it is important to reevaluate the suitability of the CSEM geometry for applications on the 7-GeV APS. A detailed evaluation of the performance of a pure CSEM configuration has been published.⁽²⁰⁾ In this section, some of the characteristics of this configuration are highlighted, and it is then compared with the hybrid configuration. The tunability of the pure CSEM device is discussed, and its suitability is evaluated for APS applications.⁽²¹⁾

The characteristics of a pure CSEM device depend almost entirely on the quality and tolerance of the permanent magnet material used in its construction. More magnet blocks are needed for choosing and pairing. The field at any point in the gap region is a

II. 9. INSERTION DEVICES

linear superposition of the fields from each block; hence, analytical models can be used to completely specify a device. Parameters such as field quality and flux closure can be predicted if the magnetic properties of each of the magnet blocks are fully characterized. In practice, however, the actual field errors are usually larger than those predicted by the analytical models. Intensive effort in sorting and pairing of the magnet blocks and in achieving tight construction tolerances can reduce the field errors to as small as 0.1%, although with less stringent effort, 1 to 2% errors are more commonly accomplished. For the 7-GeV APS applications, it would be desirable to reduce the errors to less than about 0.5%.

A related feature of a pure CSEM device is the compensation required for the field integral at any gap. Although this compensation should be automatic at all gaps, most devices built thus far need an additional, gap-dependent field-compensation procedure based on electromagnets.

The field lines of a pure CSEM geometry can be easily perturbed by nearby high-permeability materials. Thus, for example, the end field clamps or shunts have been observed to produce measurable degradation in the field quality of the device. This is an added complication in the use of these devices in the proposed segmented-undulator scheme for the APS.

The tunability requirements of an undulator for the APS were discussed by the National Task Group.⁽⁴⁾ The recommendation of achieving a tunability of the first-harmonic from 4.7 to 14 keV by varying the gap of a pure CSEM configuration was addressed in detail. In Figs. II.9.12-1 and II.9.12-2, the tunability of pure CSEM devices and of hybrid devices with different periods is shown. The following important facts are noted:

- The pure CSEM configuration will not meet the tunability recommendation of the National Task Group when the storage-ring energy is set at 7 GeV.
- The minimum gap of 1.0 cm and the maximum gap defined by the gap-to-period ratio (R) of 0.8 provide a tunability from 4.0 to 12 keV for a pure CSEM device with a period of 3.6 cm. A pure CSEM geometry with a period of 3.1 cm provides a tunability from 6 to 14 keV. On the other hand, a hybrid configuration with 3.1-cm period provides tunability from 4.7 to 14 keV when installed on a 7-GeV storage ring.

In Table II.9.12-1, various technical characteristics of a pure CSEM configuration are compared with those of a hybrid configuration.

The cost of a pure CSEM geometry is lower than that of a hybrid configuration when the design goal is to limit the peak field error to a range of 1 to 3%. Approximately 50% more magnet material is necessary in a hybrid design, compared with a pure CSEM design, to achieve large peak fields. This factor, along with the additional

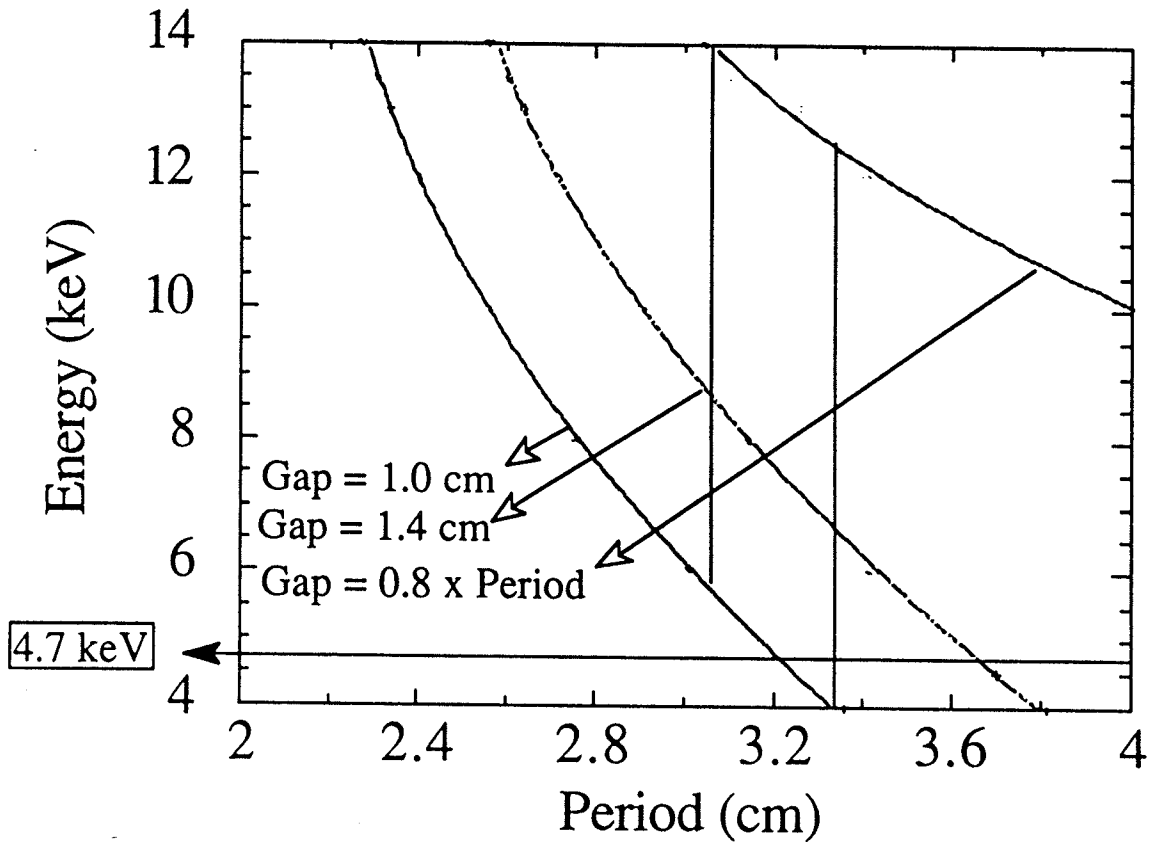


Figure II.9.12-1

Tunability of undulators of different periods with pure CSEM configuration using Nd-Fe-B magnets. None of the undulators provide the first-harmonic tunability from 4.7 to 14 keV recommended in Ref. 4. The limits of tunability are defined by the minimum gap (1.0 or 1.4 cm) and the maximum gap (0.8 x period).

II. 9. INSERTION DEVICES

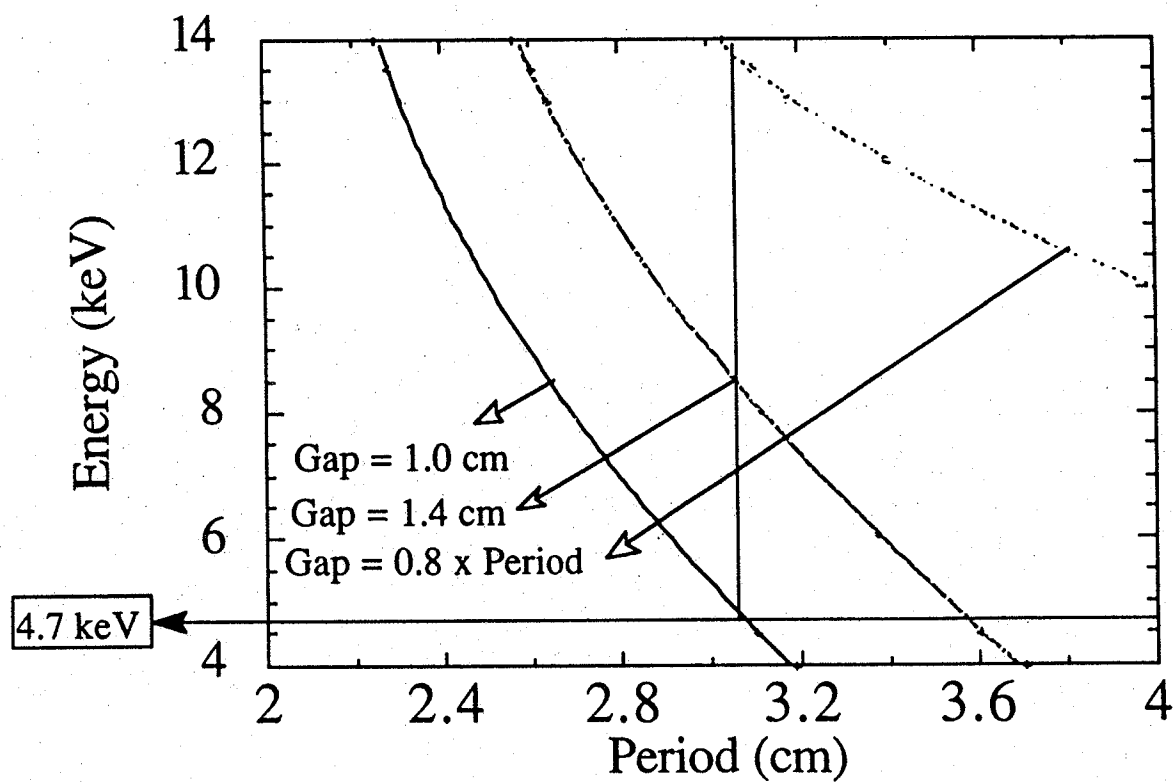


Figure II.9.12-2
Tunability of hybrid undulator using Nd-Fe-B magnets. The undulator with about 3.1-cm period provides the tunability range recommended in Ref. 4.

II. 9. INSERTION DEVICES

Table II.9.12-1 [Additional Material]

A Comparison of the Characteristics of a Pure CSEM Configuration
and a Hybrid Configuration

Characteristics	Pure CSEM	Hybrid
Magnet Design	Analytical modeling	Numerical modeling
Peak Field	About 10% lower than hybrid geometry	About 10% larger than pure CSEM geometry
Field Distribution	Depends on magnet material	Depends on pole/magnet geometry
On-Axis Harmonic Content	About 98% in the fundamental geometry; 96% is typical	Depends on pole/magnet
Field-Error Evaluation	Analytical methods	Numerical methods
Error Values		
Typical	1-3%	1-3%
Minimum achieved	0.1%	0.1%

cost of the pole pieces, generally increases the cost of a hybrid device. Since the desirable error values for the APS applications are about 0.5%, it is necessary to carry out a detailed cost study for both configurations. In addition, the new scheme of using magnetic shims might reduce the cost of grinding the pole pieces for a hybrid configuration to realize field errors of better than 0.5%. The cost estimates are being developed for both types of devices suitable for the 7-GeV APS applications.

In summary, the pure CSEM geometry has an intrinsic limitation in meeting the required tunability of undulators on the 7-GeV APS from 4.7 to 14 keV in the first harmonic. However, in experimental situations where wide tunability is not important, this geometry may be adequate. In such cases, the decision will be based on a cost comparison with a hybrid configuration, which is being prepared.

II. 9. INSERTION DEVICES

9.12.2 Relaxation of the Minimum-Gap Requirement through New Undulator Configurations [New Section]

During mature operation of the storage ring, the vacuum chamber for the straight section will have an aperture for the positron beam with a vertical clearance of 0.8 cm. This value is dictated by the minimum undulator gap of 1.0 cm essential to achieve the desired x-ray energy tunability. It has been found that this aperture is adequate for satisfactory performance of the storage ring. On the other hand, any increase in aperture will make operation easier and more reliable. One way of accomplishing this objective is to develop newer, hybrid undulator configurations that will meet the prescribed tunability requirements with gaps larger than 1.0 cm.

During the past year, new hybrid configurations that can enhance the peak field values have been proposed. One of these configurations results from a three-dimensional field optimization of undulator geometry in the lateral direction,⁽²²⁾ while the second one is based on a wedge pole geometry, originally suggested by Quimby and Pindroh.⁽²³⁾ Both these configurations provide a higher on-axis field by means of a larger concentration of the flux lines through the pole pieces. The new geometries allow the magnet surface that faces the gap to be driven to full magnet coercivity. A third geometry, combining the above two geometries, is expected to enhance the peak field along the undulator axis by about 20% over the conventional hybrid configuration. This would increase the minimum gap to about 1.2 cm, with the result that the minimum aperture requirements would be relaxed to about 1.0 cm.

In Fig. II.9.12-3, the laterally compensated hybrid geometry and the wedge pole hybrid geometry are shown. In both these geometries, the flux-line concentration is larger than that in the conventional hybrid geometry. In a standard hybrid geometry, addition of permanent magnet material in the lateral air gap improves the lateral flux path through the pole pieces. The wedge pole configuration not only increases the flux density but also results in a reduction in the higher harmonic content in the longitudinal variation of the magnetic field, compared with conventional hybrid geometries. A three-dimensional flux calculation shows that for a 3.3-cm-period undulator the peak field enhancement is about 4% for the laterally compensated configuration, 15% for the wedge pole configuration, and 20% for the combined configuration mentioned above.

9.12.3 Straight-Section Vacuum Chamber Design [New Section]

A prototype of the aluminum vacuum chamber was extruded for the straight section that will accommodate the insertion device. As described in Sec. II.9.4, these chambers have an aperture of 0.8 cm and minimum wall thickness in the vertical direction of 1 mm.

A 5-m length of this chamber was subjected to various tests. The deflection under vacuum was measured to be less than 25 μm . A support structure has been built for this

II. 9. INSERTION DEVICES

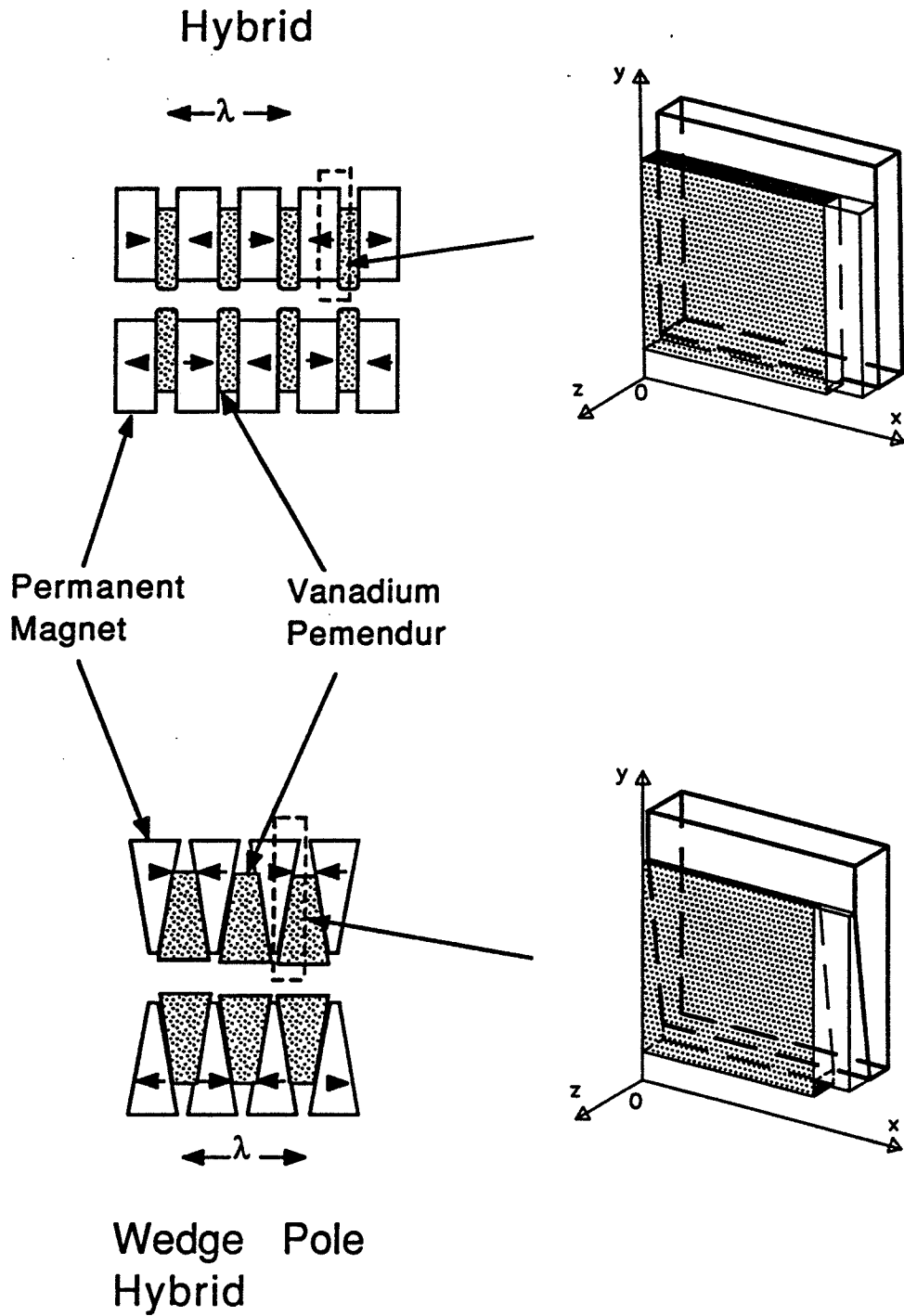


Figure II.9.12-3
Laterally compensated hybrid geometry and wedge pole hybrid geometry for undulators.

II. 9. INSERTION DEVICES

chamber capable of keeping the chamber flat over its 5-m length. Flatness and linearity of the mounted chamber were measured to be better than 0.2 mm over the length.

In order to improve the pumping capability for these long, narrow beam chambers, a new design has been developed. This design, shown in Fig. II.9.12-4, is similar to the earlier design with regard to the beam-chamber geometry, but it has an enlarged antechamber to accommodate a larger NeG strip, additional pumps, and vacuum-monitoring probes. Channels are also provided for cooling the antechamber and the beam chamber. The structural calculations are being carried out prior to the production of an extruded prototype of this chamber for further mechanical and vacuum tests.

9.17 References [Additional Material]

18. G. K. Shenoy, P. J. Viccaro, and D. M. Mills, "Characteristics of the 7-GeV Advanced Photon Source: A Guide for Users," Argonne National Laboratory Report ANL-88-9 (Feb. 1988).
19. P. J. Viccaro, G. K. Shenoy, S. Kim, and S. Bader, "A Soft X-ray Undulator for Photoelectron Spectroscopy at NSLS," to be presented at the Synchrotron Radiation Instrumentation Conference, Aug. 29-Sept. 2, 1988, Tsukuba, Japan.
20. K. Halbach, Nucl. Instrum. Methods A246, 77 (1986).
21. P. J. Viccaro, "Comparison of the Characteristics of Pure Permanent Magnet and Hybrid Undulators," Argonne Report, Light Source Note LS-120 (1988).
22. S. Kim, "Field Enhancement in an Undulator," Argonne Report, Light Source Note LS-121 (1988).
23. D. C. Quimby and A. L. Pindroh, Rev. Sci. Instrum. 58, 339 (1987).

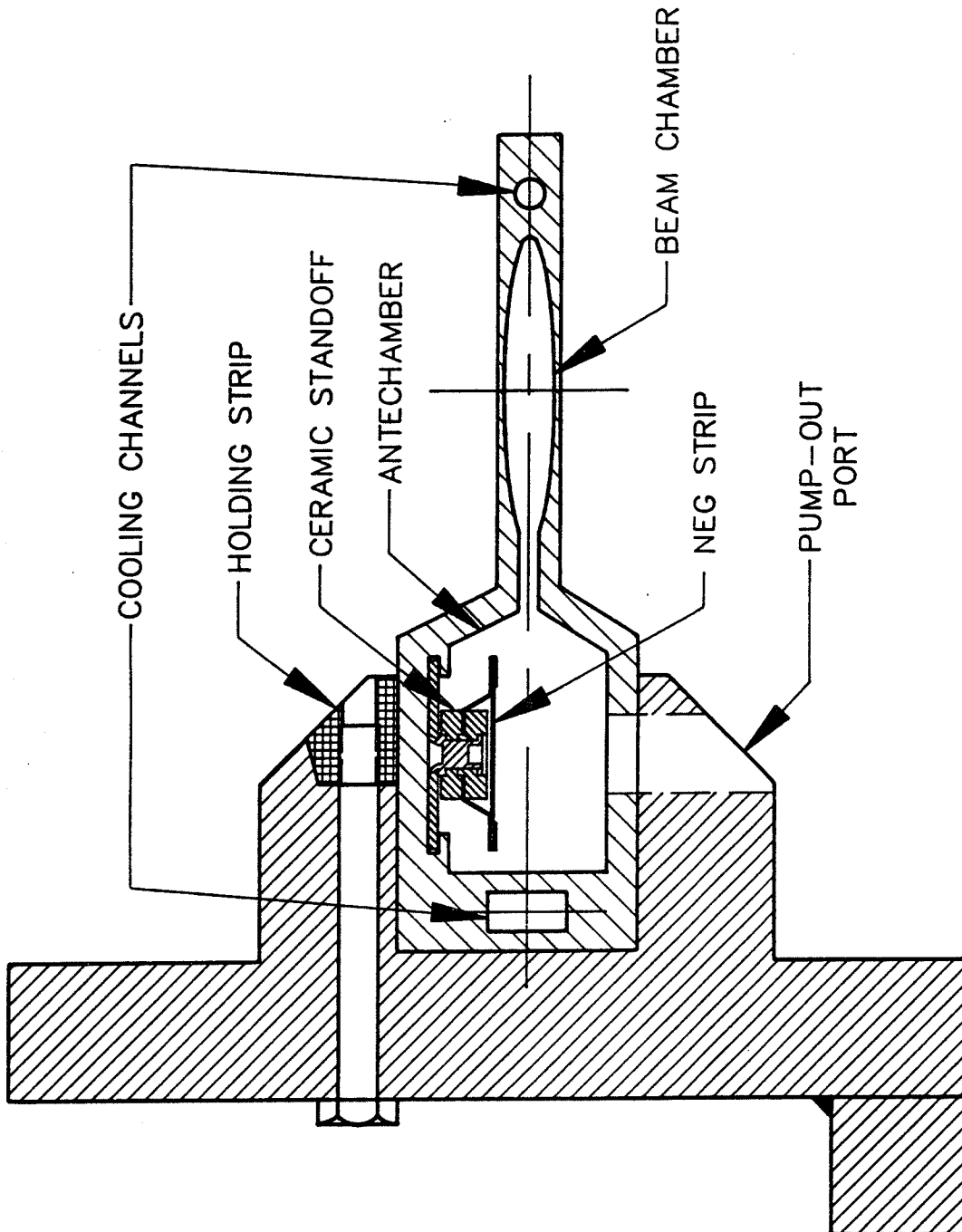


Figure II.9.12-4
A cross-section of the ID vacuum chamber and its support.

II. 9. INSERTION DEVICES

II. 10. INJECTION SYSTEM

10.1 Introduction - The Positron Injection Process [Replacement]

The main components used for production and acceleration of positrons for the 7-GeV Advanced Photon Source are as follows:

200-MeV Electron Linac (2.8 GHz, Rep. Rate 60 Hz),
Tungsten Positron-Production Target,
450-MeV Positron Linac (2.8 GHz, Rep. Rate 60 Hz),
Energy Compressor (Debuncher),
450-MeV Positron Accumulator Ring (PAR), and
450-MeV to 7-GeV Injector Synchrotron (Rep. Rate 2 Hz).

The electron linac accelerates electrons to 200 MeV at a 60-Hz rate. Each electron-linac macropulse is about 30 ns long and contains about 50 nC of charge. The 200-MeV electrons are focused to a 3-mm-diameter spot at the positron-production target.

The tungsten positron-production target is 7 mm thick. The target yield is 0.0083 positrons per incident electron within a solid angle of 0.15 sr and an energy range of (8 ± 1.5) MeV. The positrons from the target are focused by a high-field pulsed solenoid for injection into the positron linac system. The acceptance of the solenoid is 330×330 (mm·mrad)².

The positron linac system accepts the focused positrons from the target and accelerates about 60% of them to 450 MeV. Each 45-MeV macropulse contains 0.25 nC (1.5×10^9 positrons/pulse). With a 1.12 linac dilution factor, the 95th percentile emittance is 6.6×6.6 (mm·mrad)². This corresponds to an rms emittance of 1.1×1.1 (mm·mrad)². The ratio of 450-MeV positrons to 200-MeV electrons is 0.005.

The energy compressor (debuncher) is made up of four 30° bending magnets and a 10-MV waveguide. The magnets cause different path lengths for positrons that have energies greater than and less than the average energy. This leads to a lengthening of the 2.8-GHz microbunches in the waveguide where the rf voltage reduces the energy spread. The energy spread after the energy compressor is $\pm 0.5\%$.

The 450-MeV positrons are injected into the horizontal phase space of the PAR at a 60-Hz rate. As many as 24 macropulses can be accumulated as a single bunch in the PAR during each 0.5-s cycle of the injector synchrotron. A 0.1-s period is provided for final compression of the PAR bunch length before transfer into one of the 353-MHz rf buckets of the injector synchrotron.

The PAR circumference is 30.577 m (1/12 of the injector synchrotron). The positron linac macropulses (approximately 30 ns long) are accumulated in a first-

II. 10. INJECTION SYSTEM

harmonic 9.8-MHz rf bucket. A 12th-harmonic cavity is turned on to damp the beam sufficiently to inject into the 353-MHz synchrotron buckets.

The total number of positrons injected into the PAR can be as large as 3.6×10^{10} (24 pulses \times 1.5×10^9 positrons/pulse). The design and operation of the PAR is very similar to that of the PIA used for the accumulation of positrons before injection into the DESY synchrotron in Hamburg, West Germany.⁽¹⁰⁾ This ring operates with an accumulation efficiency of 50-60%. There is no further loss of beam during injection and acceleration of the positrons in DESY.

The injector synchrotron operates at a repetition rate of 2 Hz. Once each cycle, the bunch accumulated in the PAR is transferred to the injector synchrotron for acceleration to 7 GeV. The rf system for the injector synchrotron has the same frequency, 353 MHz, as that of the storage ring. At 7 GeV, the bunch is extracted and injected into a designated rf bucket of the storage ring.

With the synchrotron operating at 2 Hz, with 24 linac pulses per cycle, and assuming a PAR efficiency of 60%, the storage-ring filling rate is 4.3×10^{10} positrons/s, which results in a filling time of 50 s.

10.2 Linac

10.2.1 Introduction [Revision]

Following the DESY operational experience, the positron accelerating sections will all operate at a field of 16 to 20 MeV/m, rather than the 7 to 11 MeV/m in CDR-87. A revised linac layout and rf power distribution are shown in Fig. II.10.2-1. The positron beam is now injected into the PAR instead of directly into the injector synchrotron.

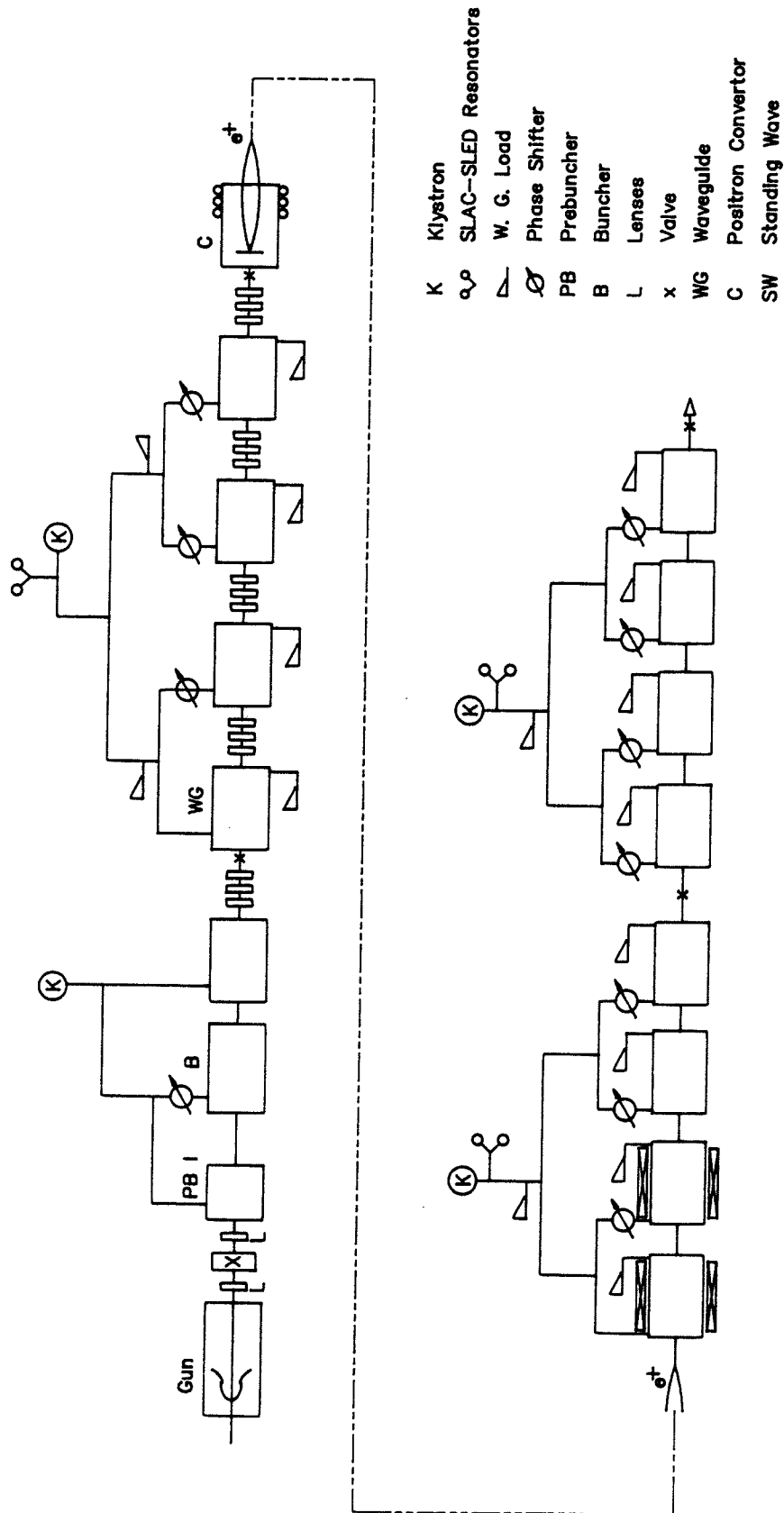
Linac parameters are listed in Table II.10.2-1.

10.2.2 Linac Injection System [Revision]

The pulse rate is changed from 8 pps to 48 pps due to the PAR scheme. The current is decreased from 3 A to 1.7 A. Also, the pulse length is increased from 16 to 30 ns, but the total charge is kept the same.

With a nominal rate of 60 Hz, 24 pulses per half second are injected into the main linac. The gun injects a beam pulse of ~ 3.0 A (it is capable of 10.0 A) and 30-ns duration at 135 keV and $\beta = 0.6$.

II. 10. INJECTION SYSTEM



II.10-3

Figure II.10.2-1
Schematic diagram of the electron and positron linacs showing the rf power distribution.

II. 10. INJECTION SYSTEM

Table II.10.2-1 [Replacement]

Nominal Linac Parameters

General	
Frequency	2.8 GHz
Klystron Power	35 MW
No. of Klystrons	4
No. of Sections/Traveling Wave	13
No. of Sections/Standing Wave	1
Repetition Rate	60 Hz
Beam Pulse Length	30.0 ns
No. of Pulses/Half Second	24
Electron Linac	
No. of Sections (incl. buncher)	5
Input Current	3.0 A
Input Energy	135 keV
Output Current	1.7 A
Output Energy	200 MeV
Output Emittance	1.2 mm ² mrad
Active Length	13 m
Converter	
Type	Tungsten
Thickness	7 mm
Conversion Efficiency e ⁺ /e ⁻ at Converter (for 200-MeV e ⁻)	0.0083
Positron Linac	
Input Current	14 mA
No. of Traveling-Wave Sections	8
Output Energy	450 MeV
Input Energy (mean)	8 MeV
Resolved Output Current	8.5 mA
Emittance (95th percentile)	6.6 mm.mrad
Energy Spread, ΔE/E (95th percentile)	±0.01
Active Length	24 m
Transmission Efficiency	60%
Overall e ⁺ /e ⁻ Efficiency	0.005

II. 10. INJECTION SYSTEM

10.2.3 Linac Accelerating Sections [Revision]

There are now eight traveling-wave sections in the positron linac in place of ten. This is due to operation of all positron accelerating sections at an accelerating field of 16 to 20 MeV/m. The higher field in the first three sections of the positron linac is now used, since the DESY linac operates successfully under these conditions.

Due to the sixfold increase of the average rf power dissipated in the waveguides, the design has been adjusted to provide for additional cooling to keep the operating temperature to $\pm 0.2^\circ\text{C}$.

10.2.4 Linac Klystron and Modulators [Revision]

The new rf duty cycle (48 pps x 5 μs) falls within the klystron's capability. The modulators are upgraded to be capable of producing 48 pps with peak power of 80 MW and average power of 25 kW each.

10.2.7 Positron Production [Revision]

The total charge in the electron pulse is the same as in CDR-87, but the pulse length is changed. Likewise, the positron pulse length is changed, but the number of positrons per pulse is the same. Despite the higher repetition rate, the original cooling scheme is adequate.

10.2.10 The Energy Compression System (Debuncher) [New Section]

The energy spread of the 450-MeV positron beam at the end of the positron linac is $\pm 1.0\%$. Even though the Positron Accumulator Ring (PAR) is designed to accept a 450-MeV positron pulse with an energy spread of $\pm 1.0\%$, it is desirable that the injected beam have an energy spread of $\pm 0.5\%$. This specification is met through the use of an energy compression system (ECS or debuncher), consisting of four 30° dipole magnets with a bending radius of 1.5 m and a magnetic field strength of 1 T, three quadrupoles, and a 1-m S-band waveguide (see Fig. II.10.2-2, Table II.10.2-3).

The anisochronous path in the transport system disperses the beam longitudinally according to energy. The accelerating section is used to differentially accelerate the dispersed beam to achieve energy compression.

The longitudinal phase-space gymnastics are shown in Fig. II.10.2-3. The longitudinal phase-space ellipse from the positron linac is oriented in the upright position. The ΔE is ± 4.5 MeV and Δt is ± 7.5 ps. It is sheared by the transport system longitudinally along the time axis to $\Delta t = \pm 25.6$ ps. The accelerating waveguide with ~ 10 MV shears the ellipse along the energy axis to an upright position. The resulting beam energy spread is less than $\pm 0.5\%$.

II. 10. INJECTION SYSTEM

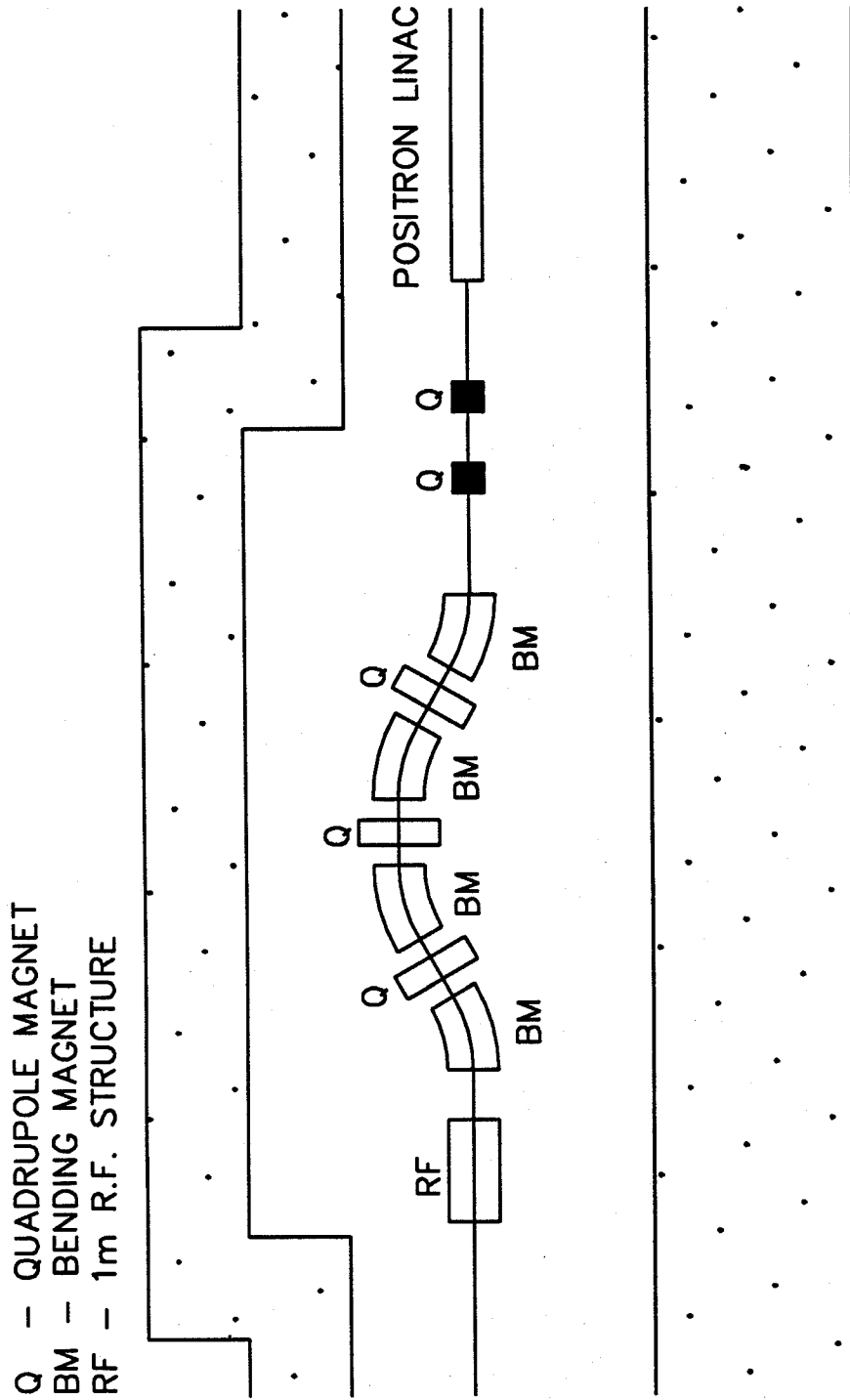


Figure II.10.2-2
 Energy compression system layout.

II. 10. INJECTION SYSTEM

Table II.10.2-3 [Additional Material]

Parameters for Energy Compression System Magnets

		Dipole	Quadrupole
Number Required		4	3
Field Strength at 450 MeV		1.0 T	3.8 T/m*
Effective Length	(m)	0.785	0.3
Gap Height or Diameter	(mm)	40	70
Total Mass	(kg)	786	125
Coils Per Pole		1	1
Conductor Height	(mm)	9.7	2.0
Width	(mm)	9.7	2.0
Hole Diameter	(mm)	5.3	edge-cooled
Turns per Coil		60	288
Coil Current	(A)	275	7.0
Current Density in Conductor	(A/mm ²)	2.0	1.5
Voltage	(V)	18	28.9
Power	(kW)	5.0	0.2
Cooling Water Circuits per Magnet		2	4
Total Water Flow	(gal/min)	1.0	0.05
Water Pressure Drop	(psi)	100	100
Water Temperature Rise	(°C)	20	15

*Maximum value.

II. 10. INJECTION SYSTEM

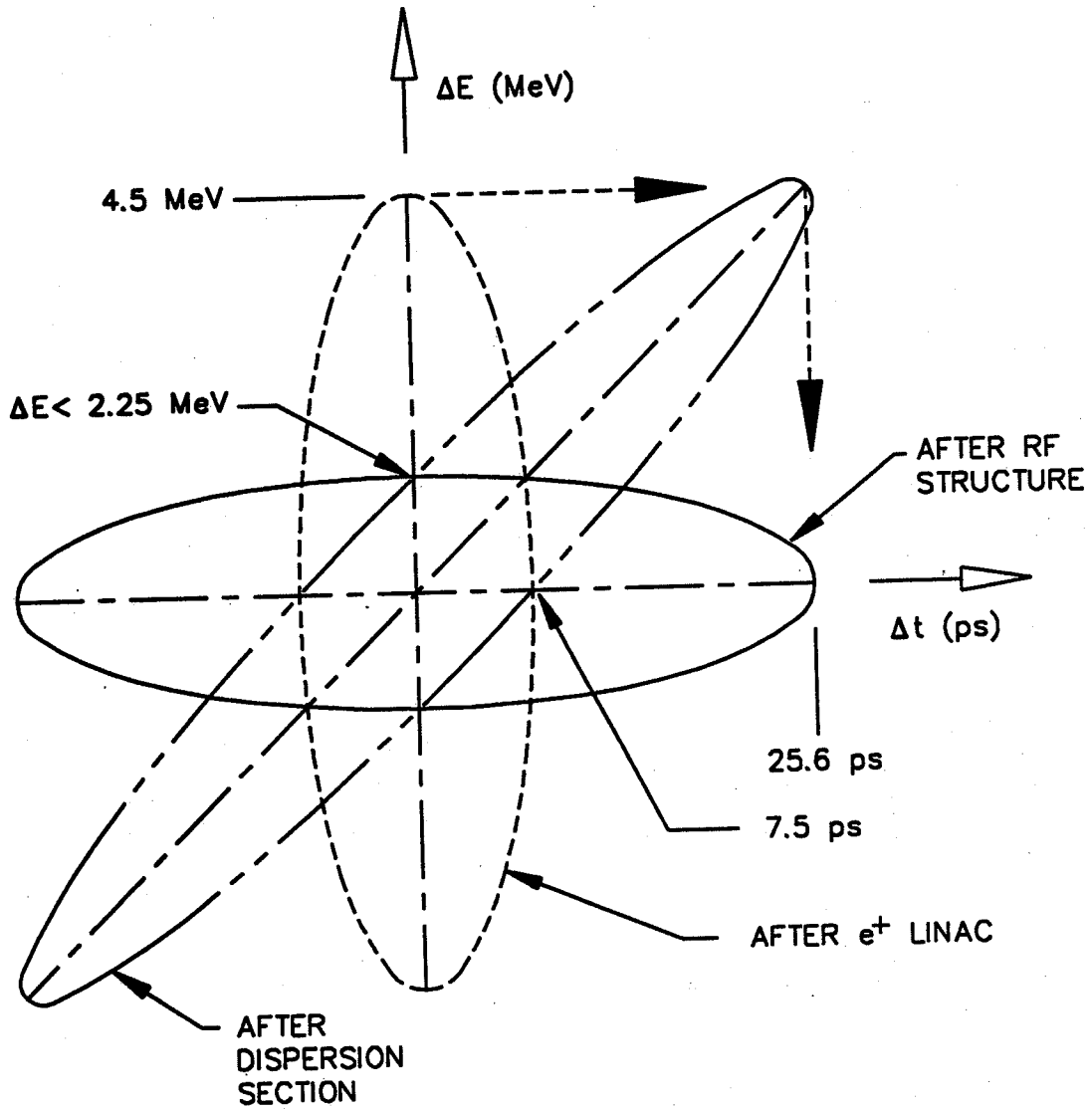


Figure II.10.2-3
Longitudinal phase-space ellipses in the energy compression system.

II. 10. INJECTION SYSTEM

10.2A Positron Accumulator Ring (PAR)* [New Section]

10.2A.1 Introduction [New Section]

Positrons from the 450-MeV linac are injected into the horizontal phase space of the accumulator ring at a 60-Hz rate. During each injection, bumper magnets are used to move the horizontal orbit as close as possible to the septum of an injection magnet. The separation of the bumped orbit from the septum of the injection magnet is determined by the extent of the damping of horizontal oscillations between successive injections. This separation in turn determines the horizontal aperture of the ring.

The horizontal damping time constant, τ_x (ms), is given by[†]

$$\tau_x = \frac{4\pi R \rho}{26.55 J_x E^3},$$

where

$2\pi R$ is the circumference of the ring (m),

ρ is the bending radius in each dipole (m),

E is the positron energy (GeV),

$$J_x = 1 - \frac{1}{2\pi} \int \frac{D(s)}{\rho} (1 - 2n) ds,$$

$D(s)$ is the dispersion function, and

$$n = \frac{-\rho B'(x)}{B_0} \text{ (field index).}$$

$B'(x)$ is the radial gradient in the bending magnets, and the integration is over the path length in the bending magnets.

In addition to the horizontal oscillation damping required for injection, the length of the single bunch in the ring must be compressed from about one-third of the circumference of the PAR to a length that can be injected without loss into the 353-MHz rf buckets of the injector synchrotron. This compression of the bunch length is accomplished by damping of the energy spread. The time allowed for the damping of the 24 accumulated pulses is 0.1 s. The energy damping time constant is given by

$$\tau_E = \tau_x J_x / J_E,$$

* E. A. Crosbie, ANL Report, Light Source Note LS-109 (March 1988).

† M. Sands, "The Physics of Electron Storage Rings," SLAC Report 121 (1970).

II. 10. INJECTION SYSTEM

where

$$J_E = 3 - J_x.$$

At 450 MeV ($B\rho = 1.501 \text{ T}\cdot\text{m}$), a small damping time constant requires high magnetic fields in the bending magnets. The bending-magnet field for the PAR is 1.476 T. The circumference of the ring must also be as small as possible and still leave room for quadrupoles, sextupoles, injection and extraction magnets, orbit correctors, and rf cavities. This circumference is 30.58 m, which is 1/12th of the circumference of the injector synchrotron.

A field index of 0.6 in the bending magnets further decreases the horizontal damping time constant without seriously increasing the longitudinal damping time constant. For the PAR lattice, J_x is 1.257 and J_E is 1.743. These values of J_x and J_E give values for τ_x equal to 20.49 ms and τ_E equal to 14.77 ms.

10.2A.2 Lattice [New Section]

A plan view of the PAR is shown in Fig. II.10.2A-1. The eight bending magnets are arranged in a two-period configuration with two long straight sections. One of the long straight sections is used for injection and extraction, and the other contains the rf cavities.

The component parameter list for 1/2 period is shown in Table II.10.2A-1. The lattice functions β_x , β_y and dispersion function D are shown in Fig. II.10.2A-2. The dispersion function is zero in the two long straight sections.

The horizontal and vertical tunes are 2.19 and 1.27. A list of the performance characteristics for the ring is shown in Table II.10.2A-2. Two families of sextupoles correct horizontal and vertical chromaticities to zero. These sextupoles are located in multipole magnets, which also contain vertical and horizontal orbit-correcting dipoles.

10.2A.3 RF Capture and Bunch-Length Damping [New Section]

Injection is into a first-harmonic, 9.8045-MHz rf bucket that has an energy acceptance of $\pm 1.4\%$. Each macropulse from the 450-MeV positron linac is about 30 ns long. Ninety-five percent of the positron beam from the 450-MeV linac is contained within an energy spread of $\pm 1\%$. The compressor system between the linac and the PAR is capable of reducing the energy spread to $\pm 0.5\%$. The compressor system is an option that provides flexibility to compensate for unexpected dilution.

II. 10. INJECTION SYSTEM

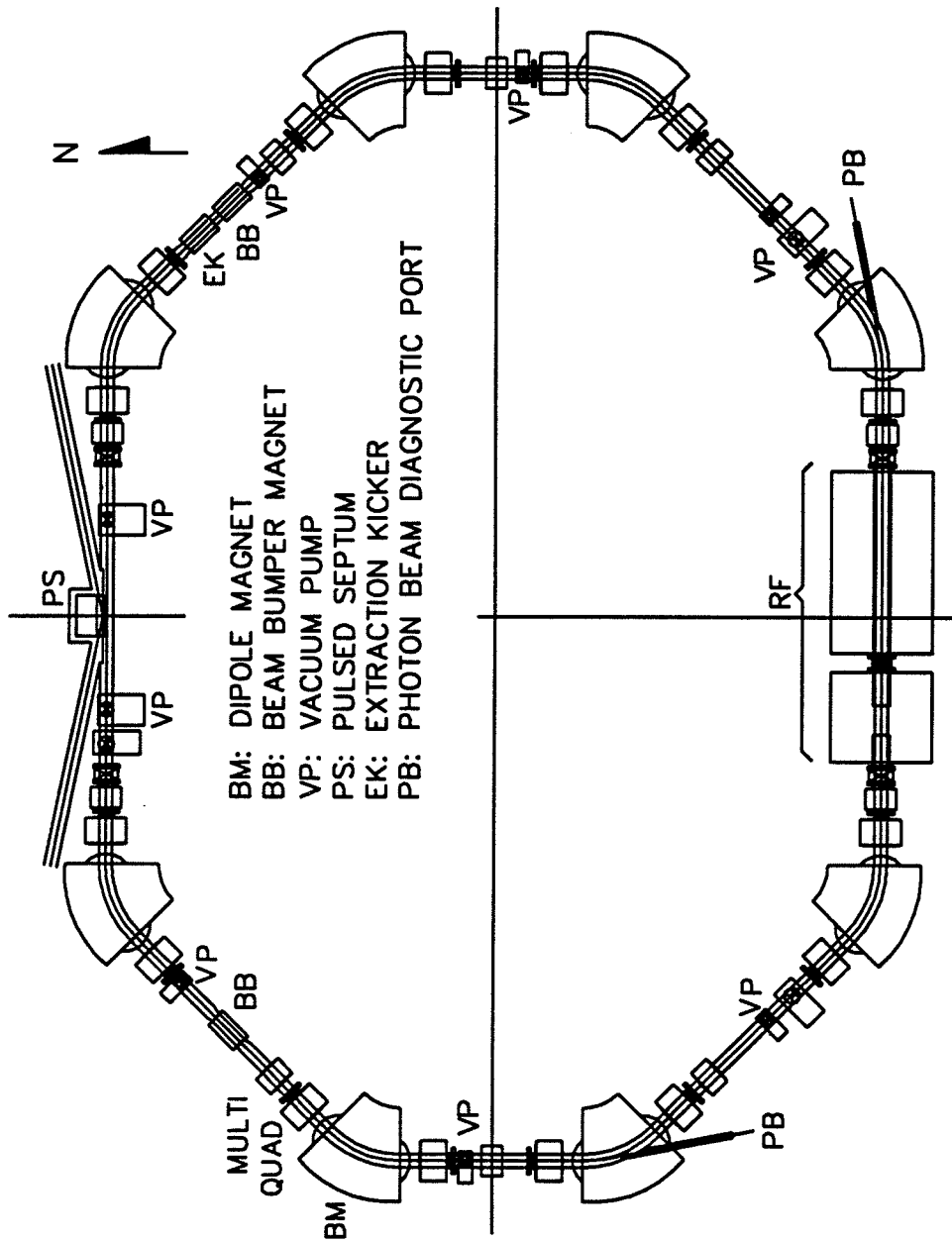


Figure II.10.2A-1
Positron accumulator ring layout.

II. 10. INJECTION SYSTEM

Table II.10.2A-1 [Additional Material]

PAR Lattice Components for One-Fourth Machine*

Element	Length (m)	Magnet Parameters
Drift	1.7092	
Multipole	0.20	
Drift	0.10	
Quadrupole Q1	0.25	$B'/B\rho = 0.543 \text{ m}^{-2}$
Drift	0.20	
Magnet	0.80	$\rho = 1.01859 \text{ m}, \frac{\rho B'}{B} = -0.6$
Drift	0.20	
Quadrupole Q2	0.25	$B'/B\rho = 1.4706 \text{ m}^{-2}$
Drift	1.39	
Multipole (sextupole, S1)	0.20	$B''\ell/B\rho = 0.23 \text{ m}^{-2}$
Drift	0.20	
Quadrupole Q3	0.25	$B'/B\rho = -1.3607 \text{ m}^{-2}$
Drift	0.20	
Magnet	0.80	$\rho = 1.01859 \text{ m}, \frac{\rho B'}{B} = -0.6$
Drift	0.20	
Quadrupole Q4	0.25	$B'/B\rho = 1.3846 \text{ m}^{-2}$
Drift	0.345	
1/2 Multipole (sextupole, S2) (Reflection point)	0.10	$B''\ell/B\rho = 0.44 \text{ m}^{-2}$
TOTAL	7.6442	

* $B \cdot \rho = 1.5010 \text{ T} \cdot \text{m}$ (0.45 GeV).

II. 10. INJECTION SYSTEM

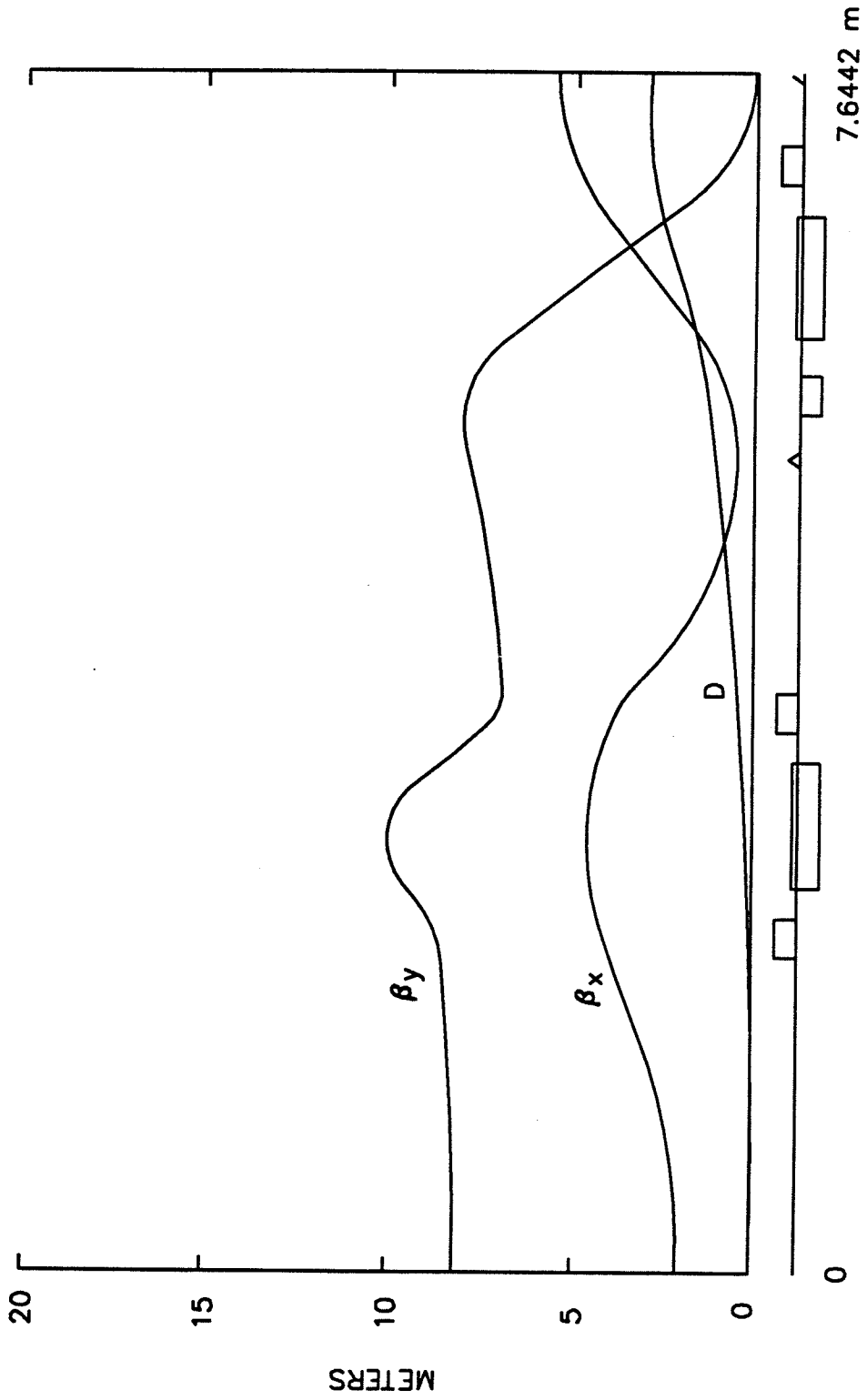


Figure II.10.2A-2
Lattice and dispersion functions for one-half of a period for the PAR.

II. 10. INJECTION SYSTEM

Table II.10.2A-2 [Additional Material]

Parameters for the Positron Accumulator Ring

Item	Value
Circumference (m)	30.5768
Revolution Time (ns)	101.994
Energy (MeV)	450
No. of Cells	2
No. of Bending Magnets	8
Dipole Field, B (T)	1.476
Bend Radius, ρ (m)	1.0186
Field Index, $-\rho B'/B$	0.6
No. of Quadrupoles	16
Tunes, ν_x/ν_y	2.19/1.27
Transition Gamma, γ_T	1.93
Chromaticities, ξ_x/ξ_y	-2.70/1.05
Partition Numbers, $J_x/J_y/J_E$	1.257/1.000/1.743
Damping Time Constants, $\tau_x/\tau_y/\tau_E$ (ms)	20.49/25.75/14.77
Energy Loss per Turn (keV)	3.56
Natural Emittance, ϵ (mm·mrad)	0.37
Natural Energy Spread, σ_E/E (damped)	0.41×10^{-3}
RF Systems	
System I	
Frequency, f (MHz)	9.8045
Harmonic Number, h	1
Peak Voltage, V (kV)	40
Synchrotron Frequency, f_s (kHz)	19.1
Natural Bunch Length, σ_τ (damped) (ns)	0.92
System II	
Frequency, f (MHz)	117.654
Harmonic Number, h	12
Peak Voltage, V (kV)	30
Synchrotron Frequency, f_s (kHz)	60.5*
Natural Bunch Length, σ_τ (damped) (ns)	0.29*

*Systems I and II both on.

II. 10. INJECTION SYSTEM

Once each cycle of the 2-Hz injector synchrotron, 24 macropulses are injected into the horizontal phase space of the PAR at a 60-Hz rate. This allows 100 ms for the final damping of the single bunch to a length short enough to be transferred to the 2.83-ns (353-MHz) injector synchrotron rf bucket. The applied rf voltage is just large enough for efficient capture without producing excessive increase in the energy spread. The latter condition is important because of the aperture requirements for injection into the horizontal phase space. The lattice dispersion function has a maximum value of 3.35 m.

Figure II.10.2A-3 shows the phase space of the injected pulse fitting within a 40-kV, first-harmonic PAR bucket. The bucket contour that encloses 95% of the injected pulse has a $\Delta\tau$ of 60 ns and $\Delta E/E$ of $\pm 1.2\%$. At least 95% of the injected beam is contained within this contour.

After 50 ms, the longitudinal phase space damps to the natural values of

$$\sigma_E/E = \sqrt{\frac{0.384}{\rho J_E}} \frac{E}{0.511} \times 10^{-3} = 0.41 \times 10^{-3}$$

and

$$\sigma_\tau = \frac{1}{2\pi f_s \gamma_T^2} \sigma_E/E,$$

where ρ is in m, E is in GeV, γ_T is the transition γ , and f_s is the synchrotron frequency.

The final bunch length provided by the first-harmonic system is not adequate for efficient capture in the injector synchrotron. Therefore, a twelfth-harmonic (117.654-MHz), 30-kV rf system has been added to the PAR. This system is turned on 50 ms after the injection of the last linac pulse. The first-harmonic system damps the beam to $\sigma_E/E = 0.44 \times 10^{-3}$ and $\sigma_\tau = 0.99$ ns. With the first-harmonic system still on, the twelfth-harmonic system is turned on with the phase equal to 180° at the bunch center. Figure II.10.2A-4 shows the $\sqrt{6}$ σ contour of the beam in the combined 40-kV first-harmonic and 30-kV twelfth-harmonic bucket. The combined system has a synchrotron frequency of 60.6 kHz and a final bunch length of $\sigma_\tau = 0.29$ ns. Figure II.10.2A-5 shows the phase-space contour for the $\sqrt{6}$ σ of the PAR bunch in the injector synchrotron 100-kV rf bucket.

10.2A.4 Injection [New Section]

Multipulse injection into the PAR is in the horizontal phase. Figure II.10.2A-6 shows the horizontal phase space that can be occupied by the beam at the septum magnet. There is a 3-cm clearance between the septum magnet and the central orbit. The beam is injected at 3.67 cm from the unperturbed central orbit, and the bumped orbit is at 1.83 cm. During subsequent turns with the orbit bumper magnets turned off, the 95% profile of the injected beam is, before damping, located anywhere in a phase-

II. 10. INJECTION SYSTEM

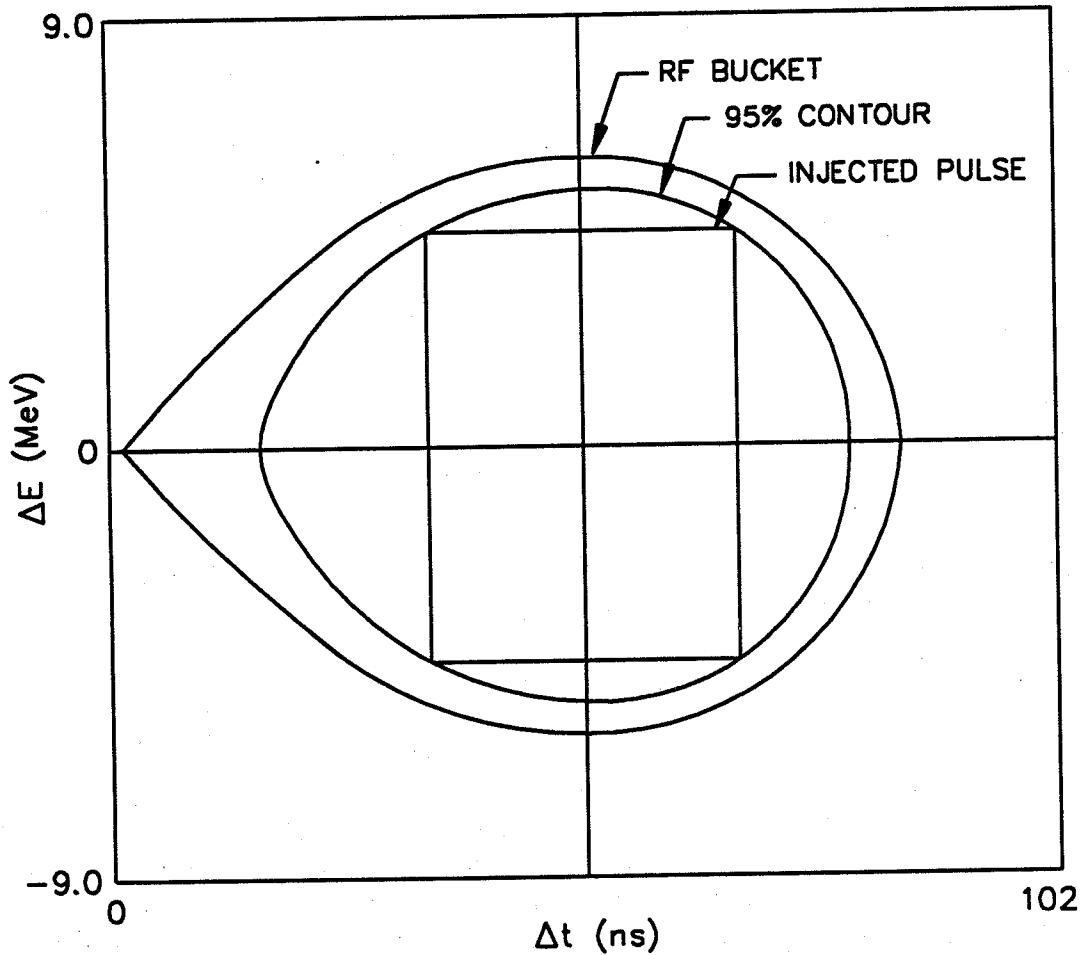


Figure II.10.2A-3
Phase space of the injected pulse ($\frac{\Delta E}{E} = \pm 1\%$, 30 ns) fitting within a 40-kV, first-harmonic PAR-rf-bucket. Also shown is the rf bucket that contains at least 95% of the injected pulse.

II. 10. INJECTION SYSTEM

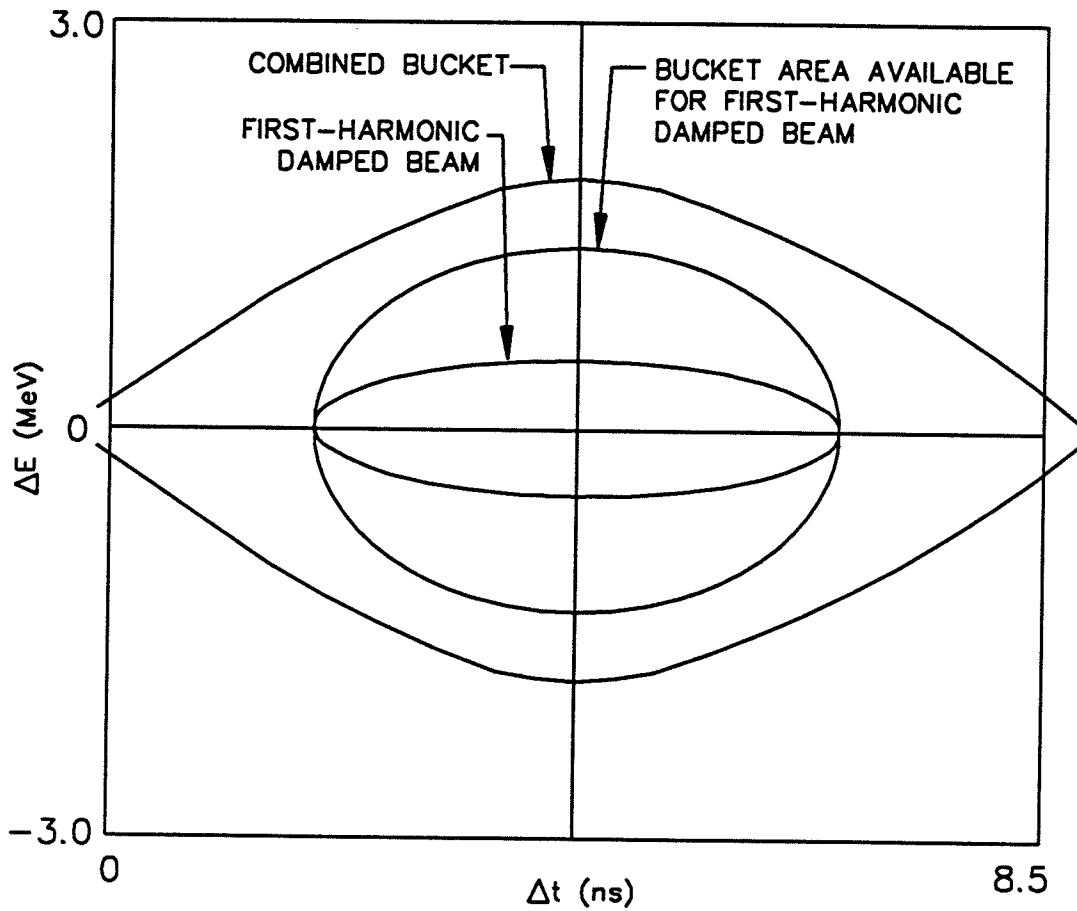


Figure II.10.2A-4

The $\sqrt{6} \sigma$ contour bunch in the combined first-harmonic and twelfth-harmonic rf bucket at the time of the twelfth-harmonic turn-on. Also shown is the bucket area available for the first-harmonic damped beam.

II. 10. INJECTION SYSTEM

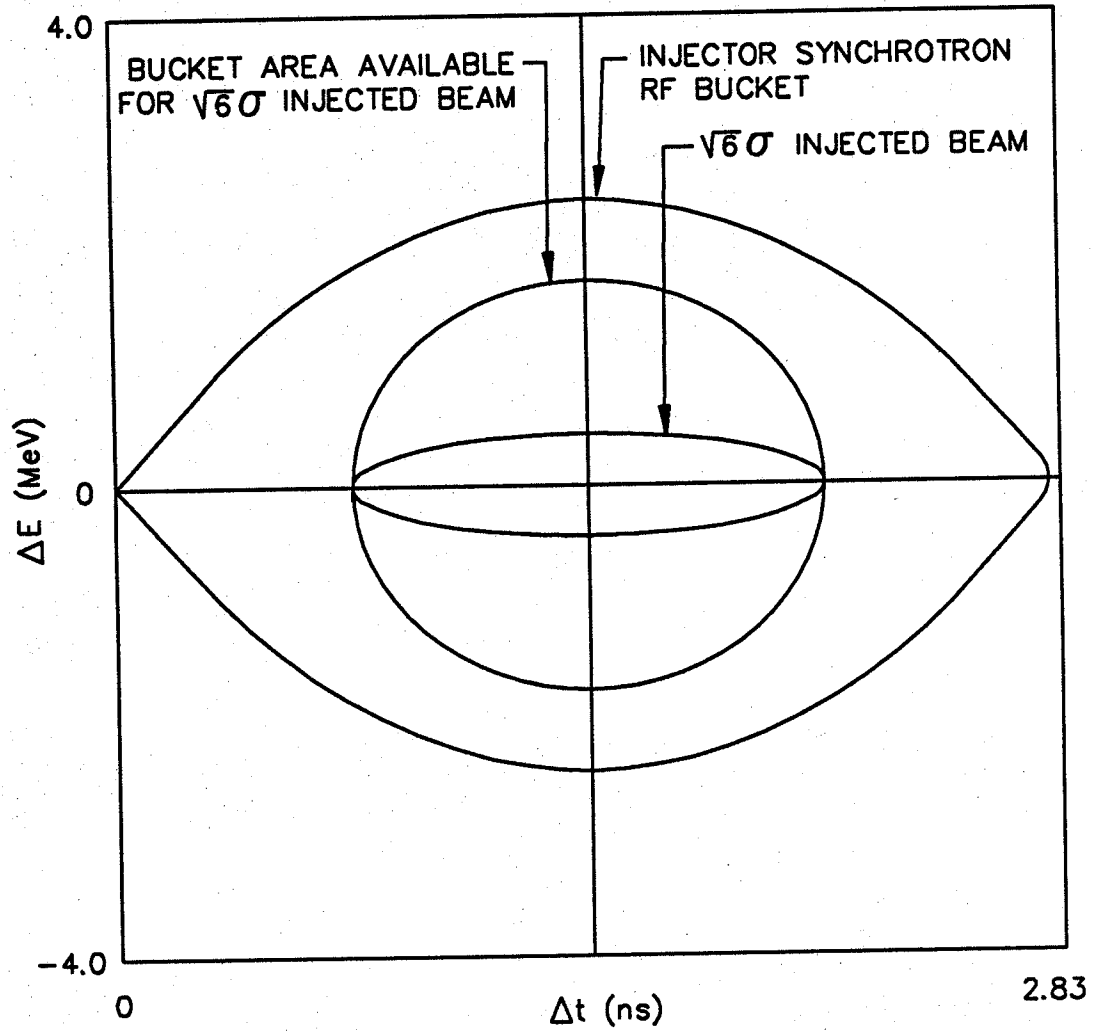


Figure II.10.2A-5
 $\sqrt{6}\sigma$ bunch from the PAR in a 100-kV, 353-MHz injector synchrotron bucket. Also shown is the bucket area available for $\sqrt{6}\sigma$ injected beam.

II. 10. INJECTION SYSTEM

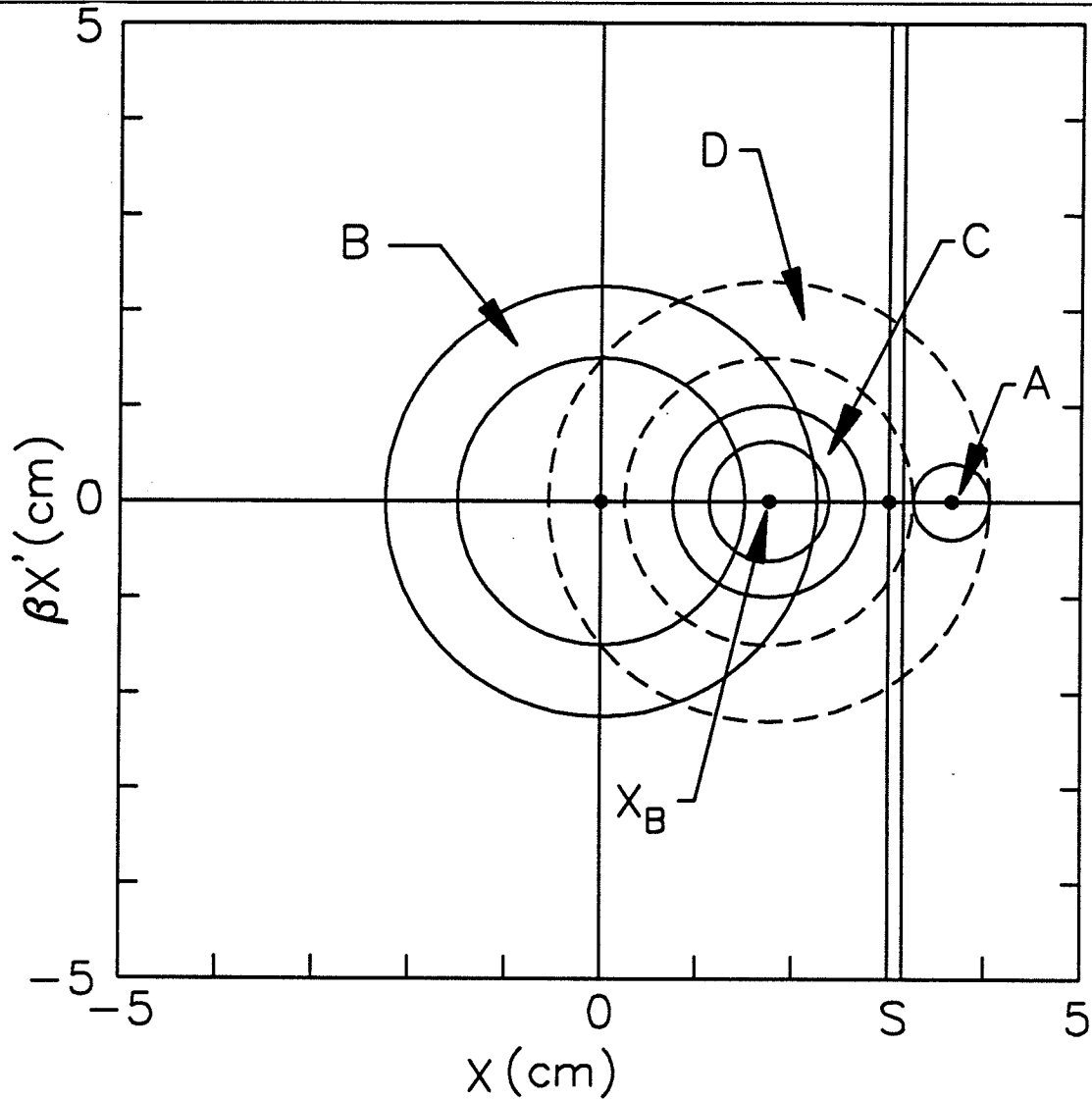


Figure II.10.2A-6

Horizontal phase space at the injection septum magnet.

- A: Injected beam
- S: Septum
- X_B : Bumped orbit position
- B: Phase space available for the injected beam before damping with the beam bumper magnets turned off
- C: Phase space available for injected beam after 16.7 ms of damping with the beam bumper magnets turned on
- D: Phase space available for the injected beam before damping and with the beam bumper magnets turned off

II. 10. INJECTION SYSTEM

space ring having radii of 1.84 ± 0.37 cm. After $1/60$ s of damping, the radii are reduced by a factor of 0.44 so that the maximum extent of the beam misses the septum magnet when the orbit is again bumped for injection of the next pulse. Pulses that have been injected previous to the pulse under consideration are damped for a longer time and occupy the space inside the rings shown in the figure. Based on the calculated natural emittance of the lattice, the horizontal oscillations damp to a final value of $\sigma_x = 0.88$ mm.

The maximum extent of the horizontal oscillations of each injected pulse is ± 21 mm at the injector septum. This width increases to a maximum of ± 35 mm at one-fourth of the circumference upstream and downstream of the septum. At these locations, the dispersion function has its largest value, 3.35 m. If the energy spread of the injected beam is $\pm 1\%$, the maximum total aperture required for injection is ± 50 mm. For this reason, the horizontal aperture of the vacuum chamber is 12 cm. The vertical gap is 3.6 cm.

Two kicker magnets are used to produce the bumped orbit at the injection magnet. They are located 90° in horizontal betatron phase upstream and downstream of the injection septum magnet. The bumped orbit is shown in Fig. II.10.2A-7. The injection kicker magnets have a rise time of 65 ns, a fall time of 90 ns, and a flat-top time of 80 ns. The kicker strength required to produce a bumped orbit of 1.83 cm at the septum magnet is 171 G·m. The designed kickers are 35 cm long and are capable of producing fields of 600 G.

10.2A.5 Extraction [New Section]

The injection kickers run continuously at 60 Hz, and extraction is accomplished by pulsing a third kicker magnet located downstream of the first bumper magnet (see Fig. II.10.2A-7). This causes the circulating bunch to enter the aperture of the injection septum magnet, which is then used as the final extraction magnet.

10.2A.6 Injection/Extraction Septum Magnet [New Section]

The same septum magnet is used for both injection into and extraction from the PAR. Both beams must clear the yokes of either the downstream or upstream bending magnet. These magnets are at distances of 2.26 m from the center of the injection straight section and have yokes that extend to 40 cm from the central orbit.

The injection and extraction angles for the PAR are 0.2 rad (11.5°). The magnet is 0.4 m long and has a field of 0.75 T and a septum thickness of 2 mm. The horizontal and vertical apertures are 7 cm and 2 cm, respectively. The magnet operates continuously at 60 Hz.

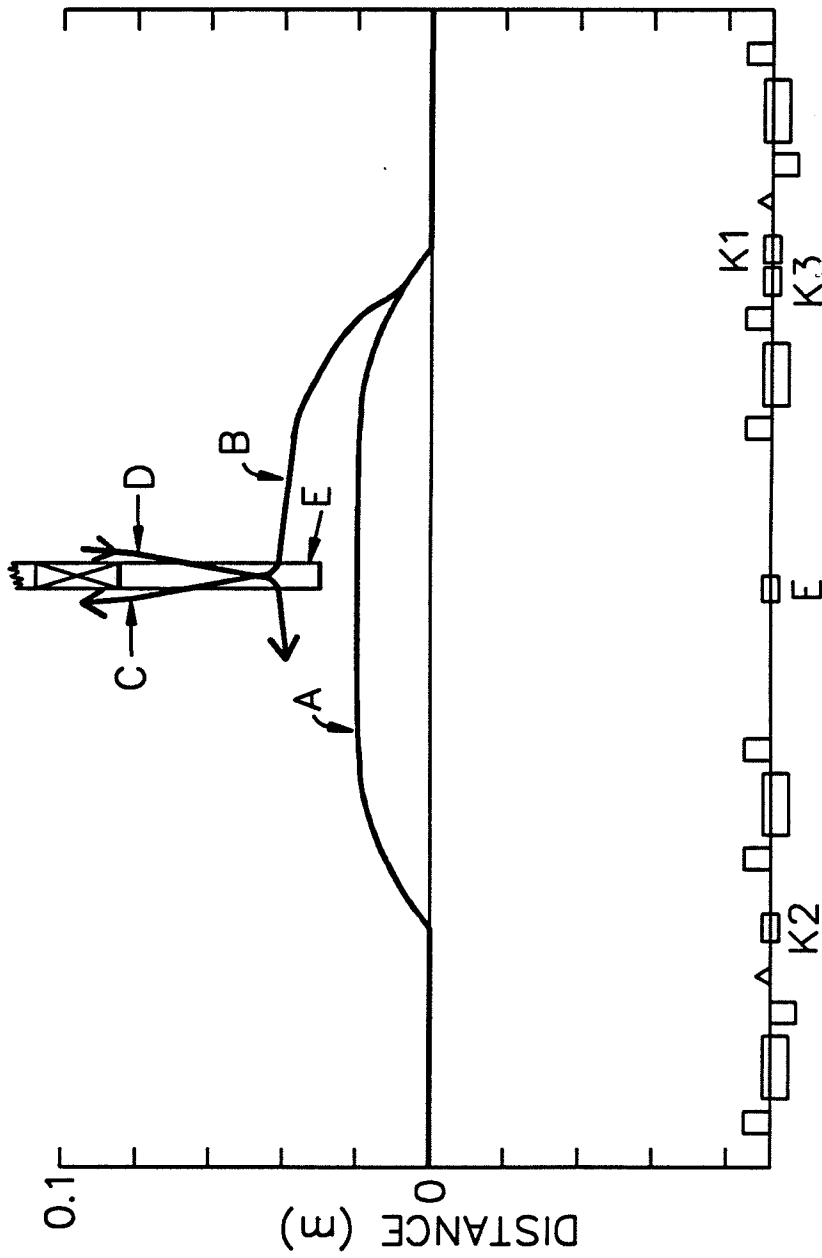


Figure II.10.2A-7
 Bumped orbit and injected and extracted beams. A: Bumped orbit using kickers K₁ and K₂, B: Beam kicked into the extraction magnet (E) using kickers K₁ and K₃, C: Extracted beam, D: Injected beam, E: Septum magnet.

II. 10. INJECTION SYSTEM

10.2A.7 Orbit Corrections [New Section]

The amplification factors for focusing element displacements for the PAR are 4.0 and 6.5 for the horizontal and vertical planes, respectively. Horizontal and vertical orbit corrections are accomplished using ten dipoles and 12 beam-position monitors for each plane (see Fig. II.10.2A-1). The correction dipoles are located in the multipole magnets.

Computer simulations of ten sample machines using 1-mm rms magnet displacement errors, 10^{-3} rms field errors, and 10^{-3} rad rms dipole roll errors resulted in closed-orbit distortions of about 7 mm in both planes. The largest single orbit distortion in the ten samples was 18 mm. The dipole strengths to correct the orbits to better than 0.1 mm had an rms average of 1 kG·cm. The largest single corrector strength in the ten samples was 2.9 kG·cm. The dipole correctors in the multipole magnets are designed to produce 4 kG·cm.

10.2A.8 Stored Beam Current [New Section]

The total number of positrons injected into the PAR can be as large as 3.6×10^{10} (24 pulses at 1.5×10^9 positrons/pulse). The average beam current \bar{I} is 56.5 mA. As the bunch is damped in the ring, the peak current increases. For a Gaussian distribution, the peak current is given by

$$I_p = \frac{\bar{I} T}{\sqrt{2\pi} \sigma_\tau}$$

where T is the revolution time (102 ns).

The minimum bunch length is 0.29 ns, producing a peak current of 7.8 A. The final energy spread, σ_E/E , is 0.41×10^{-3} .

The impedance limit for longitudinal stability is customarily written as

$$\left| \frac{Z_{\parallel}}{n} \right| \leq \frac{E}{\gamma_T^2 I_p} \left(\frac{\Delta p}{p} \right)^2$$

where $\frac{\Delta p}{p}$ is the full width at half maximum ($2.355 \sigma_E/E$). The impedance is 14.5 Ω , which is easily achieved in modern machines.

II. 10. INJECTION SYSTEM

10.2A.9 Magnets, Supports, and Power Supplies [New Section]

10.2A.9.1 Magnets [New Section]

10.2A.9.1.1 Dipoles, Quadrupoles, and Multipoles

The principal magnets for the PAR consist of eight dipoles, 16 quadrupoles, and 10 multipole (12-pole) magnets. Views of these three magnets are shown in Figs. II.10.2A-8, II.10.2A-9, and II.10.2A-10, respectively. These figures show some of the dimensions and major components of the assembled units. The ring vacuum chamber is also shown for reference in each drawing.

The calculated (2-D geometry) relative field deviations and leading coefficients for the ring magnets at 450 MeV are listed in Table II.10.2A-3.

The eight main dipoles are combined-function magnets containing both a 1.47-T dipole field and a superimposed defocusing gradient field of 0.8659 T/m. The cores of the dipole and multipole magnets are made from solid, low-carbon (SAE 1010) steel. The core of each quadrupole is assembled from 1.5-mm-thick, low-carbon-steel laminations with 10.0-mm-thick end-plates. The core is held under compression with tie rods and secondary assembly components welded to the end-plates and to each lamination. The coils for each magnet are made from copper conductor and insulated with fiberglass that is vacuum-impregnated with epoxy resin.

Each of the multipole magnets contains three independent sets of coils; one produces a sextupole field, and the other two produce vertical and horizontal dipole fields. Each set of dipole coils consists of windings on ten poles; the ampere-turns around each pole are proportional to the distance of the pole from the relevant midplane. Each pole contains from one to three windings combined into a monolithic structure. The parameters for the PAR magnets are listed in Table II.10.2A-4.

10.2A.9.1.2 Injection/Extraction Septum-Magnet Design

The septum magnet is a pulsed device similar in design to that used for injection into the storage ring. It operates at a peak field of 0.75 T and at 60 Hz. The thickness of the septum is 2 mm at both ends and increases along the length towards the center to improve the mechanical and thermal properties. The parameters for this magnet are listed in Table II.10.2A-5.

II. 10. INJECTION SYSTEM

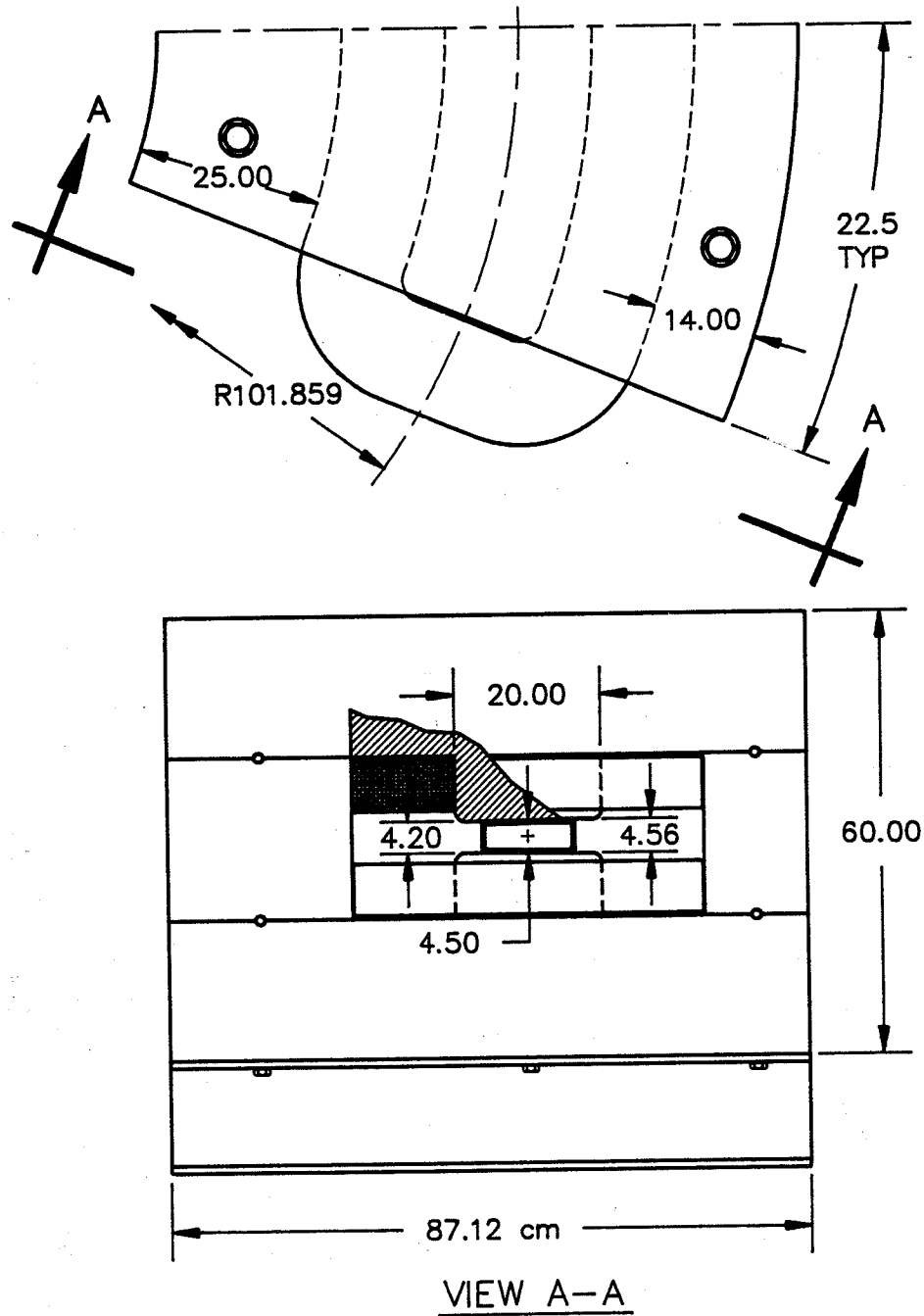


Figure II.10.2A-8
Top and end views of the PAR dipole magnet.

II. 10. INJECTION SYSTEM

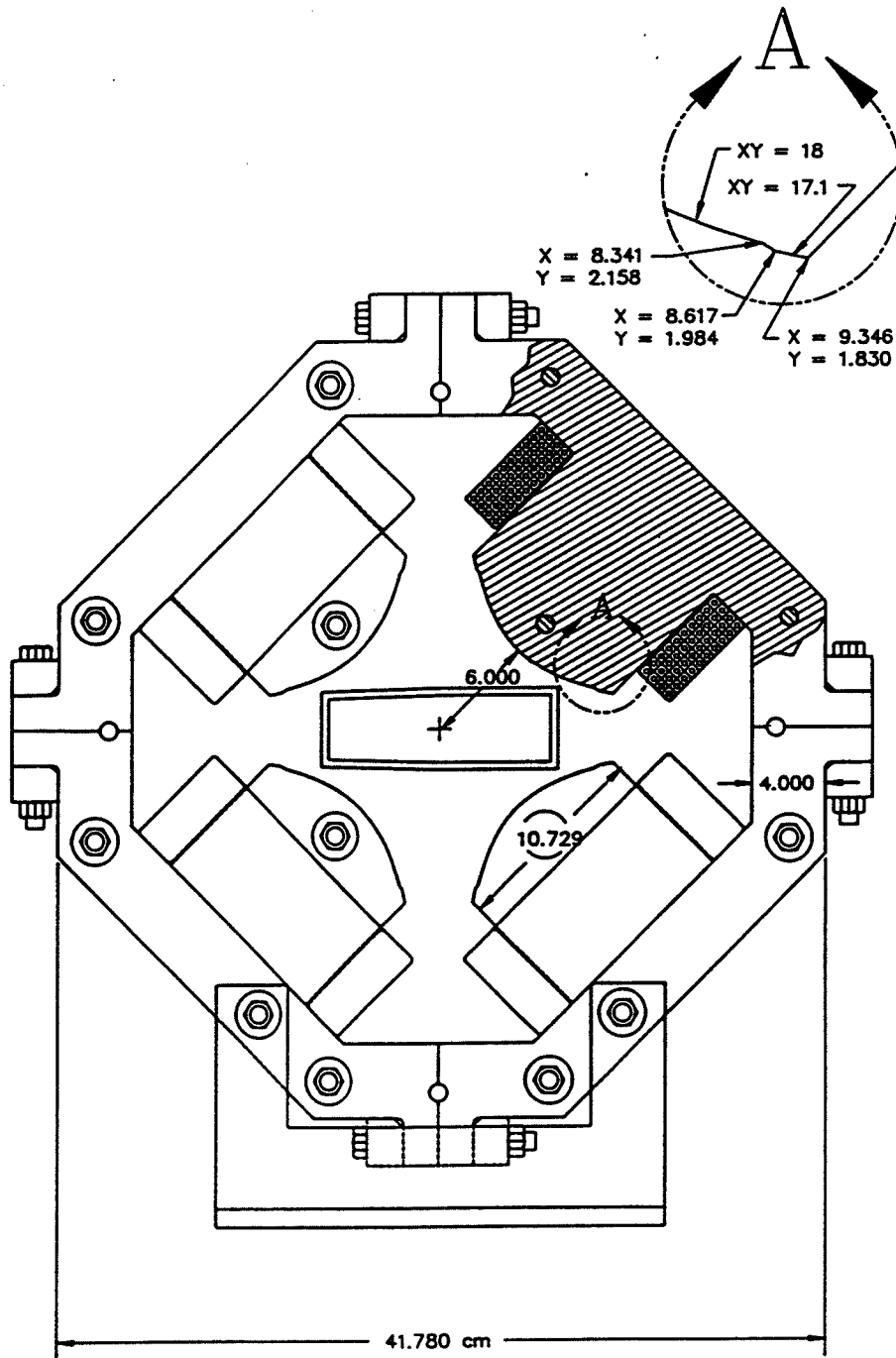


Figure II.10.2A-9
End view of the PAR quadrupole magnet.

II. 10. INJECTION SYSTEM

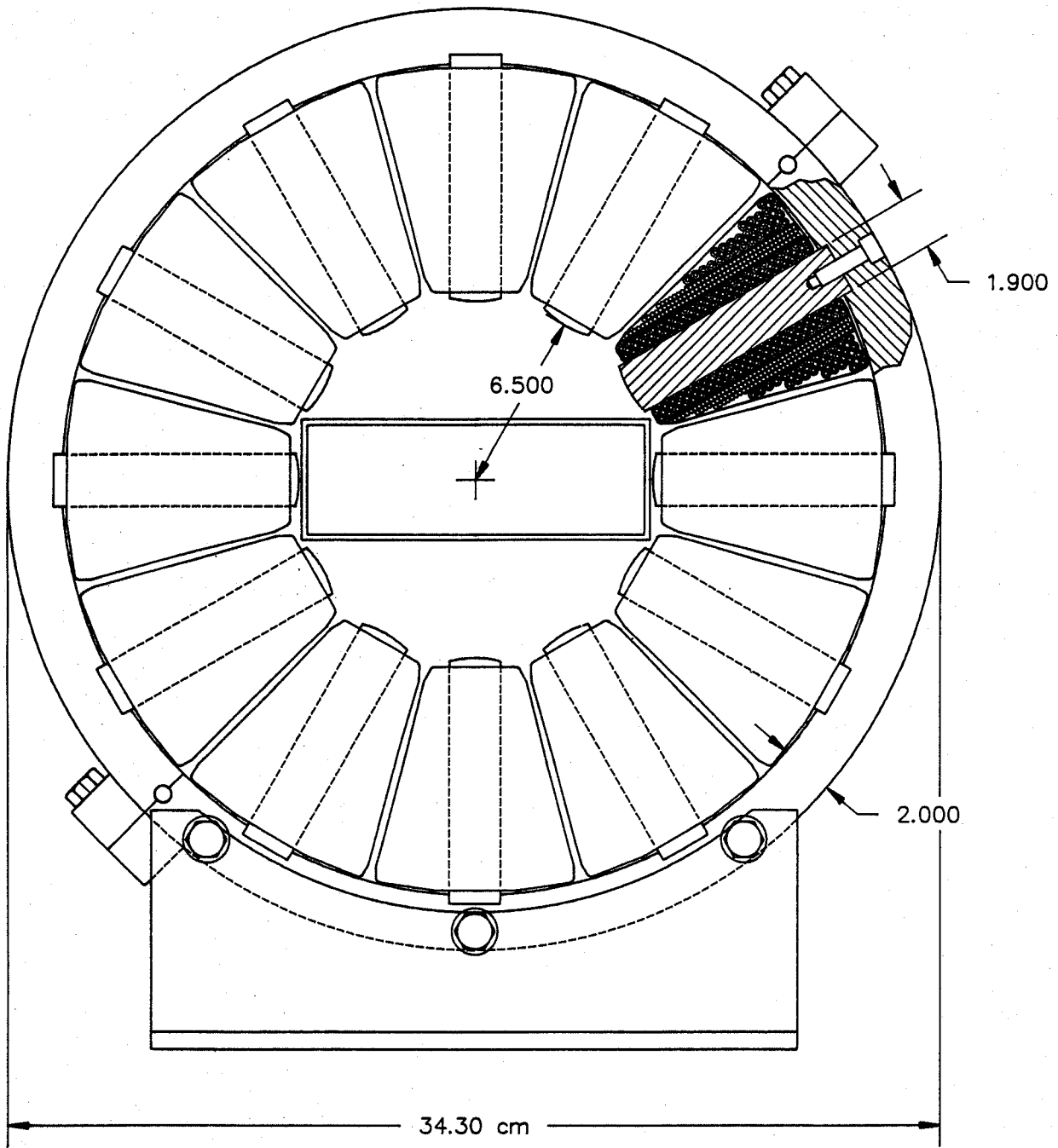


Figure II.10.2A-10
End view of the PAR multipole magnet.

II. 10. INJECTION SYSTEM

Table II.10.2A-3 [Additional Material]

Field Qualities of PAR Magnets

Magnet	Relative Deviation (10^{-4})	Multipole Coefficients, b_n (10^{-6} cm $^{-n}$)
Bending Magnet	$\left(\frac{\Delta G}{G_o}\right) = \begin{matrix} +30 \\ -20 \end{matrix}$	$b_1 = -5891$ $b_2 = 3.7$ $b_3 = 0.7$
Quadrupole	$\left(\frac{\Delta G}{G_o}\right) = \begin{matrix} +1 \\ -15 \end{matrix}$	$b_5 = 0.6$ $b_9 = 0.002$
Multipole: Sextupole	$\left(\frac{\Delta K}{K_o}\right) = \begin{matrix} +90 \\ -300 \end{matrix}$	$b_8 = -0.9$ $b_{14} = -0.0014$
Multipole: H&V Dipole	$\left(\frac{\Delta B}{B_o}\right) = \begin{matrix} +30 \\ -0.5 \end{matrix}$	$b_2 = 210$ $b_3 = 3.4$

10.2A.9.1.3 Kicker/Bumper Magnets

Three fast kicker/bumper magnets are required. They are 0.35 m long, with identical cross sections. The field is 0.06 T, the rise time is 65 ns, the flat-top time is 80 ns, and the fall time is 90 ns. The gap region is 110 mm wide and 53 mm high. Each magnet has two coils, and the inductance of each is 458 nH.

The cross section of the magnet is shown in Fig. II.10.2A-11. The design parameters for this magnet are listed in Table II.10.2A-6.

10.2A.9.2 Magnet Supports [New Section]

10.2A.9.2.1 Dipole and Quadrupole Magnet Supports

One dipole magnet and two quadrupole magnets are mounted on a common rigid girder. The dipole magnet is first mounted to the rigid girder, and its magnetic center is

II. 10. INJECTION SYSTEM

Table II.10.2A-4
Parameters for Principal PAR Magnets

Parameter	Dipole				Multipole		
	Main	Trim	Quadrupole	Sextupole	Dipole Correction*		
Number Required	8	8	16	10	20		
Strength at 450 MeV	1.47 T	0.075 T(max)	4.0 T/m(max)	10 T/m ² (max)	0.02 T(max)		
Field Index	-0.6						
Bending Radius	(m) 1.019						
Effective Length	(m) 0.8	0.8	0.25	0.2	0.2		
Gap Height or Diameter	(mm) 45	45	120	130	130		
Total Mass	(kg) 3000		154	90	-		
Conductor Height	(mm) 9.7	2.0	4.8	1.5	3.2		
Width	(mm) 9.7	2.0	4.8	1.5	3.2		
Hole Diameter	(mm) 5.3	solid	2.6	solid	1.6		
Number of Turns per Pole	72	120	40	118	208		
Total Inductance	(mH) 106	229	16	116	0.6		
Total Resistance	(mΩ) 90	2874	128	3115	191		
Time Constant	(ms) 1178	80	125	37	3		
Supply Current	(A) 379	13.2	143	3.8	19.4		
Current Density in Coil	(A/mm ²) 2.8	2.4	4.1	0.4	1.6		
Voltage	(V) 34	38	18	12	3.7		
Power	(kW) 12.9	0.5	2.6	0.05	0.07		
Cooling Circuits per Magnet	6	-	4	-	2		
Total Water Flow	(gal/min) 3.2	-	0.5	-	0.06		
Water Pressure Drop	(psi) 50	-	50	-	50		
Water Temp. Rise	(°C) 16	-	22	-	5		

*10 horizontal and 10 vertical.

II. 10. INJECTION SYSTEM

Table II.10.2A-5

Parameters for PAR Septum Magnet

Min. Septum Thickness (mm)	2.0
Peak Field (T)	0.75
Physical Length (m)	0.5
Effective Length (m)	0.4
Gap Height (mm)	20.0
Gap Width (mm)	70.0
Number of Primary Turns	3
Total Inductance (mH)	0.006
Total Resistance (m Ω)	2.5
Peak Supply Current (A)	4018
Peak Power (kW)	445
Average Power (kW)	0.34

aligned with four vertical 2-ton jacks. The two quadrupole magnets are then aligned with the common magnetic center by means of simple adjustable supports on the girder.

10.2A.9.2.2 Multipole and Septum Magnet Supports

The multipole and septum magnets are rigid, welded structures with sufficient stiffness to be supported directly. Each magnet has its own stand and a simple adjustable support that is used to align it with the common magnetic center.

II. 10. INJECTION SYSTEM

Table II.10.2A-6

Design Parameters for Kicker/Bumper Magnets

Item	Value
Rise Time (ns)	65
Flat-Top Time (ns)	80
Fall Time (ns)	90
PFN* Voltage (kV)	35.4
PFN Charge Current (mA)	58.6
PFN Cables (m)	4 X 12.7 in parallel
Cable Type	YR-10914
Cable Impedance (Ω)	14
Configuration	1 cell, 2 half-turn coils
Peak Field (T)	0.0600
Peak Magnet Current (kA/coil)	2.531
Magnet Inductance (nH/coil)	458
Charge Power Dissipation (W)	870 (60-Hz CW) 29 (2-Hz CW)
Load Power Dissipation (W)	435 (60-Hz CW) 15 (2-Hz CW)
per Coil (W)	
Magnet Gap Dimensions	
Height (cm)	5.3
Width (cm)	11.0
Length (m)	0.35
Ferrite Type	Ceramic Magnetics Type CMD-5005

*Pulse-forming network.

10.2A.9.3 Power Supplies [New Section]

10.2A.9.3.1 Introduction

A stability of 50 ppm is the design goal for the main bending and focusing magnets (dipoles and quadrupoles). For the correction magnets, the requirements are less stringent; these requirements range from 300 ppm for sextupoles and orbit trim windings in the main dipoles to 400 ppm for dipole correction magnets. All power supplies have an upper limit of operation corresponding to 8% higher than 450 MeV.

The main bending magnets are connected in series and fed from a single 140-kW, 12-phase power supply connected to the 480-V power line. The quadrupole magnets are

II. 10. INJECTION SYSTEM

grouped in four families of four magnets each. The sextupole windings of six of the 10 multipole magnets are connected in two families: one family of four magnets connected to one power supply, and the other family of two magnets connected to the other power supply.

The power supplies for dipole and quadrupole magnets and the sextupole windings of the multipole magnets are unidirectional. The correction dipole windings of the multipole magnets are bipolar. Table II.10.2A-7 lists the power supplies, their output ratings, and other performance specifications. The current stability and reproducibility include effects due to normal power-line fluctuations, load variations, component drifts, and temperature coefficients over the range from 10 to 40° C.

10.2A.9.3.2 Main Dipole and Quadrupole Power Supplies

The main dipole magnets are connected in series and energized from a 12-phase dc power supply. The voltage to ground of ± 165 V causes current leakage through the cooling water paths. Magnet field imbalances caused by these leakage currents are compensated by the dipole trim coils. The magnet cooling-water inlet temperature is regulated to $32^{\circ}\text{C} \pm 1.1^{\circ}\text{C}$. The corresponding dimensional changes of the dipole (~ 12 ppm/ $^{\circ}\text{C}$) do not affect f_{Bd} ; the changes in gap height are compensated by an equivalent change in length.

The dipole and quadrupole power supplies are of the same type and are commercially available. Figure II.10.2A-12 shows a typical power circuit configuration. The delta- and wye-connected secondaries of the rectifier transformer feed two series-connected silicon-controlled-rectifier (SCR) bridges. The 12-phase raw dc output is filtered by a ground-symmetrical, damped passive LC-filter to attenuate the fundamental 720-Hz ripple to the required levels. In this configuration, the DAC-programmed regulator controls, by means of rectifier phase control, the power-supply output.

10.2A.9.3.3 Sextupole Power Supplies

Two identical power supplies are used to energize the sextupole windings in the multipole magnets. Due to the low power (2200 W), linear amplifiers are used. Such amplifiers are commercially available.

10.2A.9.3.4 Correction and Trim Dipole Power Supplies

A total of 28 independently controlled power supplies are provided with ratings from 100 to 600 W. The need for smooth control of the current through zero dictates the use of bipolar linear amplifiers with push-pull output stages. Such amplifiers are commercially available.

Table II.10.2A-7 [Additional Material]

Magnet Power Supplies for PAR

Magnet Circuit	No. of P.S.	Rating @450 MeV			$\Delta I/I_{\max}$				Resolution of Reference (bits)
		I (A)	V (V)	P (kW)	Stability	Reproducibility	Current Ripple	Tracking Error	
Dipole (8 in series)	1	412	326	134.4	$\pm 5 \times 10^{-5}$	$\pm 1 \times 10^{-4}$	$\pm 2 \times 10^{-4}$	$\pm 5 \times 10^{-4}$	15
Dipole Trim Coils	8	13.2	42	0.6	$\pm 3 \times 10^{-4}$	$\pm 6 \times 10^{-4}$	$\pm 1 \times 10^{-3}$	$\pm 4 \times 10^{-3}$	12
Quadrupole (4 in series)	4	143	81	11.5	$\pm 5 \times 10^{-5}$	$\pm 1 \times 10^{-4}$	$\pm 2 \times 10^{-4}$	$\pm 5 \times 10^{-4}$	15
Multipole (12-pole)									
Sextupole (winding) (4 in series)	1	3.8	52	0.2	$\pm 1 \times 10^{-4}$	$\pm 2 \times 10^{-4}$	$\pm 3 \times 10^{-4}$	$\pm 5 \times 10^{-4}$	14
Sextupole (winding) (2 in series)	1	3.8	26	0.1	$\pm 1 \times 10^{-4}$	$\pm 2 \times 10^{-4}$	$\pm 3 \times 10^{-4}$	$\pm 5 \times 10^{-4}$	14
Dipole (winding) V-Correction	10	19.4	4	0.1	$\pm 3 \times 10^{-4}$	$\pm 6 \times 10^{-4}$	$\pm 1 \times 10^{-3}$	$\pm 4 \times 10^{-3}$	12
Dipole (winding) H-Correction	10	19.4	4	0.1	$\pm 3 \times 10^{-4}$	$\pm 6 \times 10^{-4}$	$\pm 1 \times 10^{-3}$	$\pm 4 \times 10^{-3}$	12

II. 10. INJECTION SYSTEM

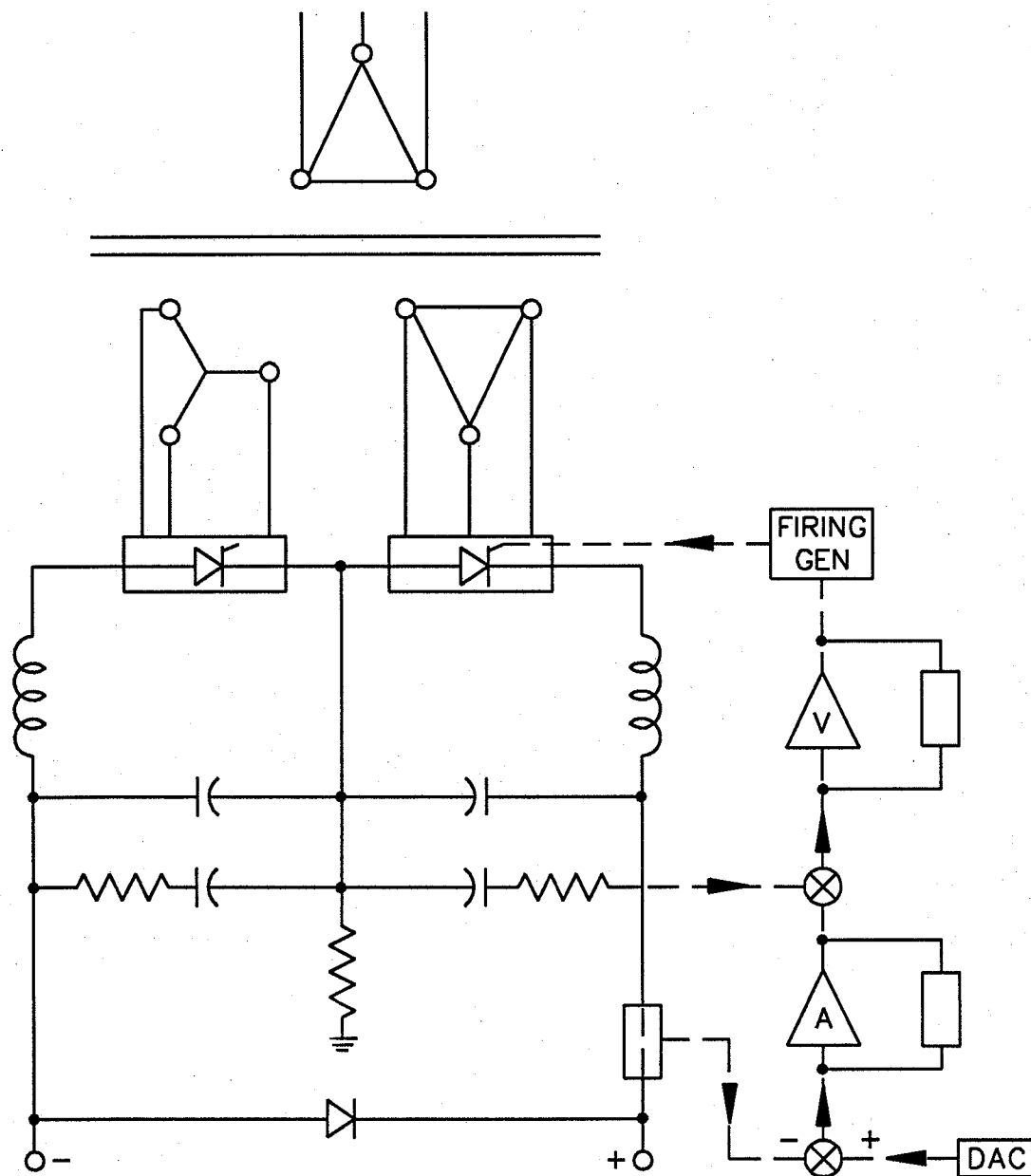


Figure II.10.2A-12
Dipole Power Supply for PAR.

II. 10. INJECTION SYSTEM

10.2A.9.3.5 Septum Magnet Power Supply

For the pulsed transformer septum magnet, the primary pulse is provided by a capacitor discharge power supply. This supply produces a pulse that is approximately a half-sine-wave with a base width of about 1/3 ms; its peak current is repeatable within $\pm 0.05\%$. The septum steel is reset by a half-sine-wave pulse of reverse polarity a few milliseconds later.

10.2A.9.3.6 Kicker/Bumper Magnet Power Supplies

Three identical fast kicker/bumper magnets are used in the injection/ extraction scheme. The first and second kicker magnets are pulsed for injection at a 60-Hz rate, and the third kicker/bumper magnet is pulsed for extraction at a 2-Hz rate. Each magnet has a separate power supply. A regulated high-voltage power supply charges the pulse-forming network (PFN) and maintains that charge. As shown in Fig. II.10.2A-13, the PFN discharges through the magnet coils to produce an 80-ns flat-top pulse when the thyatron is triggered. Two load resistors are used for each magnet.

10.2A.10 PAR Vacuum System [New Section]

10.2A.10.1 Vacuum Chamber

The vacuum chambers for the PAR are fabricated from 2-mm-thick 304 stainless steel. The chamber cross section is essentially rectangular with 4.0 cm x 12.4 cm outside dimensions. Flanges, position monitors, bellows, etc. are attached by conventional welding techniques and then leak-tested.

10.2A.10.2 Pumping

Ion pumps are the primary pumping source to maintain an average pressure of 1×10^{-9} Torr or better in the 30-m-circumference ring. The pumping system consists of 400 L/s ion pumps located in the injection/extraction area and 60 L/s ion pumps located in the ring where the chamber is conductance-limited. Preconditioning of the chambers includes chemical cleaning and bakeout and, if necessary, glow-discharge cleaning.

Pump-down from atmosphere is accomplished by using oil-free mechanical pumps to a pressure of 50 Torr, after which sorption pumps reduce the pressure to less than 10^{-2} - 10^{-3} Torr. Turbomolecular pumps further reduce the pressure to ion-pump starting pressure.

II. 10. INJECTION SYSTEM

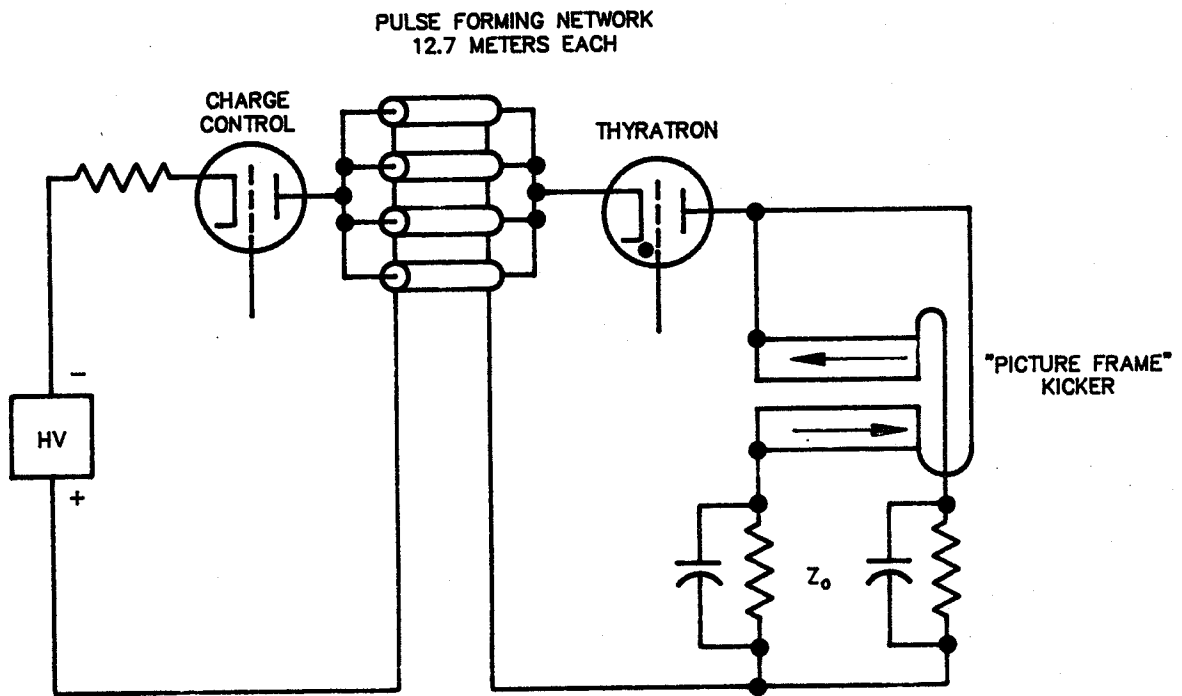


Figure II.10.2A-13
Power supply for kicker/bumper system.

II. 10. INJECTION SYSTEM

10.2A.10.3 System Monitoring

Ion gauges are distributed around the ring for pressure measurement. Ion pump current can also be monitored. Isolation valves on each of the long straight sections permit venting part of the ring without affecting the vacuum in the remainder of the ring.

10.2A.11 PAR RF Systems [New Section]

10.2A.11.1 Introduction

There are two rf systems in the PAR. One operates at 9.8 MHz, and the other at 118 MHz. Each consists of two cavities, two rf amplifiers, and associated control circuitry. The control system also synchronizes operation with the linac during injection and with the injector synchrotron during extraction.

The linac beam is injected into the 9.8-MHz bucket. The synchronous phase angle is about 175° to compensate for radiation loss while the bunch is damped. When the bunch is damped sufficiently, the 118-MHz system is turned on, and further damping occurs until extraction.

The 118-MHz system is deactivated during the first 450 ms of the 500-ms PAR cycle to prevent self-bunching of the beam at 118 MHz.

10.2A.11.2 First-Harmonic (9.8-MHz) Cavity

The cavity is a folded quarter-wavelength, coaxial re-entrant type that is capacitively loaded to resonate at a frequency of 9.8 MHz. Figure II.10.2A-14 shows a half section of the cavity, and the parameters are listed in Table II.10.2A-8.

The cavity is made of aluminum with a ceramic cylinder across the accelerating gap for vacuum isolation. Only the beam tube is evacuated, keeping the vacuum system cost low and avoiding multipactoring problems in the bulk of the cavity. Fine tuning will be done by a capacitive adjustment located at the loading capacitor.

The power amplifier is located outside the shield wall but close enough to the cavity to minimize resonances in the transmission line.

Since beam loading is incremental, with 24 linac bunches injected over a 400-ms period, a modest feedback control system keeps the cavity voltage constant and the power amplifier load impedance real. Programming of the power amplifier input voltage and cavity fine tuning is included to offset the transient from each injected bunch (see Fig. II.10.2A-15). Feed-forward techniques can be added if necessary.

II. 10. INJECTION SYSTEM

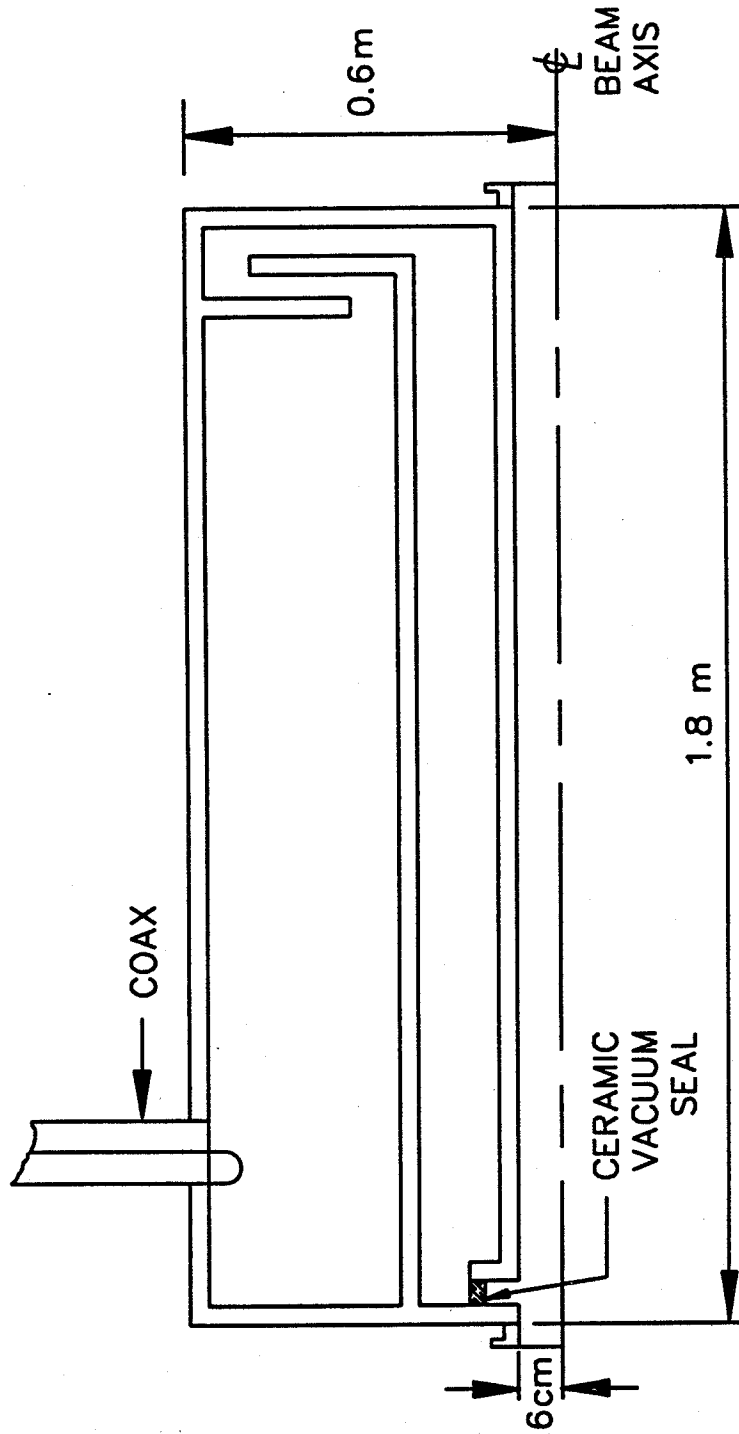


Figure II.10.2A-14
Schematic of first-harmonic (9.8-MHz) cavity, half section.

II. 10. INJECTION SYSTEM

Table II.10.2A-8

PAR Cavity Parameters

Parameter	First-Harmonic	Twelfth-Harmonic
f (MHz)	9.8	117.6
V (kV)	40	30
Type	$\lambda/4$, loaded	$\lambda/2$
Length (m)	1.8	0.9
Z_0 (Ω)	50	50
Power (kW)	4.70	0.222
R_s ($k\Omega$)	170	2020
Q	7,630	25,300
τ ($2Q/\omega$) (μs)	248	68

No high-order-mode suppression is provided, although ports are available and could be used for mode-damping circuits.

10.2A.11.3 Twelfth-Harmonic (118-MHz) Cavity

The twelfth-harmonic cavity is a half-wavelength coaxial cavity (see Fig. II.10.2A-16) slightly foreshortened by the accelerating gap capacitance. The cavity is made of aluminum with the vacuum seal at the accelerating gap to minimize the vacuum volume and multipactoring difficulties. The cavity is tunable over a range of 1 MHz.

The cavity is electronically adjusted during operation of the 9.8-MHz cavity so as not to interact with the beam, since only the fundamental cavity is used during the injection time of the PAR cycle. PIN diodes are used to connect resistors into the cavity to lower the gap impedance by at least a factor of ten. If needed, the resonance is shifted away from 118 MHz by similar PIN diode switches connecting a reactance into the cavity. Also, higher-order-mode suppression is implemented so that the beam is undisturbed during operation of the cavity.

When the cavity is switched from a passive (imitating a beam pipe) to an active state, beam loading is rapid. A fast tuning and voltage control system, including feed-forward techniques, is used. Large induced voltages (224 kV) are avoided with programmed tuning. Figure II.10.2A-17 shows the control circuit for the cavity with both feedback signals from the cavity and feed-forward signals from a beam monitor. The

II. 10. INJECTION SYSTEM

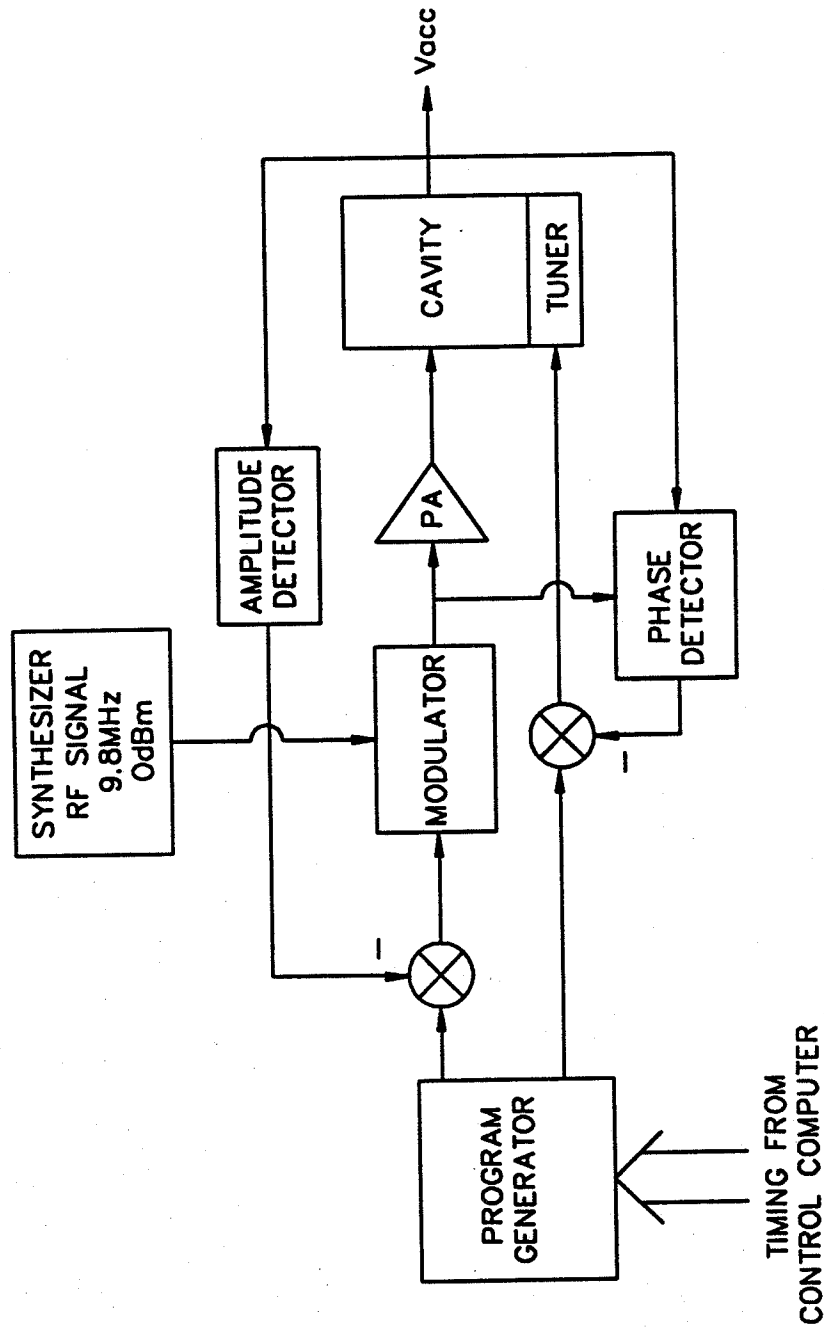


Figure II.10.2A-15
9.8-MHz rf system block diagram showing program generator.

II. 10. INJECTION SYSTEM

amount of circulating beam controls the program signals to the power amplifier and to the tuning device, so that as the cavity is turned on for the last 50 ms of the PAR cycle, the accelerating voltage has the correct phase with respect to the 9.8-MHz bucket and the power amplifier sees a real load. The program can be a learning (adaptive) program to monitor the feedback error signals and adjust the program to minimize the errors. This correction can be done in several ways: over many PAR cycles, using only the last PAR cycle, or using a weighted running average. Using a correction signal improves the operation of the cavity; thus, for a given tolerance on cavity parameters, the feedback loop dynamic range and gain can be smaller.

The unloaded shunt impedance of the cavity is $2.0 \text{ M}\Omega$ and the maximum twelfth-harmonic beam current is 112 mA, so the maximum induced voltage without compensation due to the beam is 224 kV. The rf amplifier produces a 30-kV accelerating voltage, and the total current without compensation would cause the voltage to be 82.4° out of phase with the empty 118-MHz buckets and the 9.8-Hz bucket. Since only 222 W is needed to power the empty cavity, resistive loading is added to the cavity to lower the shunt impedance and reduce the phase shift between beam current and generator current. This makes the programming and feedback systems less sensitive to variations in beam loading and increases the stability of the feedback system.

The power amplifier is located outside the shield wall, and power is fed to the cavity via a coaxial cable. This is a 2-kW amplifier (1600 for resistive loading). If beam and feedback control circuitry work well enough, the resistive loading may be removed. If rf feedback is needed, these amplifiers could be mounted on the cavity to minimize phase delay at 118 MHz.*

10.2A.11.4 Synchronization and Frequency Control

Since the rotation frequency, 9.8045 MHz, of the PAR is not an exact multiple of 60 Hz, the linac is triggered by the PAR control system at a nominal 60-Hz rate. This ensures that the subsequent linac beam pulses are in the same place in the bucket as the first beam pulse.

Similarly, the PAR is synchronized to the injector synchrotron rf at extraction so the bunch is correctly placed with respect to previous bunches in the 353-MHz buckets.

The 353-MHz frequency source is a synthesizer with direct digital synthesis (DDS) capability and a resolution of 0.1 Hz. The DDS allows phase continuity when switching frequencies so that no transient is present to disturb the stored beam. Switching is done by the control computer via a parallel bus. The correction signal is derived from the bunch signal in the storage ring. Two other synthesizers are referenced to the 353-MHz source, one for each of the PAR cavities (see Fig. II.10.2A-18).

* D. Boussard, "Control of Cavities with High Beam Loading," IEEE NS-32, No. 5 (Oct. 1985).

II. 10. INJECTION SYSTEM

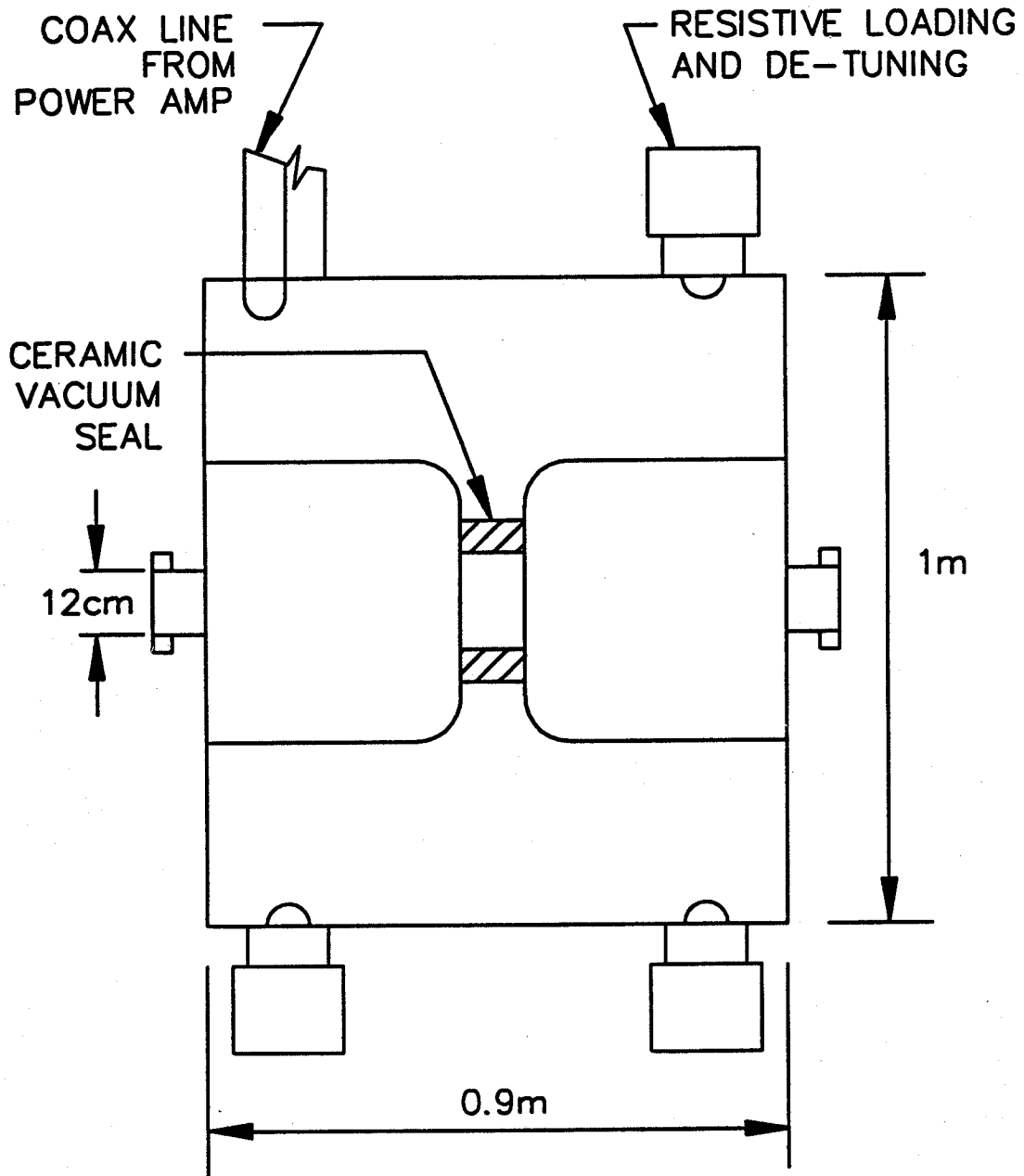


Figure II.10.2A-16
Schematic of twelfth-harmonic (118-MHz) cavity.

II. 10. INJECTION SYSTEM

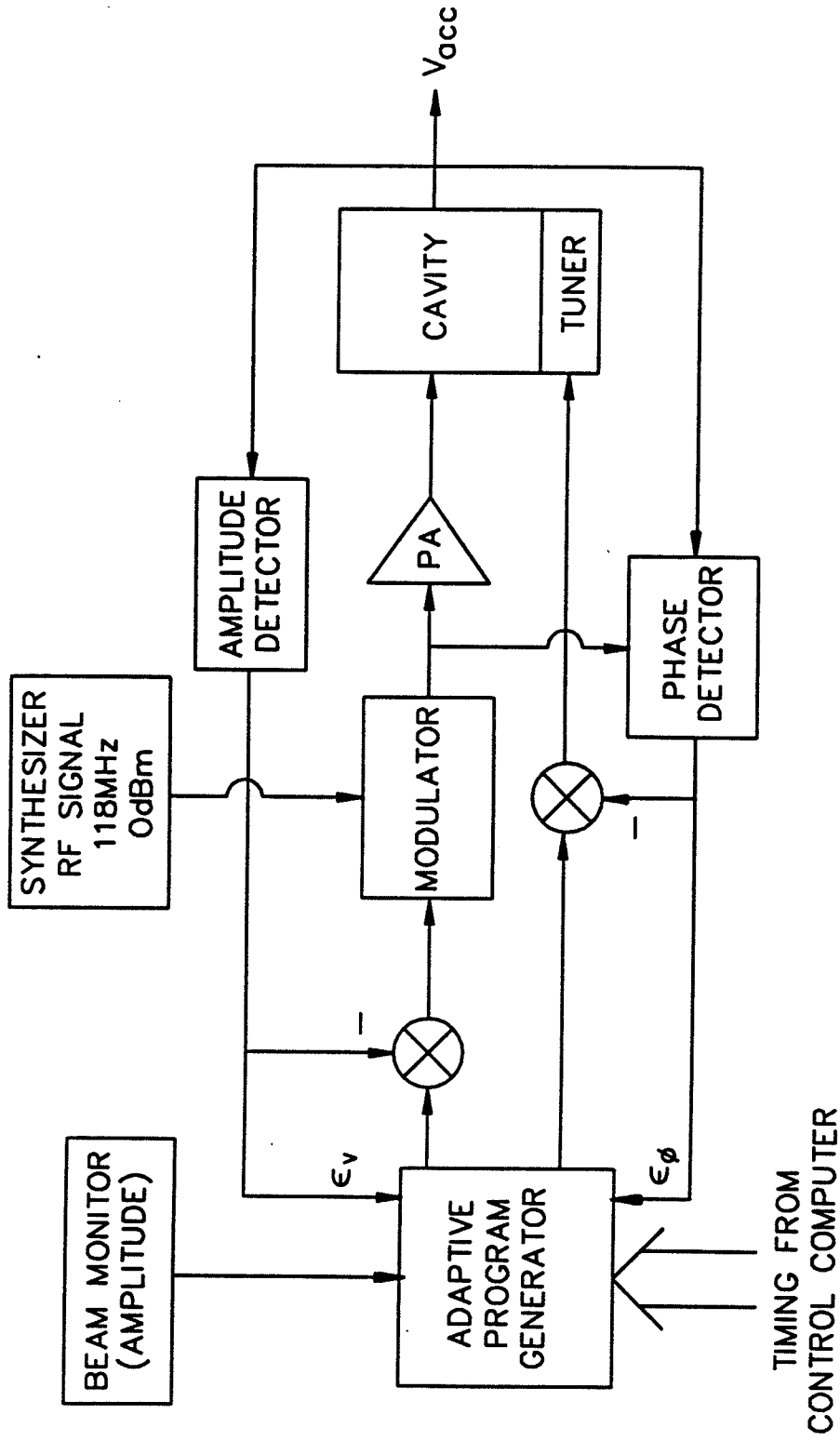


Figure II.10.2A-17
Twelfth-harmonic (118-MHz) rf system block diagram.

II. 10. INJECTION SYSTEM

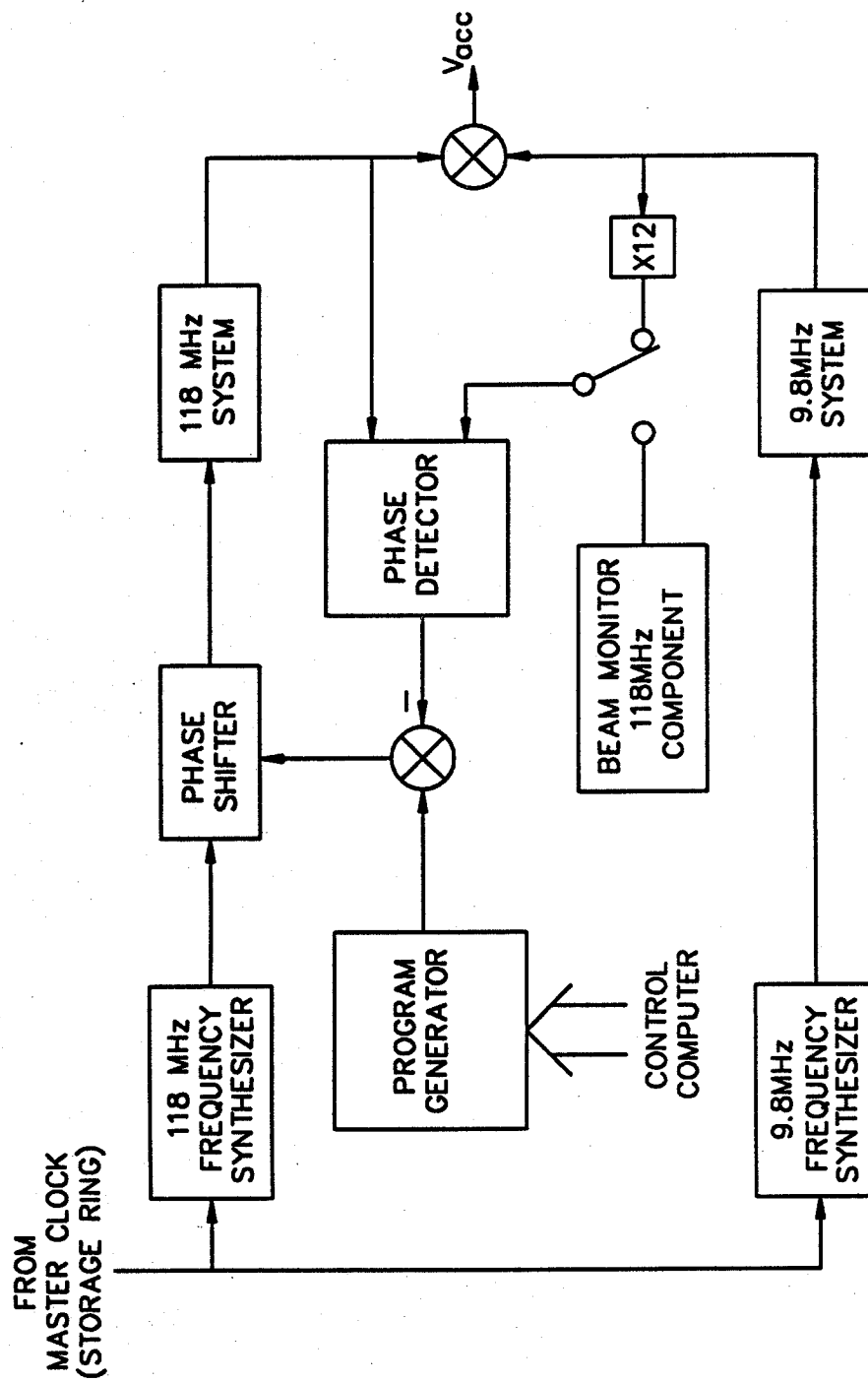


Figure II.10.2A-18
PAR rf systems showing synchronization scheme.

II. 10. INJECTION SYSTEM

10.3 Injector Synchrotron

10.3.1 Introduction [Revision]

Due to the addition of the PAR, the repetition rate is changed from 1 Hz to 2 Hz, the number of bunches injected per synchrotron cycle is reduced from 8 to 1, and the low-frequency (39.22-MHz) system is removed.

Figure II.10.3-1 is revised.

10.3.3 Injector Synchrotron Performance [Revision]

The emittance of the injected beam is reduced from 1.1 mm²mrad to 0.37 mm²mrad due to the PAR; therefore, the vacuum-chamber horizontal width is more than adequate.

The circulating beam current in the synchrotron is increased from 1.7 mA to 5.0 mA.

The addition of the PAR allows direct injection into the 353-MHz rf bucket without using the 39.22-MHz rf cavity. The bunch length, σ_{τ} , of the beam from the PAR is 0.29 ns. The energy spread, σ_E/E , is 0.4×10^{-3} . With 100 kV of applied voltage, the relative bucket height, $\Delta E/E$, is $\pm 2.6 \times 10^{-3}$. This bucket easily contains the injected beam pulse.

The replacement table for the injector synchrotron parameters is Table II.10.3-2.

10.3.4.3 Injector Synchrotron Ring Magnet Power Supplies [Replacement]

The ring magnets of the injector synchrotron are cycled, as shown in Fig. II.10.3-9(a) for the dipole magnets. There is a 1-ms injection time, a 249-ms rise and fall time, and a 1-ms flat top. The repetition rate is 2 Hz. The tracking error, $\Delta I/I$, between the quadrupoles and dipoles is within $\pm 5 \times 10^{-4}$. With the relatively slow rate of rise and the 1.5-mm core laminations, eddy current effects in the iron are negligible. A general synchrotron current shape is shown in Fig. II.10.3-9(b).

A repeatable residual field will be attained after a long shutdown by pulsing the magnets at rated current for several minutes before the beam is injected. Table II.10.3-5 lists the power supplies for the ring magnet system and indicates their output characteristics and performance data. The current stability and reproducibility include the effects due to load variations, component drifts, and temperature coefficients over the range of 10 to 40°C, as well as line fluctuations. The current tracking error applies to the nominal acceleration ramp of 20 GeV/s. All the power supplies have an upper limit of 7.7-GeV operation.

II. 10. INJECTION SYSTEM

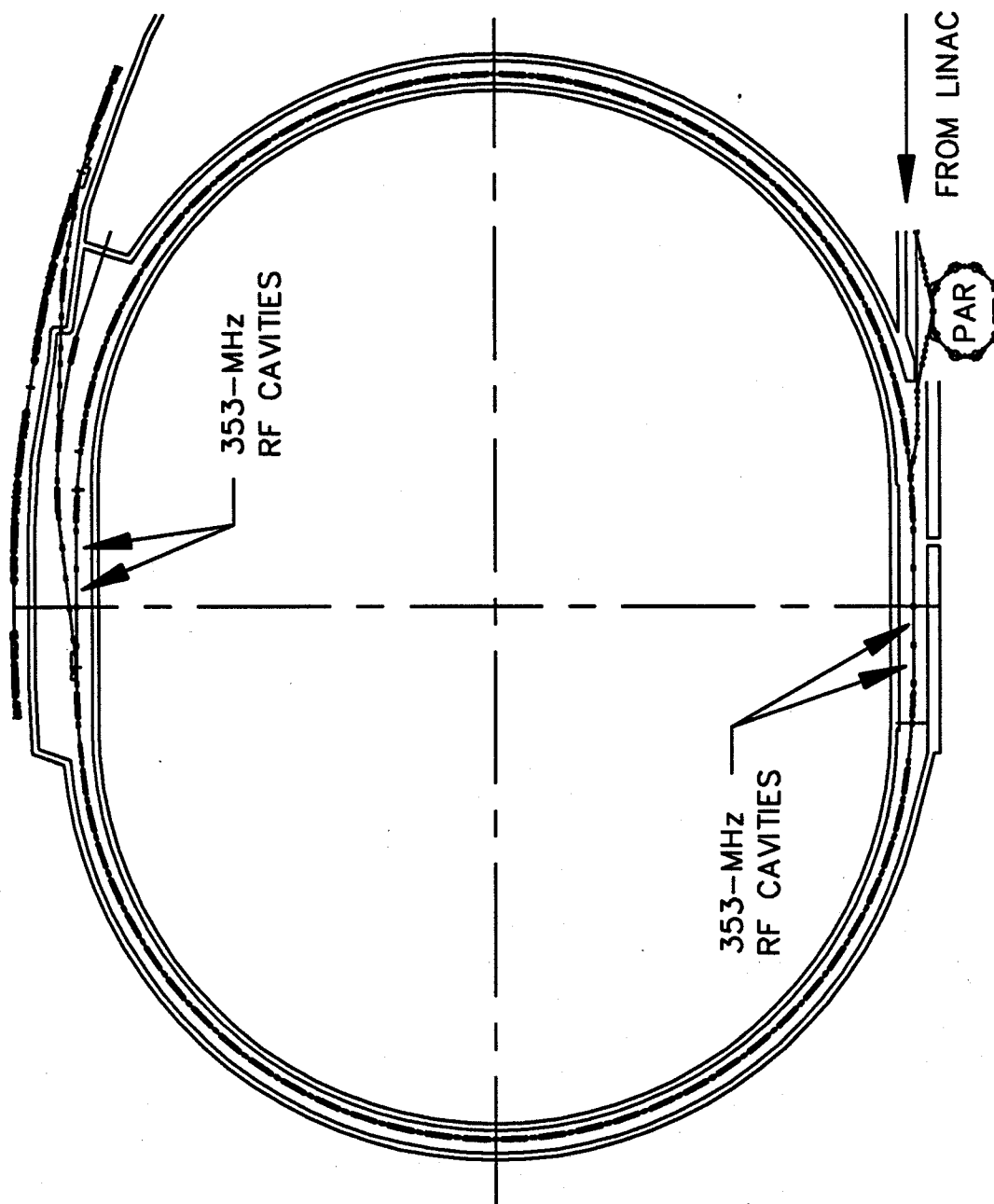


Figure II.10.3-1
Physical layout of the injector synchrotron.

II. 10. INJECTION SYSTEM

Table II.10.3-2 [Replacement]
Injector Synchrotron Parameters

Parameter	Value
Circumference (m)	366.923
Revolution Time (μ s)	1.224
Injection Energy (GeV)	0.45
Nominal Energy (GeV)	7.0
Maximum Energy (GeV)	7.7
Repetition Time (s)	0.5
Acceleration Time (s)	0.25
No. of Super Periods	2
No. of Cells	40
No. of Bending Magnets	68
Magnetic Field at: Injection (T)	0.0447
Extraction (T)	0.6960
Tunes, ν_x/ν_y	11.713/9.760
Transition Gamma	10.112
Betatron Damping Time at 7 GeV (ms)	2.7
Natural Emittance at 7 GeV (m)	1.321×10^{-7}
Energy Loss Per Turn at 7 GeV (MeV/turn)	6.33
Synchrotron Damping Time at 7 GeV (ms)	1.35
Bunch Length, σ_t , at 7 GeV (ps)	61
Energy Spread, σ_E/E , at 7 GeV	1×10^{-3}
Average Beam Current (mA)	4.8
Energy Gain per Turn (keV)	32.0
RF Parameters	
Frequency, f (MHz)	352.962
Harmonic Number, h	432
Voltage, V, at 7 GeV (MV)	8.3
Synchrotron Frequency, f_s , at 7 GeV (kHz)	21.3

II. 10. INJECTION SYSTEM

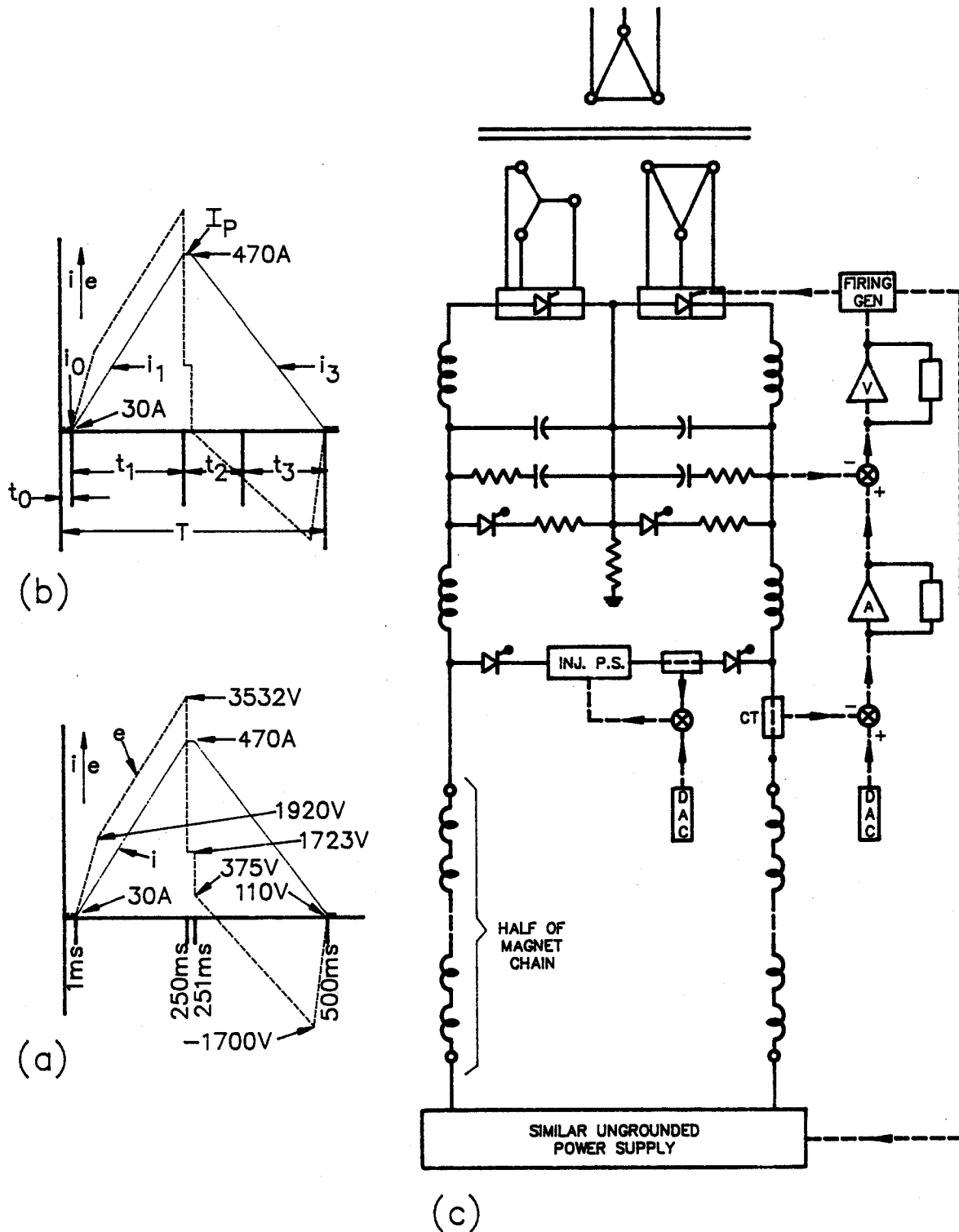


Figure II.10.3-9

Current and voltage shapes and block diagram of the dipole ring magnet power supply for the injector synchrotron.

II. 10. INJECTION SYSTEM

Table II.10.3-5 [Revision]

Magnet Power Supplies for Injector Synchrotron

Magnet	Number of Units	I_{\max} (A)	V_{\max} (V)	P_{\max} (kW)	P_{rated} (kW)	Reproducibility	$\Delta I/I_{\max}$			Ref. Resol. (bits)
							Current Ripple	Tracking Error		
Dipoles	2	470	+3532 -1700	1660	480	$\pm 1 \times 10^{-4}$	$\pm 2 \times 10^{-4}$	$\pm 5 \times 10^{-4}$	15	
Quadrupoles	2	645	+ 598 - 54	386	179	$\pm 1 \times 10^{-4}$	$\pm 2 \times 10^{-4}$	$\pm 5 \times 10^{-4}$	15	
Sextupoles	2	80	+ 159	13	7	$\pm 2 \times 10^{-4}$	$\pm 3 \times 10^{-4}$	$\pm 5 \times 10^{-4}$	14	
H Corr. Mag.	40	± 19	± 29	0.55	± 0.5	$\pm 1 \times 10^{-3}$	$\pm 1 \times 10^{-3}$	$\pm 4 \times 10^{-3}$	12	
V Corr. Mag.	40	± 15	± 40	0.50	± 0.5					

II. 10. INJECTION SYSTEM

10.3.4.3.1 Dipole Power Supply [Revision]

The current at injection is maintained for only 1 ms with the PAR, instead of 1/6 s. The main power supply output voltage is increased to 1920 V instead of 1458 V because of the faster ramp rate. The repetition rate is 2 Hz.

10.3.6 Injector Synchrotron RF System

10.3.6.1 Introduction [Replacement]

Since the injection is from the PAR and the bunches are shorter, the 39.22-MHz system is not required.

The injector synchrotron rf voltage is provided by four five-cell cavities operating at the storage-ring frequency of 353 MHz, the 432nd harmonic of the revolution frequency. Injection is into a stationary bucket with a peak voltage of 100 kV. The rf voltage increases to match the synchrotron radiation losses. At extraction, the rf voltage is 10.4 MV, and the synchrotron radiation loss per turn is 6.33 MeV. The energy gain per turn is negligible compared with the synchrotron radiation losses.

The four cavities are driven by a single 1-MW klystron identical to those used for the storage ring.

10.3.6.2 [Deleted]

10.3.6.3 [Deleted]

10.3.6.4 353-MHz RF Cavity [Replacement]

The cavities for the 353-MHz injector synchrotron rf system are essentially copies of the LEP/PEP^(11,12) five-cell, $\lambda/2$ resonant cavity. They have a 10.0-cm-diameter beamhole with a reentrant nose. The cell length is $\lambda/2$ (42.49 cm). The radius from the center line to the inside of the outer shell is 30.2 cm. The cells are magnetically coupled with two off-axis slots. The structure is loop-excited in the center cell using a post-coupler from the WR2300 waveguide. Tuners are provided in the two cells adjacent to the center cell. Vacuum separation between the waveguide and the cavity is provided by a cylindrical ceramic window surrounding the waveguide post. The cavity body is made from forged disks and forged seamless cylinders of copper. These are machined to close tolerances and electron-beam welded.

II. 10. INJECTION SYSTEM

A list of parameters for the cavity is given in Table II.10.3-8. The four 353-MHz cavities are divided into two groups and placed symmetrically on opposite sides of the synchrotron.

10.4 Transport and Injection into Injector Synchrotron

10.4.1 Transport Lines from Linac to PAR to Injector Synchrotron [Replacement]

The transport line between the linac and injector synchrotron is shown in Fig. II.10.4-1. The 46-m transfer line has two sections. The first section is a 24-m transport line between the linac and the PAR that includes the 9-m energy compressor system (ECS). The ECS consists of four 30° bending magnets and three quadrupoles designed to provide an achromatic transport producing the temporal dispersion necessary for energy compression in the ECS rf structure. The B1 magnet bends the beam by 0.2 rad. The section between B1 and the PAR injection septum (B2) is an achromatic cell in which the total horizontal phase advance is 360° . Figure II.10.4-2 shows the beta and dispersion functions for this section of the transport line. The maximum beta function is 20 m. This corresponds to an rms beam size of 4.7 mm.

The second section of the transport line to the injector synchrotron is that part between the PAR and the synchrotron. The 10-m line between the PAR septum and the

Table II.10.3-8 [Replacement]

Parameters for the Five-Cell, $\lambda/2$, 353-MHz Cavity

Bore-Hole Diameter	10.0 cm
Cell Length (center line to center line)	42.49 cm
Cell Length (inside of cell, wall to wall)	38.9 cm
Cell Radius	30.2 cm
Number of Cells	5
Active Length of Cavity	2.12 m
Total Length of Cavity	2.32 m
Shunt Impedance	26.1 M Ω /m
Average Accelerating Voltage	1.39 MV/m
rf Power @ 2.95 MV/cavity	156.9 kW

II. 10. INJECTION SYSTEM

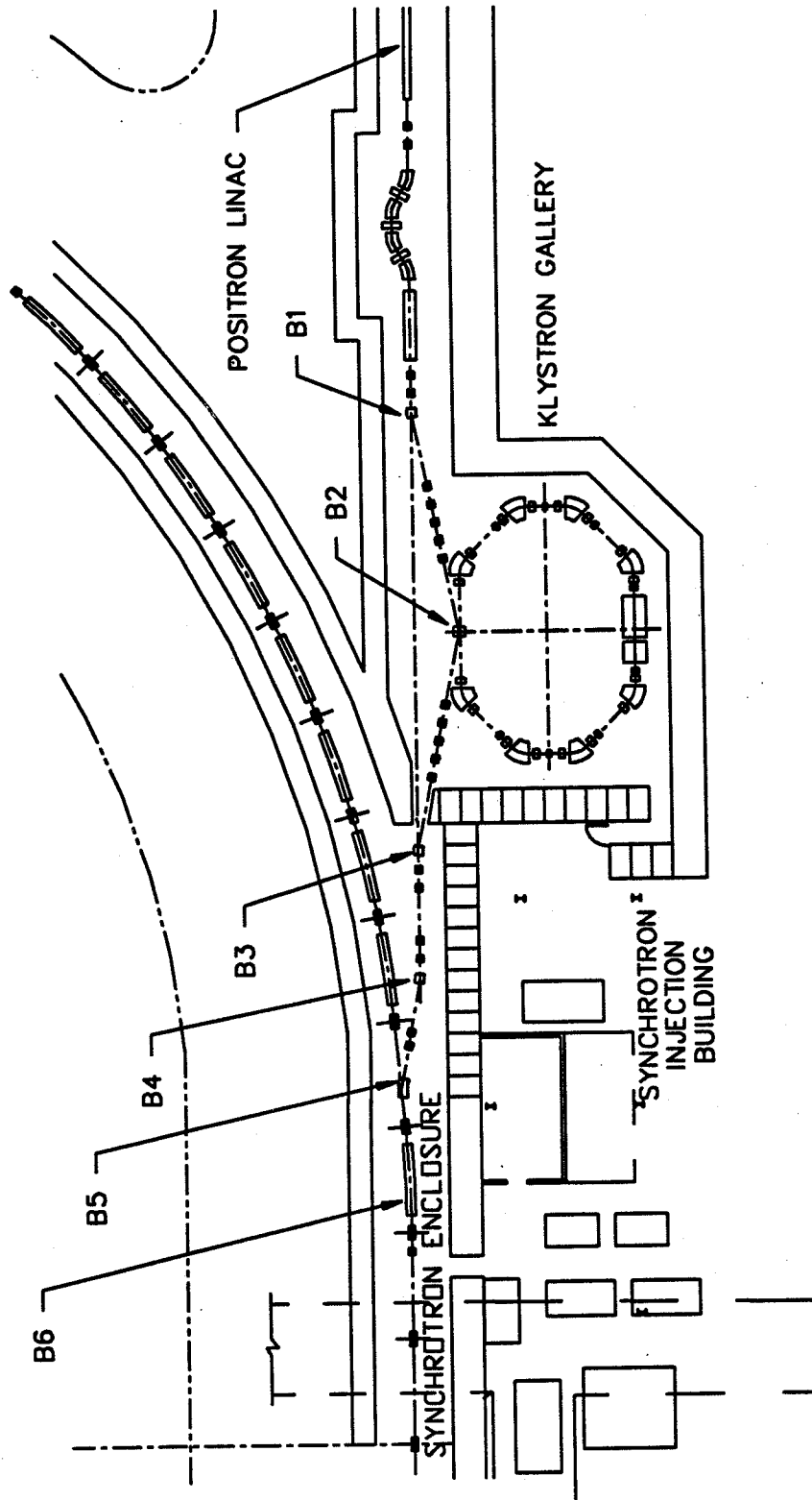


Figure II.10.4-1
Layout of linac-to-PAR-to-injector-synchrotron transport line.

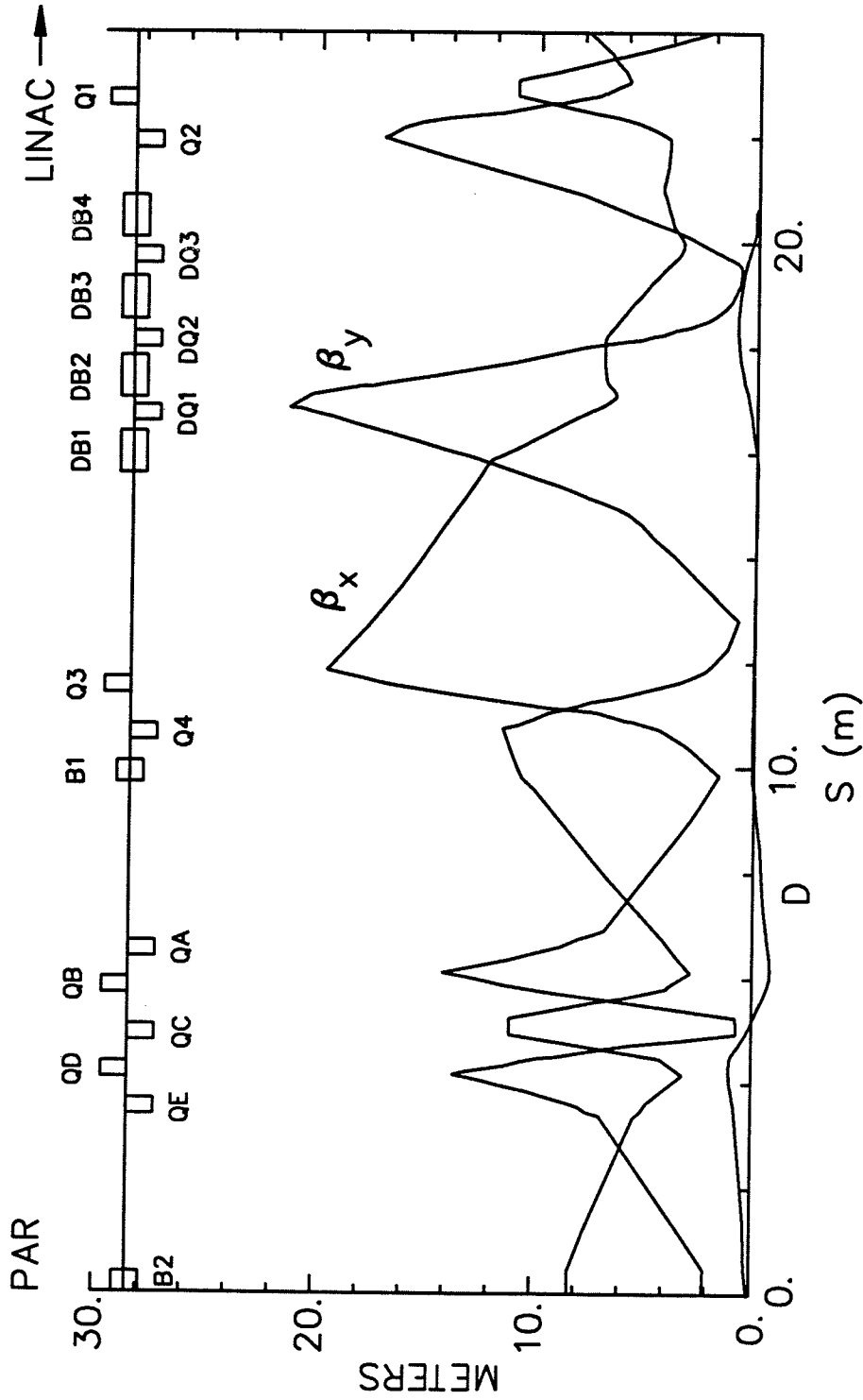


Figure II.10.4-2
Beta and dispersion functions for the linac-to-PAR transport line.

II. 10. INJECTION SYSTEM

B3 magnet is identical to the B1-B2 line in the linac-to-PAR transport system. The section between B4 and the synchrotron bending magnet B6 is an achromatic cell. The total horizontal phase advance between B4 and B6 is 180° . Fig. II.10.4-3 shows the beta and dispersion functions for this section of the transport line. The maximum beta function is 30 m. This corresponds to an rms beam size of 3.34 mm.

The magnet elements are listed in Table II.10.4-1.

10.4.2 Injection Geometry and Procedure [Replacement]

The injection geometry is shown in Figs. II.10.4-1 and II.10.4-3. Since the injection is into a stationary rf bucket of the synchrotron, the geometry is designed for on-axis injection using a kicker and a septum magnet. The septum magnet is located in the empty half cell of the dispersion suppressor cell, and the kicker is located about half a cell after the septum magnet. The integrated kicker strength is 0.0077 T·m. The injection trajectory and its associated beam envelopes are shown in Fig. II.10.4-4.

For each 0.5-s cycle of the injector synchrotron, a single bunch having a half length (σ_τ) of 0.29 ns is injected into one of the 353-MHz rf buckets. With 100 kV of applied voltage, the relative bucket height extends to $\pm 5.6 \times 10^{-3}$. Since the energy spread, σ_E/E , from the PAR is 0.41×10^{-3} , the synchrotron rf bucket easily accommodates the injected pulse. The kicker magnet is described in Sec. II.10.4.4.

10.4.3 Injection Septum Magnet [Revision]

Since the injector synchrotron receives one bunch of positrons from the PAR for each synchrotron cycle, the septum pulse rate is changed from 60 pps to 2 pps.

10.4.4 Injection Kicker Magnet [Revision]

The injection kicker magnet pulse can remain the same as stated in CDR-87, but it no longer needs to accommodate a 16.5-ns bunch length. The bunch length from the PAR is 1.8 ns.

10.5.1 Extraction Procedure and Geometry [Revision]

With the addition of the PAR to the positron injection system, a 1/3-s flat top in the injector synchrotron is no longer required at extraction. One bunch is accelerated in the synchrotron and extracted per cycle.

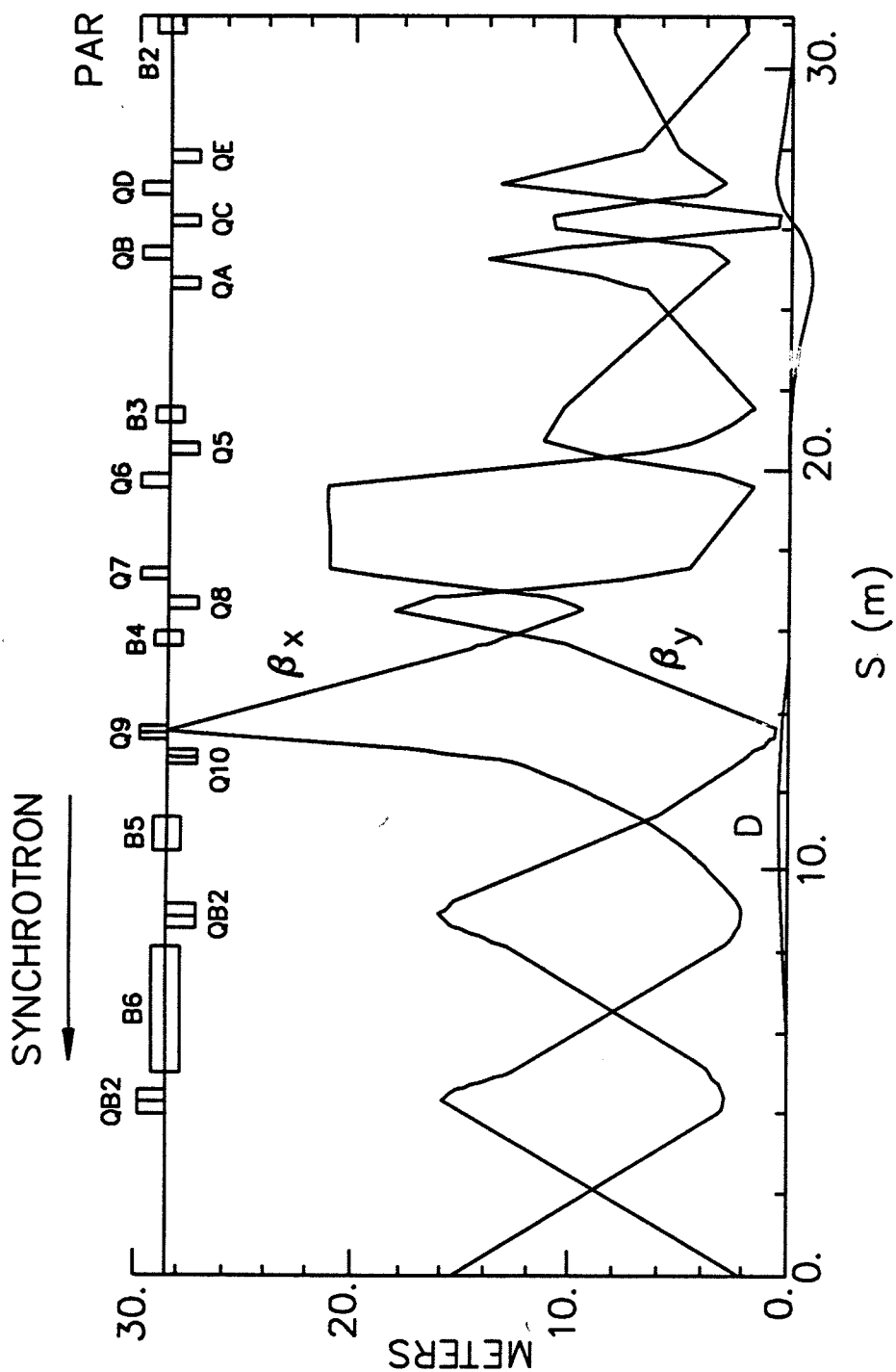


Figure II.10.4-3
Beta and dispersion functions for the PAR-to-injector-synchrotron transport line.

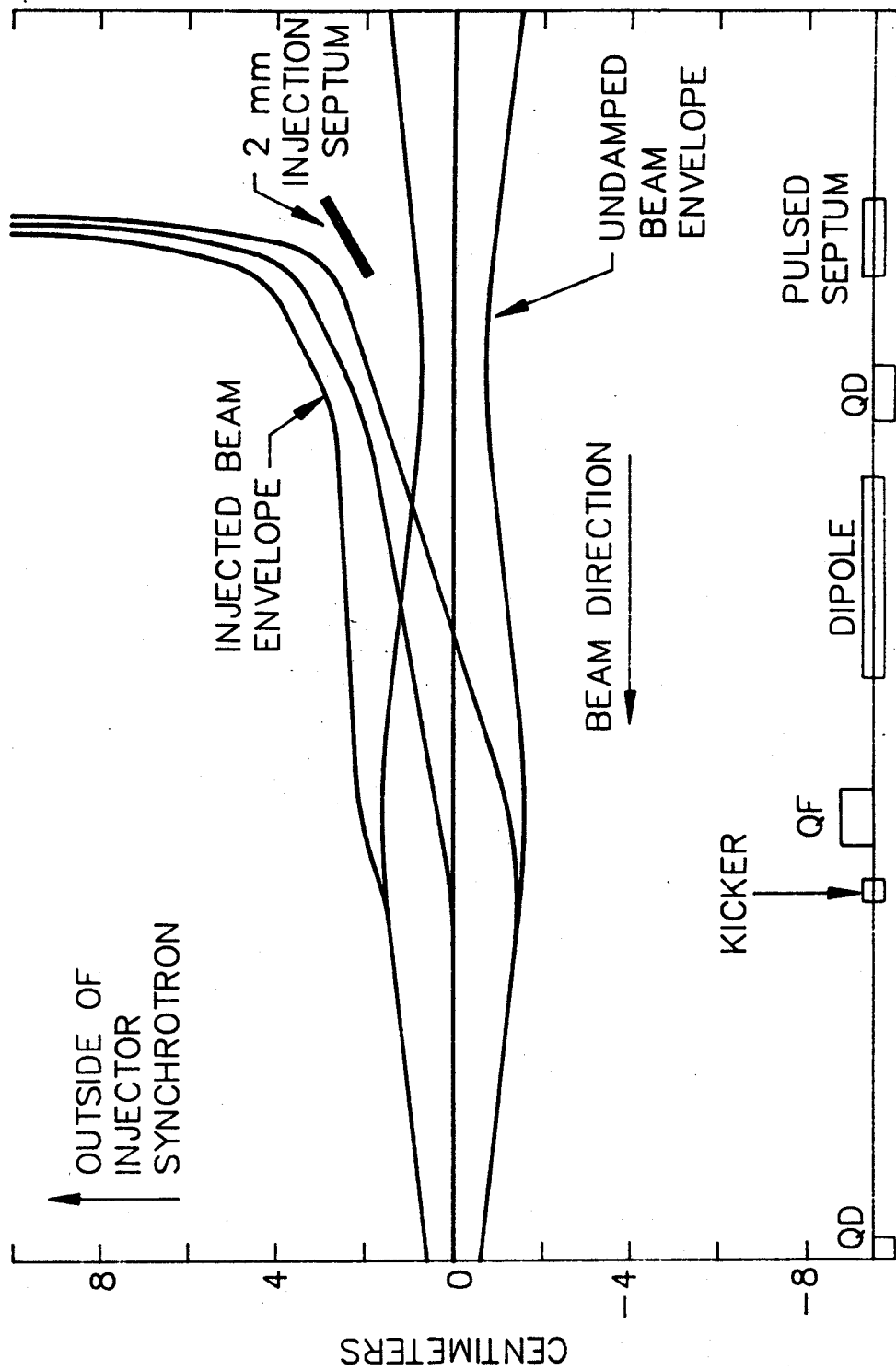


Figure II.10.4-4

Beam trajectory and $4\text{-}\sigma$ envelope for the injected and undamped beams in the injection region of the injector synchrotron. The 2-mm injection septum is 21 mm from the unperturbed orbit.

II. 10. INJECTION SYSTEM

Table II.10.4-1

Parameters for Magnets in Transport Line between
Linac and Synchrotron*

Parameter		Dipole	Quadrupole
Number Required		3	20
Field Strength at 450 MeV		0.75 T	9 T/m (max)
Effective Length	(m)	0.4	0.3
Gap Height or Diameter	(mm)	40	70
Total Mass	(kg)	360	128
Coils Per Pole		1	1
Conductor Height	(mm)	8.0	2.0
Width	(mm)	8.0	2.0
Hole Diameter	(mm)	4.4	edge-cooled
Turns per Coil		60	288
Coil Current	(A)	203	15.7
Current Density in Conductor	(A/mm ²)	2.4	3.6
Voltage	(V)	12	66
Power	(kW)	2.5	1.0
Cooling-Water Circuits per Magnet		2	4
Total Water Flow	(gal/min)	0.8	0.17
Water Pressure Drop	(psi)	100	100
Water Temperature Rise	(°C)	12	23

*Excluding magnets for the ECS

II. 10. INJECTION SYSTEM

10.5.3 Septum Magnet [Revision]

Because of the addition of the PAR, the pulse rate of the septum magnet is changed from 60 Hz to 2 Hz.

10.7 Injection Control System [Revision]

The PAR uses the same control system components as those used by the storage ring and the other injection systems. Microprocessor-based clusters are used to interface with various injection systems. The addition of the PAR, the removal of the low-frequency rf system from the synchrotron, and the reassignment of 450-MeV beam-line control clusters results in a total of eight microprocessor clusters instead of seven for the injection system.

III. 2. FRONT-END OF A BEAM LINE

2.6 Front-End [New Section]

During the past year, the Subcommittee on Conventional Facilities set up by the APS Users Organization Executive Committee recommended that the shield wall be moved towards the source point so that the first-optics can be located as close as possible to the radiation source. This optimization has two parts: first, reduction of the front-end length that remains between the shield wall and the source, and second, movement of the shield wall closer to the source. The first-optics was moved closer to the source by moving the wall and making it thinner. In this process, it was assured that there would be adequate space to access various storage-ring, crotch, and front-end components during commissioning and maintenance. A full-scale mock-up of a sector of the storage ring has greatly assisted in this effort.

The front-end was reevaluated for its effective operation while reducing its length to six meters. This was accomplished without any redesign of the subcomponents.⁽⁶⁾ The new design of the shield wall geometry is discussed in detail in Sec. IV.3.1.6.

2.7 Liquid-Gallium-Cooled X-Ray Optics⁽⁷⁾ [New Section]

The insertion devices on the APS will deliver large power loads and power densities to the first-optics. Optimal solutions for handling such power densities and efficiently delivering the maximum x-ray flux to the sample under investigation are being developed. Use of liquid gallium as a coolant for the first-optics, compared with the conventional use of water, has great promise. During the past year a liquid-gallium pump has been built and tested for its performance. The liquid gallium was made to flow through channels in a silicon crystal, and this assembly was tested at the CHESS wiggler beam line.

The electromagnetic induction pump is built from a modified 5-hp, 3-phase induction motor, where the central rotor is replaced with a stainless steel tube spiral. The interaction of the moving magnetic field and the current generates a force on the liquid gallium in the stainless steel spiral to produce a pumping action. The pump has developed a static head pressure of 43 psi and can pump 3 gal/min through channels in a silicon crystal. The higher thermal conductivity of liquid gallium compared with water makes the heat transfer at the liquid-solid interface very efficient.

The design of the cooling channels in a silicon crystal is based on a finite-element analysis to obtain the optimal geometry. A series of tests was conducted using the radiation from a six-pole wiggler at CHESS. By removing existing filters on this beam line, a large heat load was realized and distributed over the liquid-gallium-cooled crystal. A comparison of water cooling and liquid-gallium cooling of silicon crystals with respect to the surface temperature and the rocking curves is shown in Figs. III.2.7-1 and

III. 2. FRONT-END OF A BEAM LINE

III.2.7-2. The cooling with liquid gallium provided at least a gain of a factor of five in the x-ray flux delivered by the monochromator to the sample. The increase in the temperature of the surface of the crystal was considerably lower when cooled with liquid gallium, compared with water. Further studies with various optimized cooling geometries will further improve the efficiency.

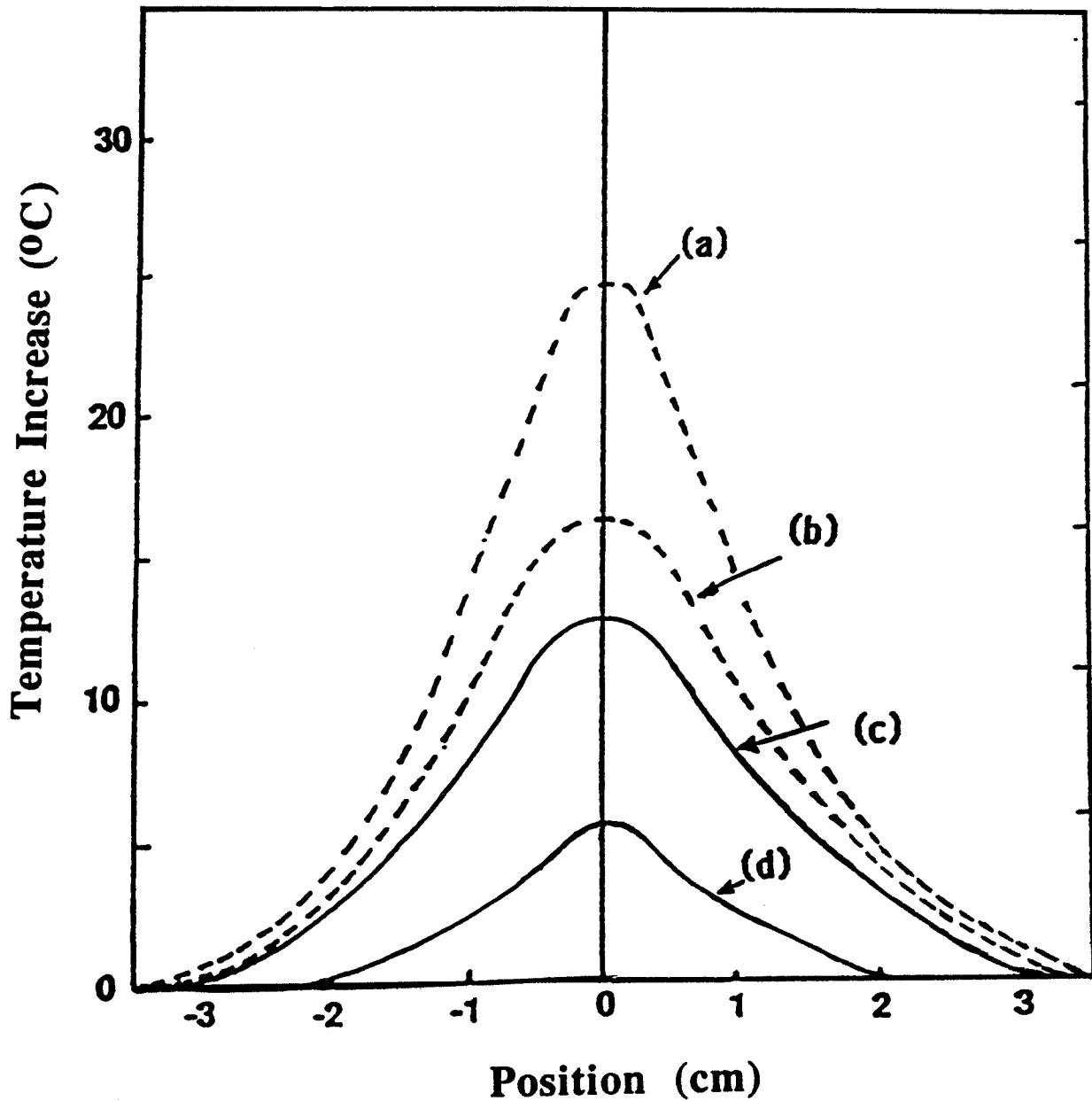


Figure III.2.7-1

Increase in the surface temperature along the x-direction for various silicon crystal cooling schemes with the CHESW wiggler operated at 46 mA of stored current at 5.4 GeV. (a) Si crystal mounted on a copper block, which is cooled with water. (b) Si crystal with channels carrying water and (c) liquid gallium. (d) Si crystal with optimized location of channels cooled with liquid gallium.

III. 2. FRONT-END OF A BEAM LINE

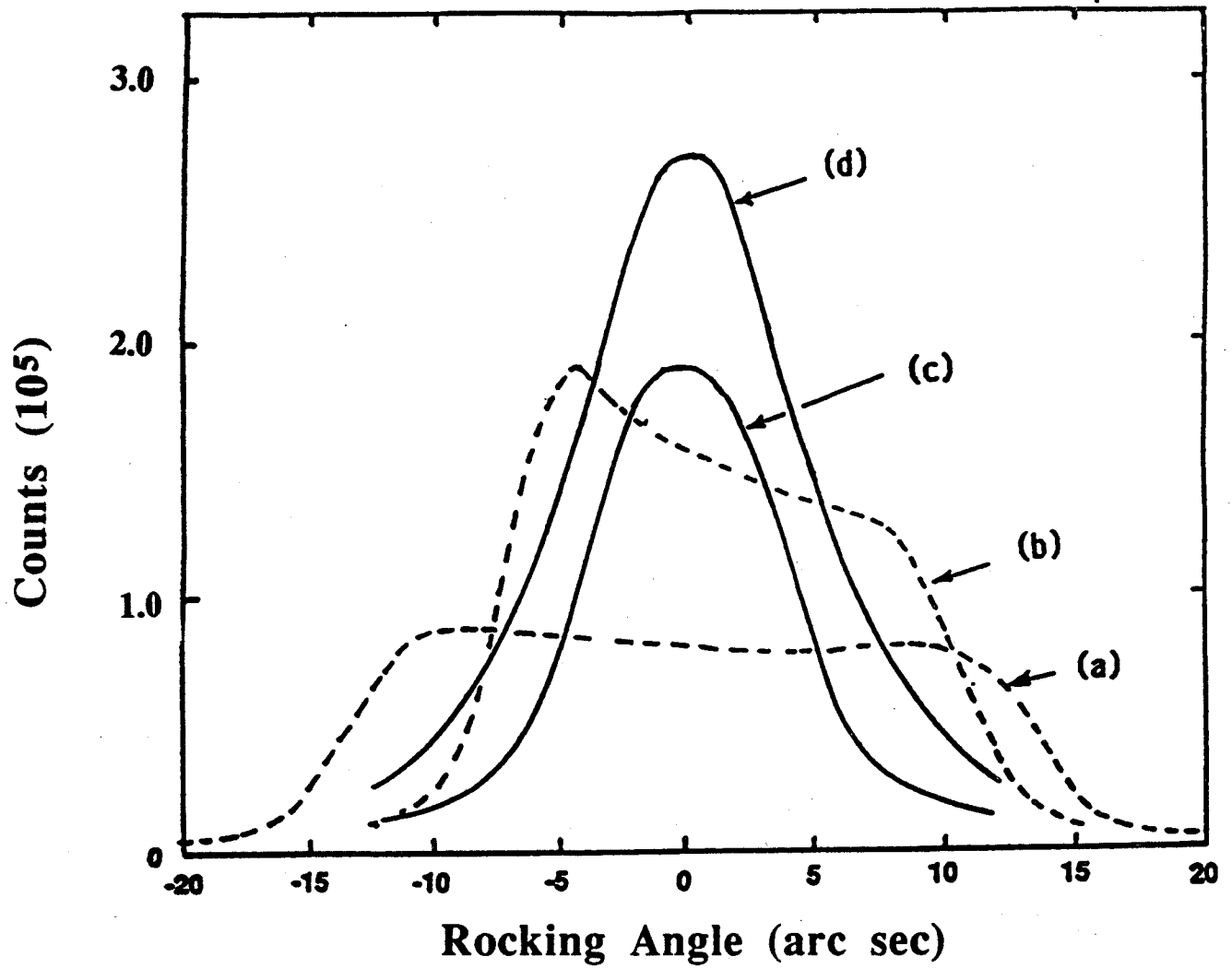


Figure III.2.7-2
Rocking curves at 20 keV for various cooling geometries described in the caption for Figure III.2.7-1.

III. 3. DESCRIPTION OF BEAM LINES

3.5 Preliminary Plans for the Beam-Line "Trust Fund" [New Section]

Although the 15 beam lines that have been designed and costed are not necessarily those that will be constructed, this work has generated a reliable cost basis for the future experimental effort to be implemented at the Advanced Photon Source. The final choice of the beam lines cannot be made at this time. Hence, as per recommendations of the DOE Review Committee (DRC), the estimated budget and contingency for the insertion devices and beam lines is designated as a "trust fund" for these components, to be used as future user needs are developed and defined. Towards this goal, a committee was formed to develop a plan to distribute the "trust fund."

The report of the committee⁽⁸⁾ describes the optimization of the distribution of the funds held in trust so that the short- and long-term research programs will be productive, making the facility most attractive from the user's point of view. Following are the main recommendations:

1. Part of the funds should be utilized for the development of eight complete beam lines: three of these will be equipped with undulators and two with wigglers, while three will use the radiation from the bending magnets. These beam lines will support storage-ring commissioning activities, development of a well-qualified APS staff, and development of performance criteria for standardized insertion devices, front-end components, and first-optics. It is estimated that about 50% of the "trust fund" will be utilized for this purpose.
2. Remaining funds should be used to build insertion devices, front-ends, and first-optics using an appropriate development plan. This will reduce the cost of a complete beam line to a collaborative team and will also provide standardized insertion-device, front-end, and first-optics technology to the users.

On the basis of the currently available cost-base for the construction of various insertion devices, front-ends, and first-optics, different plans can be developed. Two illustrative plans with specific options are presented in Table III.3.5-1. In these plans, the first option includes the insertion device and the front-end to be constructed by the facility. In the second option, the first-optics will also be provided. There are two possible plans for the length of the undulators that have been considered. Plan A provides for full 5-m-long undulators, while Plan B provides for devices half this length (2.5 m). In this phase of the development of the experimental facilities, it is desirable to build half-length undulators to gain experience in handling radiation heat loads. Decisions on the distribution of undulators and wigglers will be made in consultation with

III. 3. DESCRIPTION OF BEAM LINES

Table III.3.5-1

Distribution Plans for the "Trust Fund" to Develop
Experimental Facilities.

	OPTION 1		OPTION 2	
	ID + Front-End		ID + Front-End + First-Optics	
	Plan A	Plan B	Plan A	Plan B
Undulator Length (m)	5	2.5	5	2.5
50% Undulators + 50% Wigglers	14	18	10	12
Fully-Developed Beam Lines	5	5	5	5
Total Developed Sources	19	23	15	17

the user community. For the present, equal numbers of each undulator type are assumed in Table III.3.5-1.

Together with the five insertion-device beam lines proposed to be fully developed by the facility, the "trust fund" will provide insertion-device sources (with front-ends and first-optics) at more than 50% of the 34 straight sections.

III. 3. DESCRIPTION OF BEAM LINES

3.6 References [Additional Material]

6. P. J. Viccaro, "A Front-End Design for the Advanced Photon Source," ANL Report, Light Source Note LS-108 (Nov. 1987).
7. R. K. Smither, G. Forster, D. Bilderback, M. Bedzyk, F. Finkelstein, C. Henderson, J. White, L. Berman, P. Stefan and T. Oversluizen, paper to be presented at Synchrotron Radiation Instrumentation Conf., Aug. 29-Sept. 2, 1988, Tsukuba, Japan.
8. "Insertion Device and Beam Line Plans for the Advanced Photon Source: A Report and Recommendations by the Insertion-Device and Beam-Line Planning Committee," Argonne National Laboratory Report ANL-88-7 (Feb. 1988).

III. 3. DESCRIPTION OF BEAM LINES

IV. 1. OVERVIEW

1.1 Objective of the Facilities' Construction [Replacement]

The APS conventional facilities are designed to accommodate a 7-GeV positron storage ring, a full energy synchrotron, a positron accumulator, a positron linear accelerator, and an electron linear accelerator. The storage ring is housed in an annular building, which also provides space for external photon beam lines and for the set-up of experiments utilizing the beam lines. Laboratories, clean rooms, and offices for the use of the experimenters are located adjacent to this experiment hall. Site access roads, parking facilities, and miscellaneous site amenities are included.

The layout of the components and spaces and the construction systems selected provide precise geometric relationships, specific environmental conditions, isolation from outside vibration, and appropriate safety and shielding measures. The design of the conventional facilities addresses the usability and operational efficiency of the overall project. Engineering design provisions follow the U. S. Department of Energy (DOE) Order 6430.1, entitled "General Design Criteria Manual."

The design of the conventional facilities takes into account the following significant criteria in arriving at the siting, configuration, and building system selections:

- The geometry of the technical component dictates the scale and organization of the conventional facilities. In general, the forms and dimensions of the buildings follow the functional organization of the linear accelerator, synchrotron, positron storage ring, and photon beam lines, as illustrated by Fig. IV.1.1-1, the Project Site Isometric.
- The 1060-m-circumference storage ring, being the largest technical component, is the primary element in organizing the conventional facilities. Requirements for housing the ring dictate the design dimensions for the arrangement of the conventional facilities.
- Safety of personnel during facility operations requires that the storage ring, linear accelerators, and synchrotron be shielded. Shielding calculations indicate the need for 3 to 6 ft of concrete, supplemented, where appropriate, by lead bricks, steel plate, or earth cover to safely contain radiation. (See Sec. IV.2.3.)
- Reliable operation of the beam lines and related technical components requires their installation on a vibration-free structure and their containment in a controlled, stable environment.

IV. 1. OVERVIEW

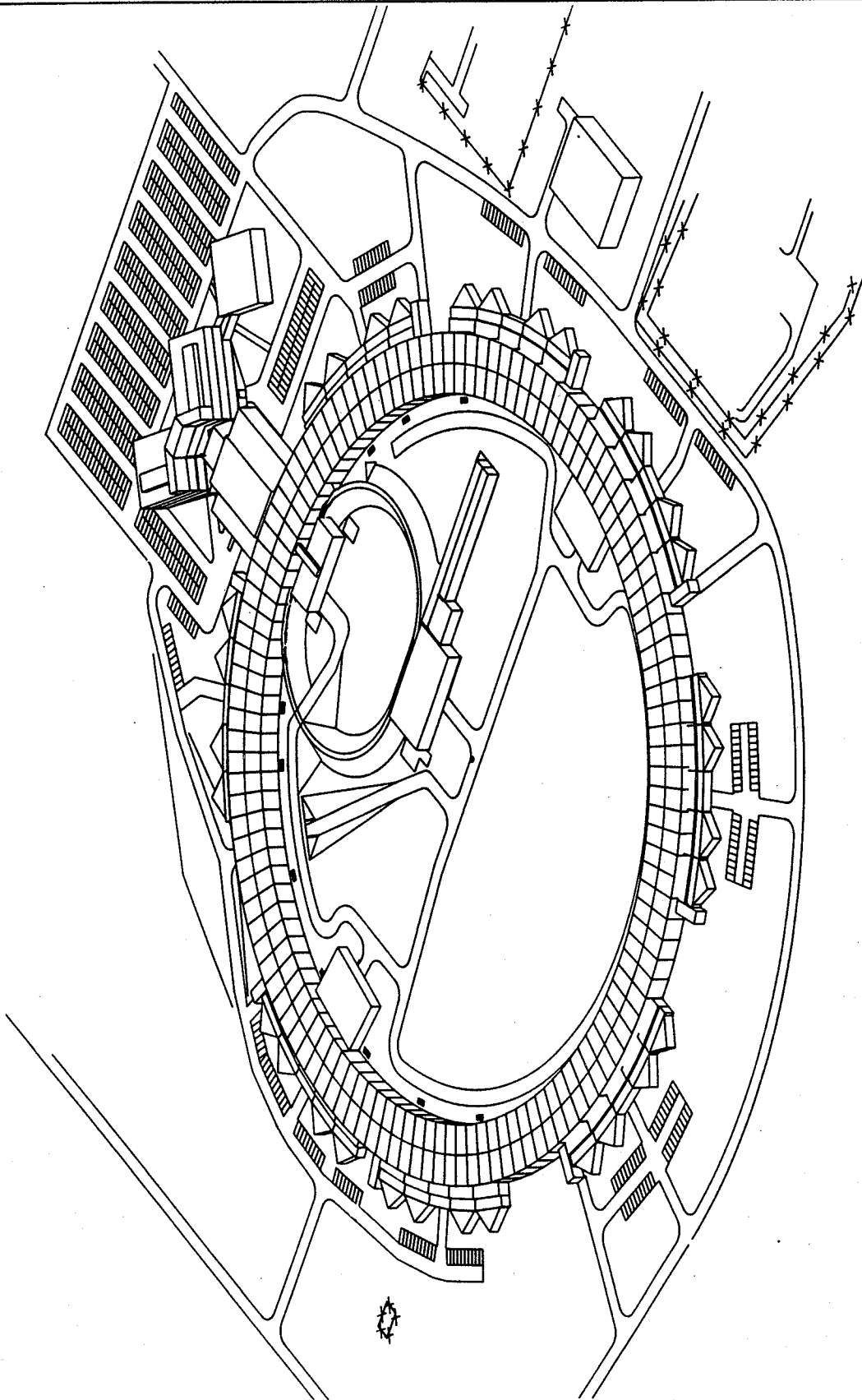


Figure IV.1.1.1-1
Project site isometric.

IV. 1. OVERVIEW

- Ease of installation, operation, and maintenance of the technical components requires safe, convenient access into the areas containing the technical components.
- Optimal use of stored beams by researchers requires the flexibility for photon beams to exit at tangents to the storage ring approximately every 4.5° . The photon beam lines range up to 80 m long in the 83-ft-wide, environmentally stable, vibration-free, column-free experiment floor, which completely surrounds the positron storage ring.
- Projected experiment installation criteria and operating conditions require the hall to have stable, level floors; a controlled, heated, and air-conditioned environment; clear heights up to 21 ft; and accessibility to utility services. The provision of these services is sufficiently flexible to anticipate varied operating routines and to accommodate an evolving technology.
- The research areas must have convenient access to laboratory, office, service and delivery, and related support spaces to maximize and enhance the experimenters' use of the facility.
- Operation of the total facility is accommodated in the central laboratory/office building, which contains offices, shops, laboratories, assembly areas, and the main control and computer rooms. The central laboratory/office building is a distinctive but functional structure that serves as the identifying "front door" for the total facility.
- The materials and character of the facility are consistent with Argonne plant standards, recognizing the long-term maintenance and operating requirements of such a large-scale facility. Utility distribution systems are designed to meet the anticipated demand loads of a fully operating research facility. Operating equipment is provided to meet initial demand levels, with provisions for planned additions as the facility usage increases. The systems are expected to maintain a high degree of reliability in their operation, without the need for installation of excessive standby components or redundancy.

Building placement and orientation were influenced by the following considerations:

- Technical component configuration

IV. 1. OVERVIEW

- Functional relationships
- Existing structures
- Existing utilities
- Radiation protection
- Subsurface conditions
- Topography
- Vibration sources
- Site access
- Environmental impact
- Archeological locations
- Possible extended beam-line projections
- Expansion potential

Figure IV.1.1-2 shows the proposed location for the APS, in the southwestern section of the Argonne site, centered on Bluff Road east of Kearney Road. The buildings are sited on a large land area away from possible adverse consequences of traffic-generated vibration, as shown on Fig. IV.1.1-3, the Project Area Plan. The site accommodates both the proposed initial and future growth expectations for the project.

1.2 Organization and Layout of Facility Components [Replacement]

The conventional facilities comprise thirteen buildings, illustrated in Fig. IV.1.2-1, the Project Site Plan. The predominant structure is the experiment hall, which encloses the storage ring; the other buildings are either located within the infield of the experiment hall or appended to the outer perimeter of the experiment hall.

The machine-support structures -- structures housing the accelerator facilities -- are located in the infield of the storage ring. They house the concrete-shielded beam enclosures and technical components for acceleration and containment of the beam. They consist of the linac building, the synchrotron injection building, the synchrotron building, the synchrotron extraction building, and the storage-ring enclosure (located within the experiment hall). These structures are connected to each other in series and linked directly to the storage ring. The two rf/power buildings that house the rf power

IV. 1. OVERVIEW

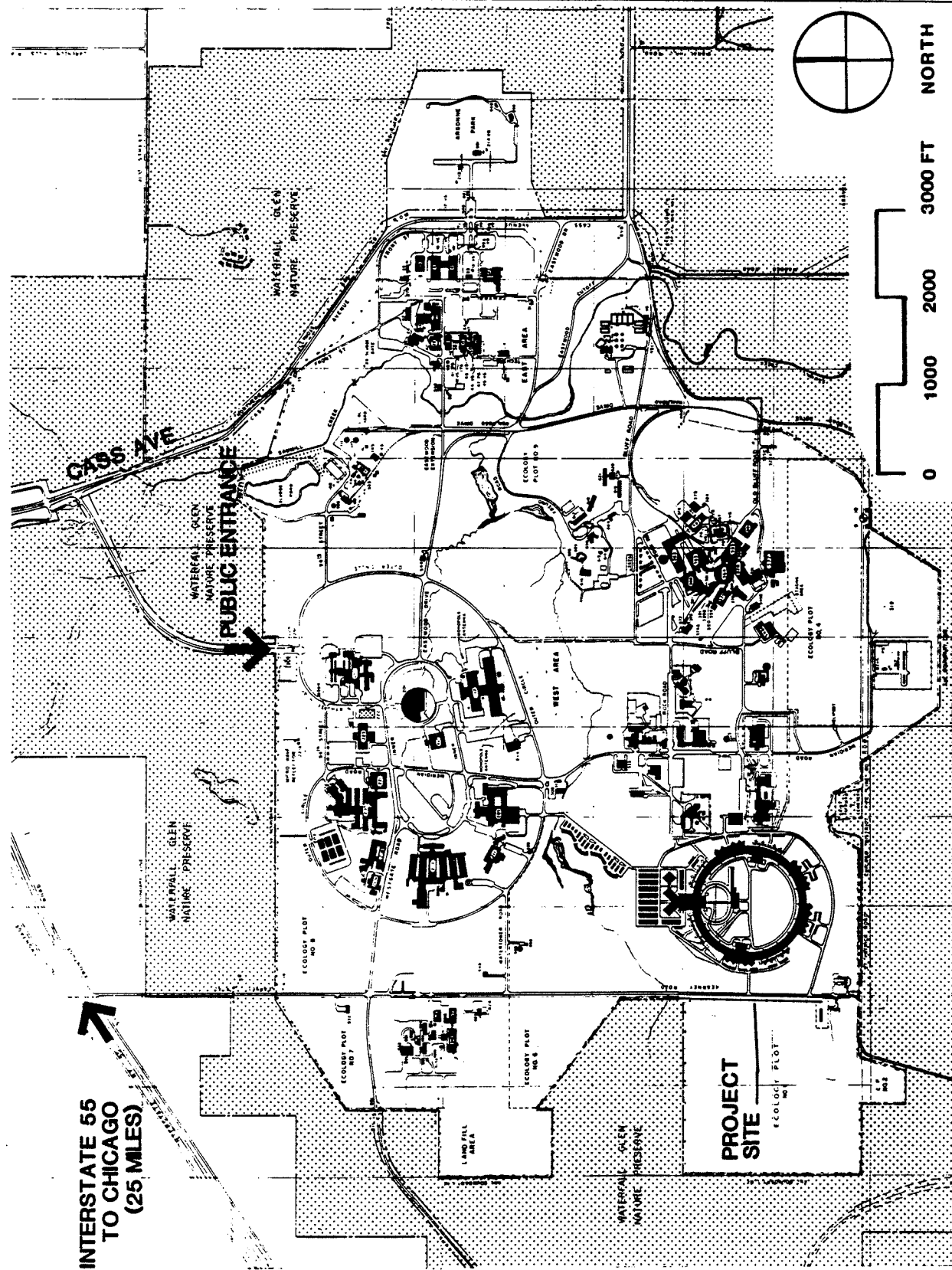


Figure IV.1.1-2
Argonne campus plan.

IV. 1. OVERVIEW

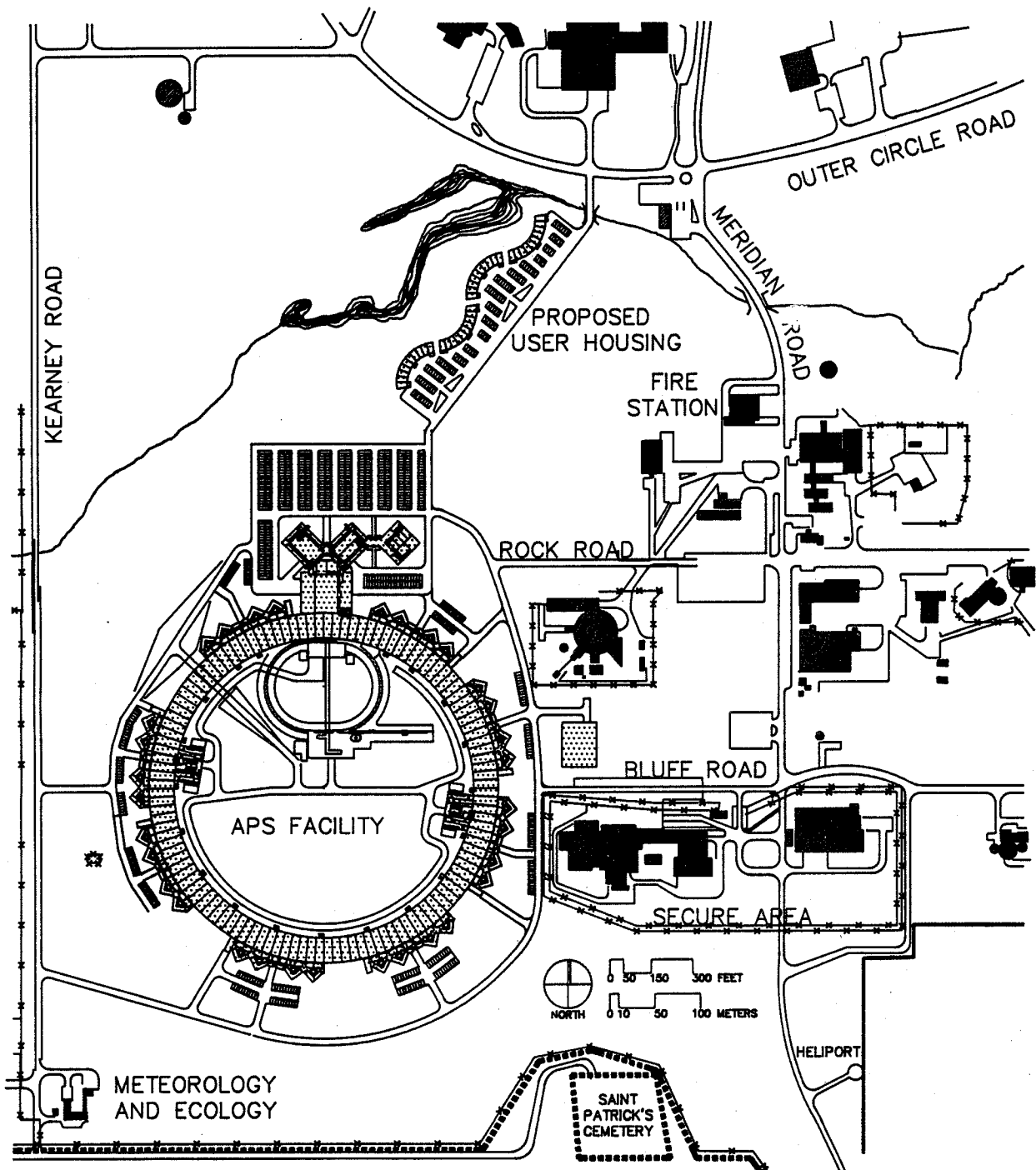


Figure IV.1.1-3
Project area plan.

IV. 1. OVERVIEW

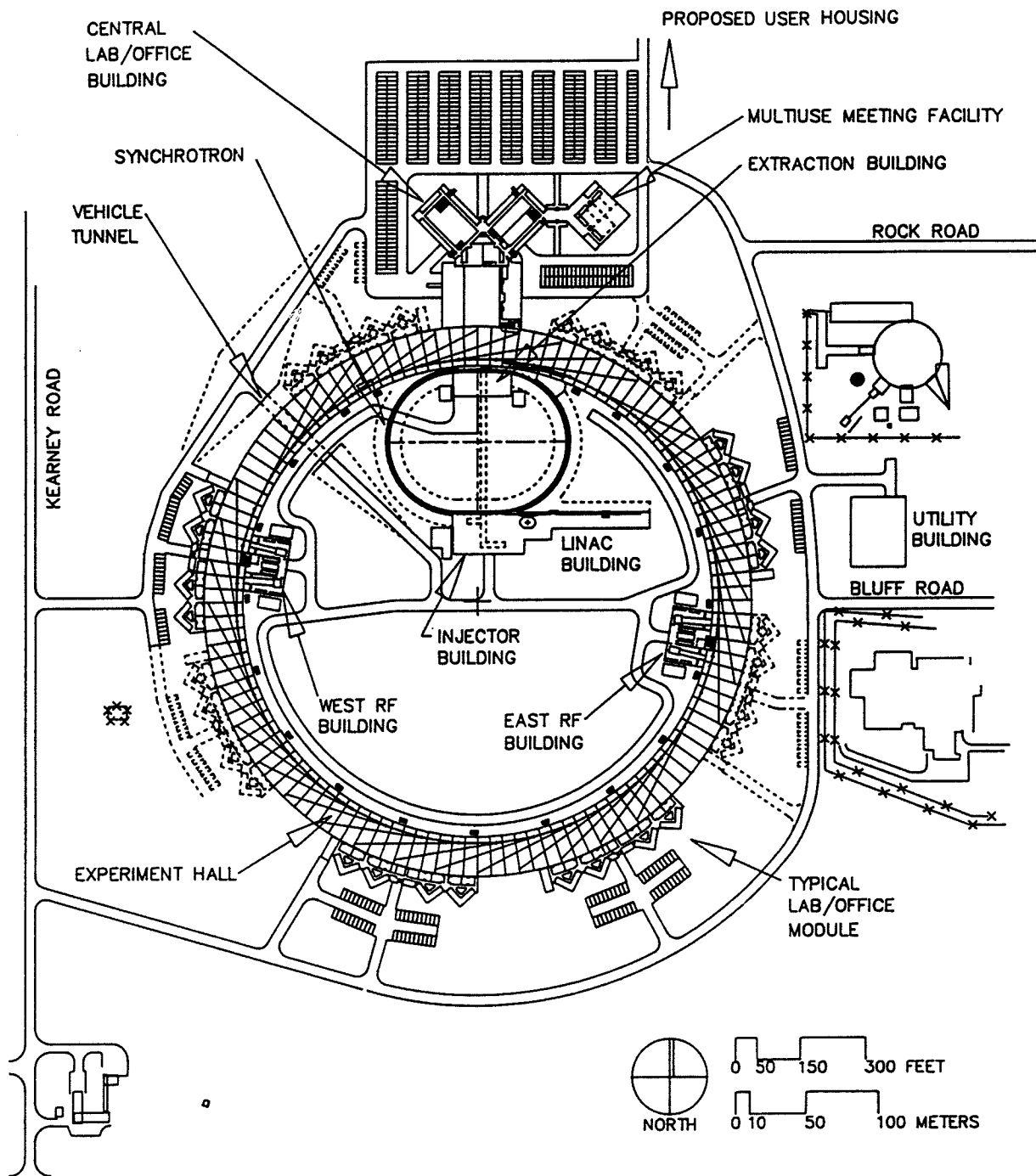


Figure IV.1.2-1
Project site plan.

IV. 1. OVERVIEW

supplies for the storage ring also connect directly to the storage-ring enclosure and the experiment hall.

The experiment-support buildings -- buildings housing people -- are extensions off the outer perimeter of the storage-ring enclosure. The experiment hall is a ring-shaped, long-span structure that contains the concrete-shielded storage-ring enclosure along the inner perimeter, with an unobstructed, continuous, column-free hall to contain the experiments between the storage ring and the outer perimeter. The central laboratory/office building contains the administrative offices and support spaces for the permanent staff assigned to manage the APS. The office wing of this building contains offices, conference facilities, laboratories, receiving area, stock room, toilet/locker rooms, and the main computer and control rooms for the entire facility. The support wing contains a high-bay assembly area, specialized labs, a clean room, and shops. A multi-purpose meeting facility is adjacent to this building. In addition, there are four laboratory/office modules - four similar, single-story buildings of 19,000 ft² each, located around the outer perimeter of the experiment hall. Each is composed of eight laboratories that connect directly to the experiment hall, 32 offices for the experimenters, and conference and support spaces; two of the modules have a truck air lock to facilitate delivery of components to the experiment hall. (The facility design can accommodate eight such modules, and eight are required to provide needed facilities for a full complement of beam lines. As APS utilization grows to fully occupy the initial complement of four modules, additional modules of appropriate design and furnishings will be built.)

Chillers, compressors, and pumps for the facility are contained in a 21,600-ft² utility building located at a distance from the experiment hall. The primary electrical distribution switchgear is also located in this structure. The utility tunnel carries piping and conduit for mechanical and electrical services from the utility building at the eastern edge of the site, under the ring road to the outer perimeter of the experiment hall. The utility loop in the experiment hall provides utility service to the rest of the site.

Two tunnels provide access directly to the infield areas from outside the experiment hall. The largest tunnel, entering the infield from the northwest corner of the site, is sized to accommodate emergency and maintenance vehicles. A smaller control tunnel provides access for utilities and pedestrians from the base of a stairway and utility chase beneath the southeast corner of the support wing of the central laboratory/office building -- under the support wing, experiment hall, and synchrotron buildings -- to a stairway and elevator in both the synchrotron extraction and synchrotron injection buildings. Building footprint, areas, and dimensions for all structures of the conventional facilities are listed in Table IV.1.2-1.

IV. 1. OVERVIEW

Table IV.1.2-1

Building Dimensions [Replacement]

Building	Clear Height (ft)	Overall Size		Footprint		Gross Floor Area (ft ²)
		Width (ft)	Length (ft)	Part (ft ²)	Bldg. (ft ²)	
Linac Building					13,151	13,151
Linac Enclosure	9.0	48.5	286	6,596		
Klystron Gallery	17.5	20.0	286	6,555		
Synchrotron Injection Building	20.0	82.0	164	13,138	13,138	14,751
Synchrotron Enclosure	9.0	11.5	1210	13,915	13,915	13,915
Synchrotron Extraction Building	14.0	49.0	132	6,470	6,470	7,060
RF/Power Buildings					21,600	21,600
East RF/Power Building	14.0	90.0	120	10,800		
West RF/Power Building	14.0	90.0	120	10,800		
Experiment Hall	24.5	91.3	3,655		334,836	334,836
Utility Corridor	11.5	7.0	2,743	19,200		
Storage-Ring Enclosure	9.0	20.7	3,478	52,000		
Experiment Floor	24.5	63.3	3,849	263,636		
Lab/Office Module					76,000	76,000
East Lab/Office Module	9.0	53.9	352	19,000		
Southeast Lab/Office Module	9.0	53.9	352	19,000		
Southwest Lab/Office Module	9.0	53.9	352	19,000		
West Lab/Office Module	9.0	53.9	352	19,000		
Central Lab/Office Building					79,820	183,700*
Office Wing	9.0	100.0	353	35,320		
Support Wing	27.0	180.0	150	32,400		
Meeting Facility Wing	17.0	110.0	110	12,100		
Utility Building	30.0	120.0	180	21,600	21,600	21,600
Subtotal					580,530	686,613
Tunnels					13,475	13,475
Utility Tunnel	15.0	15.0	153.0	2,300		
Control Tunnel	15.0	15.0	545.0	8,175		
Vehicle Tunnel	15.0	20.0	150.0	3,000		
Total					594,005	700,088

*Includes 35,320 ft² service level and 7,500 ft² fan room.

IV. 1. OVERVIEW

IV. 2. TECHNICAL AND LEGAL DETERMINANTS

2.1 Siting Constraints [Replacement]

The configuration of the technical components, especially the machine itself, is the primary determinant of the site layout. Ring shapes for the storage ring and synchrotron and relationships in the beam transfer area are a critical part of the machine design. The locations of the conventional facilities housing the machine are fixed by the chosen configuration of the machine. The rf power supply connections to the storage ring must be located directly opposite one another, requiring compatible locations for the rf/power buildings. The shape, location, and width of the experiment hall are all determined by the number, length, and tangent locations of the photon beam lines.

Beyond the configuration requirements of the machine itself, certain functional relationships are critical to the layout of the APS facility. The central laboratory/office building houses the control room and the operating staff for the machine. Because of the need to interface with the injection facilities, a close relationship between the central laboratory/office building and the infield buildings is required.

The 545-ft-long control tunnel that connects these buildings provides direct access for both pedestrians and cabling, as well as other utilities. The support wing of the central laboratory/office building is located between the office wing and the experiment hall because of the need for direct passage between these two areas. The laboratory/office modules are spaced around the outer perimeter of the experiment hall to minimize the distances that experimenters must traverse between their labs and offices and their beam lines.

In order to meet federal guidelines, a buffer zone between the radiation sources and the Argonne property line is provided. The skyshine radiation calculations help to establish how far the facility must be located from the west and south boundaries of the site. (See Sec. IV.2.3, Shielding Requirements.) Topography and subsurface conditions, although relatively uniform over the entire site, are less suitable in the northern portions of the site. In order to provide the firmest foundations for the critical machine supports, the complex was positioned as far to the south as possible and oriented to allow the storage-ring foundations to benefit from the most consistent conditions.

Sources of vibration outside the boundaries of this facility could cause unacceptable levels of vibration in the experiment areas. Vehicular traffic, particularly that of heavy trucks, is to be avoided in the vicinity of the APS. The proposed site is located at a remote corner of the Argonne campus, away from the major traffic arteries and truck delivery routes. Adjacent non-Argonne land is not expected to contribute vibration because of its use as a nature preserve and recreation area.

To facilitate access, the central laboratory/office building (the primary population area of the facility) is located closest to Rock Road, which provides the primary

IV. 2. TECHNICAL AND LEGAL DETERMINANTS

vehicular access from Meridian Road and Argonne's main entrance off Cass Avenue. The roadways encircling the facility have direct connections to Bluff and Kearney Roads. The cooling towers and utility building housing mechanical equipment are positioned at the eastern edge of the site closest to Bluff Road and all connections to the main Argonne site utility distribution systems.

The environmental impact of the facility is expected to be slight. This minimal impact is in part due to the siting of the facility so as to avoid encroachment on wetland areas at the northern edge of the site.

Although several areas of some archeological interest are included in the site, it has been possible to avoid disturbing a number of them by close coordination with the archeological investigators.

The need for expansion of selected portions of the facility has been anticipated, and space to allow future expansion has been provided in the required locations. The central laboratory/office building is laid out to allow independent expansion of the office wing, the clean rooms, support labs, and shop areas. The utility building is designed to accommodate a full complement of experimental facilities and is organized to allow the addition of mechanical equipment if the demand on the facility increases beyond this level.

Spaces have been provided in several places for the extension of future beam lines beyond the outer walls of the experiment hall. Each module may be expanded from its outer walls to provide additional work spaces in such a way as to avoid interference with these extended beam lines.

The topographic and geologic characteristics of the site are typical of much of the Laboratory. The site is well suited for this development, including both the building construction phase and the intended operation of the APS. The specific characteristics of the site that support its selection include the relatively level terrain, an adequate stay-clear area, space for extended beam lines, and close proximity to a security area for classified work.

Several alternative sites were considered. One of these is an area just east of Building 362, near the former 12-GeV Zero Gradient Synchrotron complex. Although at that location the adjacent existing buildings with their associated services and utilities offer some conveniences, the essential stay-clear areas necessary for reducing vibrational effects and for future extensions of beam lines are limited.

A level-terrain site on the eastern boundary of the Laboratory is limited by the lack of a similar stay-clear area on the east, adjacent to heavily traveled Cass Avenue. Studies showed that the rerouting of Cass Avenue was not a viable solution. The "800" area on the far western boundary has terrain limitations, as well as size and location limitations.

IV. 2. TECHNICAL AND LEGAL DETERMINANTS

2.2 Geotechnical Evaluation

2.2.1 Geology [Replacement]

The geology of the site consists of an approximately 30-m-thick deposit of glacial drift on top of the Niagaran and Alexandrian dolomite bedrock of Silurian age (about 400 million years old). These formations are underlain by Maquoketa shale of Ordovician age and older dolomites and sandstones of Ordovician and Cambrian age. Precambrian crystalline bedrock lies at a depth over 1000 m beneath the site. The beds are nearly horizontal.

The Niagaran and Alexandrian dolomite is about 60 m thick in the Argonne area; it is widely quarried in northeastern Illinois and is important as a source of ground water. The Maquoketa shale separates the upper dolomite aquifer from the underlying sandstone and dolomite aquifers; the lower aquifer has a much lower piezometric level and does not appear to be affected by pumpage from the overlying Silurian bedrock.

During the Pleistocene epoch, glaciers deposited drift over most of Illinois. Arcuate-shaped moraines, roughly parallel to the shoreline of Lake Michigan, were formed in the Chicago area during the last glacial stage (the "Wisconsinian" stage). The younger moraines are generally closer to Lake Michigan. Argonne is on the "Keeneyville Moraine," which is part of the Valparaiso morainic system.

Detailed geological and geotechnical measurements have been undertaken at the site to identify any variations in the physical properties of the glacial drift that might affect the design, construction, or exact location. In particular, a geotechnical investigation has been initiated for the purpose of determining general subsurface soil types, ground water conditions, and various soil characteristics. Twelve borings, six of which were to bedrock, have been made at the site. Soil profiles were determined in the field, and soil samples were tested in the laboratory to determine moisture content, dry unit weight, and unconfined compressive strength.

Test results have shown that the surface soils are glacial tills composed predominantly of clay-silt mixtures with lesser portions of sand and gravel. At the deeper elevations, rock debris is frequently present. The underlying bedrock consists of a thin- to medium-grained grayish-white dolomite. The site soils are preconsolidated and are usually high in density and strength. The site is well suited for construction of the APS facility.

Additional field tests are under way to determine dynamic properties of the soil, in particular the compression, shear, and Rayleigh wave speeds. Further borings will be required to obtain these data. Wave speeds will be measured by using in situ seismic testing techniques such as the crosshole test method. Among other things, the shear wave speeds will be used to calculate the shear modulus for the soil, which, in turn, is required as input for dynamic analyses of the experiment hall foundation and floor slab

IV. 2. TECHNICAL AND LEGAL DETERMINANTS

(see Sec. IV.2.5.3.4). Data relative to the general subsurface soil types and static soil characteristics will also be obtained from the new borings to supplement the data from the original twelve borings.

2.3 Shielding Requirements

2.3.1 Introduction [Replacement]

The shielding approach limits the radiation doses to DOE guidelines for both on-site and off-site exposure. The approach also addresses access to particular areas during certain operations. The shielding is designed for the radiation resulting from several types of operations that involve normal beam-loss mechanisms, as well as for certain abnormal beam-loss scenarios. The shielding design is based on experimental data obtained from existing accelerator and synchrotron light source facilities, used in conjunction with theoretical formulations based upon well-known attenuation characteristics. Details of the calculations and the parameters used for the specified shielding requirements are given in Refs. 1-5.

2.3.2 Shielding Design Objectives [Replacement]

The basic occupational exposure limit for DOE contractors is 5 rem per year for whole body exposure.⁽⁶⁾ However, in its guidance for ALARA (As Low As Reasonably Achievable) contained in the same DOE Order, the design objective for new facilities is to limit exposures to 1/5 of the basic limit. In addition, DOE has proposed as an ALARA guide that the predicted exposure to individual members of the public should not exceed 25 mrem per year.⁽⁷⁾ These guidelines for on-site and off-site locations are used as the basis for shielding for normal operation of the facility.

Considering only normal loss conditions, the wall shielding provided for the storage ring (0.8 m of normal concrete on the inner wall and 0.56 m of heavy concrete on the outer, ratchet wall) limits the on-site dose rate from continuous loss of the beam around the ring circumference for a 10-h mean lifetime to ~ 0.04 mrem/h,⁽¹⁾ well within the guidelines. This assumes a circulating current of 300 mA of positrons at 7 GeV. The computation is based on semi-empirical formulas suggested by Swanson et al.⁽⁸⁾ that assume a uniform loss around the ring.

For the case of off-site doses, the skyshine component contribution, in relation to the low permissible level (25 mrem/yr), becomes an important consideration. Since the distance to the boundary is 220 m, a prudent approach to estimating the potential yearly dose from this component was taken.⁽¹⁾ The results of several calculations indicated that 1 m of normal-concrete roof shielding is required to limit the off-site contribution to 8.3 mrem/yr, for an assumed 8000 h of operation. The calculation that predicts this

IV. 2. TECHNICAL AND LEGAL DETERMINANTS

dose rate of 8.3 mrem/yr contains a safety factor of three due to formulation uncertainties that are borne out by field measurements.⁽⁹⁾

An accidental loss of the entire beam at a single point is an extremely unlikely event. However, sufficient shielding is provided to ensure that the potential dose to an individual on the outside of the shield in the vicinity of the incident is not dangerous. With respect to such a rare accidental occurrence, the objective is to supply sufficient shielding to limit the dose per occurrence to less than 500 mrem. Assuming a circulating current of 100 mA of 7-GeV positrons and a shield thickness of 0.56 m of heavy concrete, an accidental loss of the beam at a point would result in a dose of < 100 mrem, if this event occurred at a location where the distance from the positron orbit to the outside of the shield is minimal. Under the assumption of a 300-mA circulating current, a thickness of 7.62 cm of lead located near the orbit at the beam plane will limit the dose to < 100 mrem at the same location.

In the case of the radiation dose rate outside the storage-ring shield but in the vicinity of the injection area during beam transfer from the synchrotron, a conservative assumption of 50% loss at a point was assumed for 7.2×10^{10} positrons/s at 7 GeV.⁽¹⁾ The computed dose rate for this condition is above the guideline, but the addition of sufficient lead and dense polyethylene at high-loss points in the injection region reduces the dose rate during the injection phase to within the guidelines (< 0.5 mrem/h).

2.3.3 Access Objectives [Replacement]

The shielding allows unrestricted access to the experimental area and all laboratories and offices, both during injection and while the stored beam is circulating. Access to areas on the infield side of the storage-ring tunnel is unrestricted. No access into the storage-ring tunnel is allowed while the beam is injected or stored.

For the synchrotron, the shielding is adequate to allow unrestricted access to the outside of the building and its infield region, but no access is permitted into the synchrotron tunnel while the synchrotron is operating. Work in the storage-ring tunnel is permitted while the synchrotron is operating and in the synchrotron tunnel while the storage ring is operating.

The shielding for the electron linac, positron converter, positron linac, and positron accumulator ring allows unrestricted access to the regions outside the linac radiation enclosure. Additional lead, dense polyethylene, and steel shielding around the converter target ensure unrestricted access to the area outside the shield in the vicinity of the converter.

IV. 2. TECHNICAL AND LEGAL DETERMINANTS

2.3.4 Shielding Approach [Replacement]

The shielding achieves the design goal of ≤ 0.5 mrem/h at accessible points on the outside of the shield during normal operations. At certain locations this requires additional lead and dense polyethylene.

The shielding requirements are satisfied by using sufficient normal or heavy concrete as a bulk shield to ensure adequate attenuation of the bremsstrahlung, giant resonance neutrons, and the high-energy component produced in the positron-photon showers. Where heavy concrete is called for, a density of 3.7 g/cm^3 is assumed. The concrete is supplemented by earth berms in some places, and steel, lead, and dense polyethylene are used to reinforce the shielding at localized regions of high-radiation fields. Points of localized loss during injection include septum magnets and other bending and focusing magnets in the injection system and downstream of the injection straight sections. Localized shielding of such loss points has been used successfully at Aladdin and NSLS. (8,10)

2.3.5 Recommended Shielding

2.3.5.1 Linac System [Replacement]

The linac system (~75 m long) features an electron linac (~20 m) to accelerate e^- pulses (1.2-A peak current, 40-ns pulse width) to 200 MeV at a 60-Hz rate for 24 pulses during each one-half-second synchrotron cycle. The electrons impinge on a tungsten target (with a thickness of two radiation lengths) to produce positrons, with an assumed conversion efficiency e^+/e^- of 0.0083. Forty percent of the positrons accepted by the second linac are lost during acceleration to an energy of 450 MeV; the remaining 60% are injected into the positron accumulator ring. The entire linac system is housed in a concrete tunnel of inner dimensions 9 ft \times 9 ft with the beam located 5 ft above the floor. Linac shielding alone is adequate for 10% of continuous operation. For operation in excess of this level, an exclusion area may have to be imposed.

The shielding consists of a concrete enclosure (or concrete-earth equivalent) 2 m thick on the sides and roof of both the electron and positron linacs. For the positron converter section, which is located in a 5-m-long section between the electron and positron linacs, the shielding consists of 0.3 m of steel and 2.0 m of concrete (or concrete equivalent) on the sides and top. Localized high beam-loss points are shielded with additional lead and dense polyethylene.

2.3.5.1A Positron Accumulator Ring (PAR) [New Section]

The PAR (30.58 m in circumference) is used to accumulate 24 linac pulses and to generate a bunch that matches the synchrotron rf system. The total charge amounts to

IV. 2. TECHNICAL AND LEGAL DETERMINANTS

3.6×10^{10} positrons per cycle at 450 MeV. The repetition rate is 2 Hz. The ceiling height within the PAR enclosure matches the linac enclosure at 9 ft. PAR shielding alone is adequate for 10% of continuous operation.

The shielding consists of 1.3-m concrete walls and a 1.5-m concrete roof. The north wall is the same as the linac enclosure and is made up of concrete and earth berm equivalent to 2 m of concrete. The west wall is made up of removable concrete blocks 1.5-m thick formed into an entrance maze. The linac and PAR are connected and constitute one radiation control zone. Localized high beam-loss points are shielded with additional lead.

2.3.5.2 Injector Synchrotron [Replacement]

A single bunch of positrons is transferred from the PAR to the synchrotron twice each second during the storage-ring filling operation. The particle bunch is accelerated to full energy and extracted at the proper time for injection into the storage ring. The shielding is adequate for operation at 7.7 GeV with the same charge. The synchrotron is housed in a 9 ft \times 9 ft cross-section concrete tunnel with earth coverage. Entry to the synchrotron tunnel to perform maintenance or repairs is permitted when a beam is circulating in the storage ring. In both beam transfer areas, where the linac shielding merges with the synchrotron shielding and the synchrotron shielding merges with the storage-ring shielding, sufficient shielding is provided to isolate radiation fields produced in the operating machine from the synchrotron tunnel. Additional lead and dense polyethylene shielding is provided at localized beam-loss points.

Except in the injection and extraction areas, where the concrete wall is 1.5-m thick, the shielding for the synchrotron consists of 0.3 m of concrete on the sides and roof of the tunnel, supplemented by earth berms to achieve an equivalent of 0.8 m of concrete shielding.

2.3.5.3 Storage Ring [Replacement]

The storage-ring shielding is adequate at 7.7 GeV and 100 mA. A lead "collar" will be added at the beam plane close to the orbit to allow operation at 300 mA. The circulating beam produces synchrotron radiation, which is directed down beam lines to the experiment area. The storage ring is housed in a concrete tunnel whose outside wall is in the form of a ratchet wheel or sawtooth configuration (see Figs. III.1.2-1 and III.2.4-1). The tunnel cross-section dimensions are 9 ft \times 9 ft in regions where the outside wall runs parallel to the storage-ring orbit, but wider in the regions of the ratchets to provide space for beam lines. The inside wall of the concrete tunnel is parallel to the storage ring.

The tunnel's inner side wall is 0.8 m of normal concrete, and the outer, ratchet-shaped side wall is 0.56 m of heavy concrete due to single-point beam-loss

IV. 2. TECHNICAL AND LEGAL DETERMINANTS

considerations. For a ratchet section, where the shield extends in the radial direction, the shielding consists of 0.8 m of heavy concrete, except for a 2-ft x 2-ft square opening centered on a photon beam line. The shielding in these openings consists of 25 cm of lead followed by 55 cm of concrete. The tunnel roof is 1.0 m of normal concrete due to off-site skyshine considerations. Additional provision has been made for lead and dense polyethylene shielding for use as needed.

2.4 Alignment

2.4.4 Storage-Ring Alignment [Replacement]

The storage ring has 80 primary control points, of which four are geodetic. It also has 80 secondary points that expedite the rough positioning of machine components (see Fig. IV.2.4-2). The geodetic points enable alignment on a quarter of the ring at a time. The control points are established by means of an electronic distance-measuring system and a laser alignment system with a tracking receiver to determine the straight-line offset between three adjacent control points.

The magnets between each dipole and insertion device are prealigned on a rigid frame and installed in the ring as a unit. All magnets and insertion devices have precision reference sockets located on their ends. As each unit is brought into the ring enclosure, it is rough-positioned from the control points. Then it is leveled by using a Wild N-3 optical level. Tilt is controlled with an electronic clinometer.

Final positioning of the magnets in the radial direction and magnet smoothing are accomplished by the accepted methods of Distinvar wire measurements and nylon wire offsets.

2.4.5 Injector Synchrotron Alignment [Replacement]

The injector synchrotron is aligned in a manner similar to that for the storage ring. There are 40 control points for the synchrotron, of which four are geodetic. The control points are located with an electronic distance-measuring system and a theodolite for radial position. From these points the magnet stand positions are marked on the floor. The same procedure as that used for the storage-ring magnets is used for leveling and radially positioning the magnets.

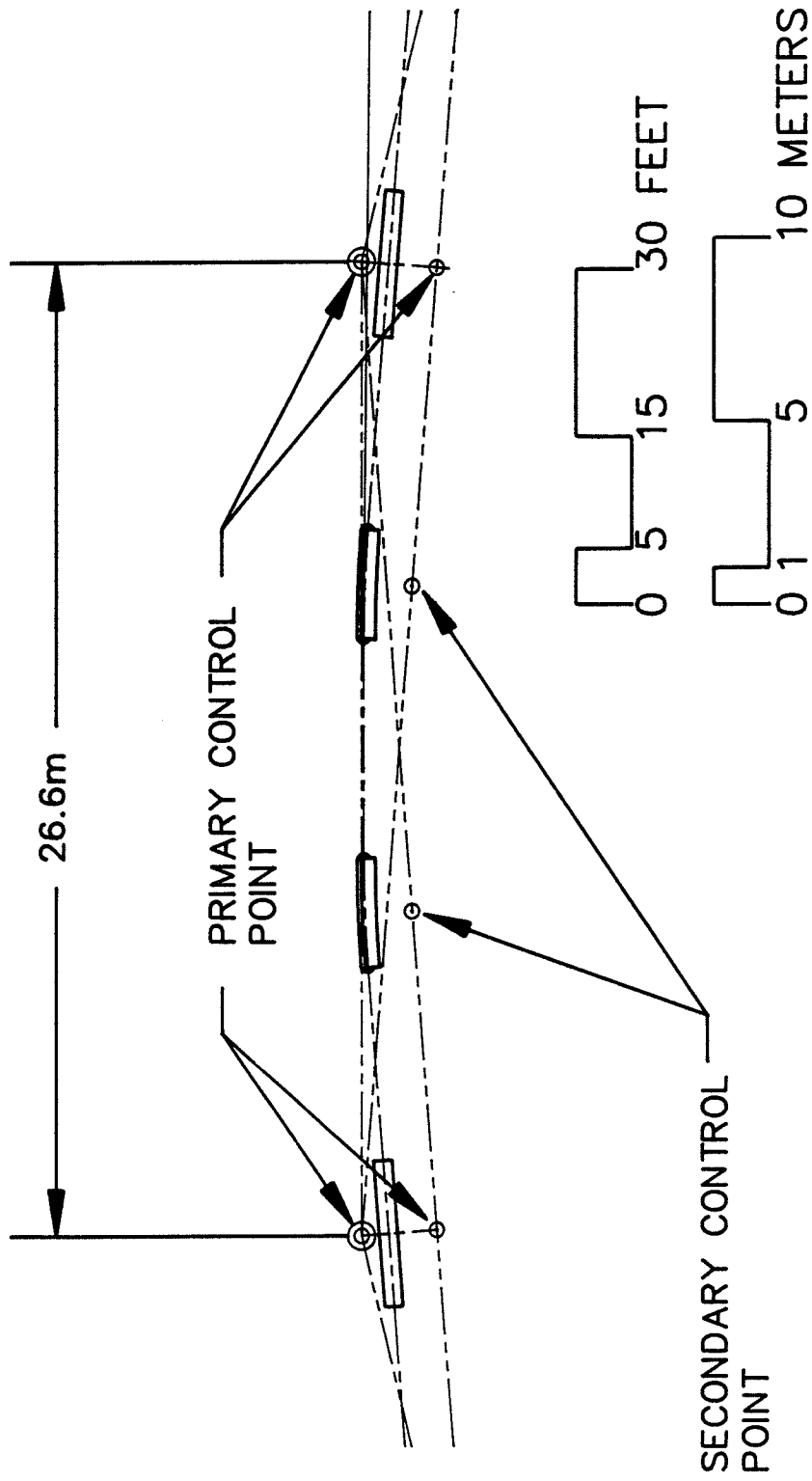


Figure IV.2.4-2
Position of control points in one cell of the storage-ring lattice.

IV. 2. TECHNICAL AND LEGAL DETERMINANTS

2.5 Vibration Control

2.5.3.1 Measurement Program [Replacement]

The vibration measurement program consists of three measurement tasks: (1) Argonne site buildings/facilities, (2) ground motion in the vicinity of the storage-ring site, and (3) wave propagation velocities in soil.

For the purpose of obtaining data and insights to support the vibration study, a vibration survey of an existing accelerator facility, the Intense Pulsed Neutron Source (IPNS) at Argonne, was performed.⁽¹¹⁾ Various vibration excitation sources associated with the design and operation of the IPNS facility were selected for study as being representative of the type of sources and energy transmission paths to consider in the design of the light source facility. These sources include the following: coolant (water) flow through the beam line magnets; energizing the magnets; and, in the experiment hall, operating a large water pump, ventilating fans, and overhead crane. A preliminary analysis of results indicates that, with one or two exceptions, the rms vibration levels are below 0.1 μm , with the energy predominantly in the low frequency range (< 20 Hz). These amplitudes are well below the required level.

While it is expected that internal excitation sources will dominate, consideration is also being given to external sources. To this end, ground-motion measurements are being made in the vicinity of the storage-ring site. The results of these measurements will allow for assessment of the level and frequency content of the ground motion and the effect of microseismic activity, road and rail traffic, Argonne site facilities operation, and the like. Additionally, the attenuation characteristics of the ground will be measured and characterized.

Exploratory measurements of ground surface vibrations have been made at the site under "quiet" and "normal" site noise conditions.⁽¹²⁾ Most vibration energy seems to be associated with frequencies less than 20 Hz. Preliminary analysis of the vibration measurements suggests that "natural" ground vibrations may be less than those due to "cultural" noise in large experimental facilities. As discussed in Sec. IV.2.5.3.4, additional ground-motion measurements are planned.

As discussed above, energy associated with external excitation sources will be transmitted to the experiment hall and storage ring via body (compression and shear) and surface (Rayleigh) waves. Also, the vibration analysis methods require knowledge of the shear modulus that can be determined from the shear wave speed. For these reasons, it is important to measure the various wave speeds. In general, the wave speed will be a function of the type of soil and soil substructure and will vary as a function of depth. Wave speed measurements are being made at the storage-ring site with in-situ seismic refraction testing methods.

IV. 2. TECHNICAL AND LEGAL DETERMINANTS

2.5.3.2 Modeling/Analysis Program [Replacement]

The vibration study modeling/analysis program includes the development of models that, among other things, account for soil structure interaction. Because of the complexities and uncertainties associated with modeling soil structure interaction, simplified models will be used to obtain insights into the dynamic behavior of the experiment hall floor slab in response to ground motion and operating equipment mounted on the floor. Initially we will model the experiment hall as a flexible slab resting on an elastic foundation. Results of elastic-half-space theory with a knowledge of shear modulus and Poisson's ratio allow us to calculate equivalent springs and dashpots for the soil for use in mass-spring-dashpot models. Results from the scoping models and ground-motion measurement will dictate whether more detailed models (for example, finite-element models) are required.

The magnet support system, on the other hand, represents a much better-defined structural system. For this system, detailed models are being developed and studied to obtain the dynamic characteristics (natural frequencies and mode shapes) of the system and the transfer functions between floor motion and magnet response.⁽¹³⁾ Among other things, the models and analysis results will be used to optimize the design of the support systems (e.g., location of supports relative to bending vibration modes of the magnet-supporting girder) to minimize the transmission of vibration energy from the floor to the magnets.

2.6 Life Safety Provisions [Replacement]

Because of the unique organization, construction, and functions of the APS facility, several kinds of life safety provisions have been implemented in the design of the conventional facilities. The storage-ring enclosure is essentially a shield around the storage ring. Door openings through this enclosure would by definition be weak points in the shielding. Such openings are therefore not acceptable for constructing exits. Although this is normally an uninhabited space, a peak population of twenty persons in a section of the enclosure during a technical component "emergency" has been postulated. Emergency exits from this enclosure are limited to four mazes from the infield side of the ring and three mazes opening to the experiment floor side from the enclosure. Maximum travel distances are about 400 ft, which is allowable for this type of structure.⁽¹⁴⁾

On the experiment floor of the experiment hall, a 3-ft-wide "stay clear" path has been defined near alternate beam lines from the ratchet wall to the outer perimeter wall. No utility lines or equipment are allowed on these paths, which constitute an assured clear exiting lane through the otherwise congested area.

Experiment hatches and office cubicles requiring internal sprinkler-type fire protection will be tied to the experiment hall sprinkler system. Additional fire

IV. 2. TECHNICAL AND LEGAL DETERMINANTS

protection, such as Halon or hand-operated extinguishers, is provided where needed as part of the hutch or cubicle construction.

Roadways are provided around both the inner and outer perimeters of the experiment hall and over the synchrotron building to the infield of the synchrotron to provide emergency vehicle access to all parts of the facility.

2.9 Environmental Compliance

2.9.1 Approach to Environmental Compliance [Replacement]

In accordance with the National Environmental Policy Act (NEPA) and to meet the U.S. Department of Energy Guidelines for compliance with NEPA (see DOE Order 5440.1B), the procedures in DOE's Environmental Compliance Guide (Rept. DOE/EV-0 132 Vol. 1, Feb. 1981) are followed. On the basis of information on the expected impact on the environment of the construction and operation of the facility, provided to DOE in an action description memorandum, permission was received from the DOE Assistant Secretary for Environment, Safety, and Health to prepare an environmental assessment (EA). The preparation of an EA for this project has been carried out by Oak Ridge National Laboratory and is now complete. The early identification of potential environmental effects will help ensure proper compliance with minimum impact on schedule by allowing coordination and integration of the NEPA process during the design-development phase.

The preparation of the EA entailed a comprehensive review of the action with regard to federal, state, and local environmental statutes and regulations. In addition, surveys for cultural resource sites of historic and prehistoric periods have been undertaken and coordinated with the State Historic Preservation Officer.

2.10 References [Replacement]

1. H.J. Moe and V.R. Veluri, "Shielding Estimates for the ANL Advanced Photon Source," ANL Report, Light Source Note LS-90 (1987).
2. H.J. Moe, "Radiological Impacts from Operation of Argonne Synchrotron X-ray Source," ANL Report, Light Source Note LS-84 (March 1987).
3. H.J. Moe and V.R. Veluri, "Shielding Estimates for the ANL 6-GeV Synchrotron Light Source," ANL Report, Light Source Note LS-55 - Revised (March 1987).
4. H. Moe, "Recalculation of Shielding for the Addition of a PAR," ANL Report, Light Source Note LS-116 (May 1988).

IV. 2. TECHNICAL AND LEGAL DETERMINANTS

5. H. Moe and M. Knott, "Dose Estimates for the Heavy Concrete Ratchet Wall Configuration," ANL Report, Light Source Note LS-117 (May 1988).
6. U.S. Department of Energy, "Requirements for Radiation Protection," DOE Order 5480.1, Chg. 6, Chap. IX-3 (1981).
7. U.S. Department of Energy, "Proposed Revision of DOE Order 5480.1A, Radiation Standards for Protection of the Public," memorandum dated Sept. 17, 1984, Ref. PE-243 (1984).
8. W.P. Swanson, P.M. DeLuca, R.A. Otte, and S.W. Schilthelm, "Aladdin Upgrade Design Study: Shielding," University of Wisconsin (1985).
9. A. Rindi and R.H. Thomas, "Skyshine-A Paper Tiger?," Particle Accelerators, Vol. 7, 23-39 (1975).
10. K. Batchelor, ed., "National Synchrotron Light Source Safety Analysis Report," Brookhaven National Laboratory (July 1982).
11. J.A. Jendrzejczyk, R.K. Smith, and M.W. Wambsganss, "Vibration Survey of IPNS Beam Line Magnets and Experiment Hall," ANL Report, Light Source Note LS-89 (1987).
12. D.L. McCowen and R. Brown, "Ground Vibration Measurements Near the Site of the Proposed ANL Light Synchrotron Radiation Facility," ANL Report, Light Source Note LS-49 (January 1986).
13. W. Chou, "Emittance Growth due to Ground Motions," ANL Report, Light Source Note LS-88 (1987).
14. M.J. Knott, "Entrance Maze Locations for the Storage Ring Tunnel," ANL Report, Light Source Note LS-83 (February 1987).

IV. 2. TECHNICAL AND LEGAL DETERMINANTS

III. 3. BUILDING SYSTEMS DESCRIPTION

3.1 Machine Support

3.1.1 Introduction [Replacement]

This section describes the buildings and facilities that support the various accelerator and storage-ring systems. All of these buildings are located in the infield region of the experiment hall in order to provide 360-degree utilization of the storage ring for experimental facilities. The structures are basically defined by the dimensional and functional requirements of the accelerators (see Fig. IV.3.1-1). The final dimensions have been determined by actual equipment sizes and placement.⁽¹⁾

The building designs are purely functional, and amenities are minimal. Air-conditioning is provided only in essential areas, such as accelerator containment structures, small electronics interfacing and control rooms, and the few laboratories and offices in the synchrotron injection building.

A control tunnel connects the accelerator buildings (linac, synchrotron injection, and synchrotron extraction) with the south end of the support wing of the central laboratory/office building, where a stairway and utility chase allow a convenient route to the control room in that building. This minimum length "spinal column" tunnel carries computer network and control signals, communication wiring, utilities, and personnel traffic between the various buildings. The same tunnel is used to house waveguides carrying rf power to the north-side cavities of the synchrotron. From the synchrotron extraction building, passage can be made to the storage-ring control area located atop the ring roof.

Control system, vacuum, and diagnostic equipment and multipole power supplies for the storage ring are located atop the ring tunnel roof, with their communication lines and utilities distributed along the inner wall of the experiment hall. Periodic slots through the ring inner shield wall at the ceiling level and an internal tray system carry wiring to the storage ring itself.

The two rf/power buildings contain the rf klystrons and waveguides for the storage ring. The third-harmonic rf system and the storage-ring magnet power supply are each contained in one of these two buildings. A small air-conditioned room is provided in each of these buildings to accommodate the critical electronics and control system components. The remainder of the buildings are provided with heating and ventilation only.

Nearly all buildings have been designed with some provision for future expansion. The linac gun-end shielding is made up with removable concrete blocks to allow expansion of the linac system. The positron linac and accumulator ring are shielded with

III. 3. BUILDING SYSTEMS DESCRIPTION

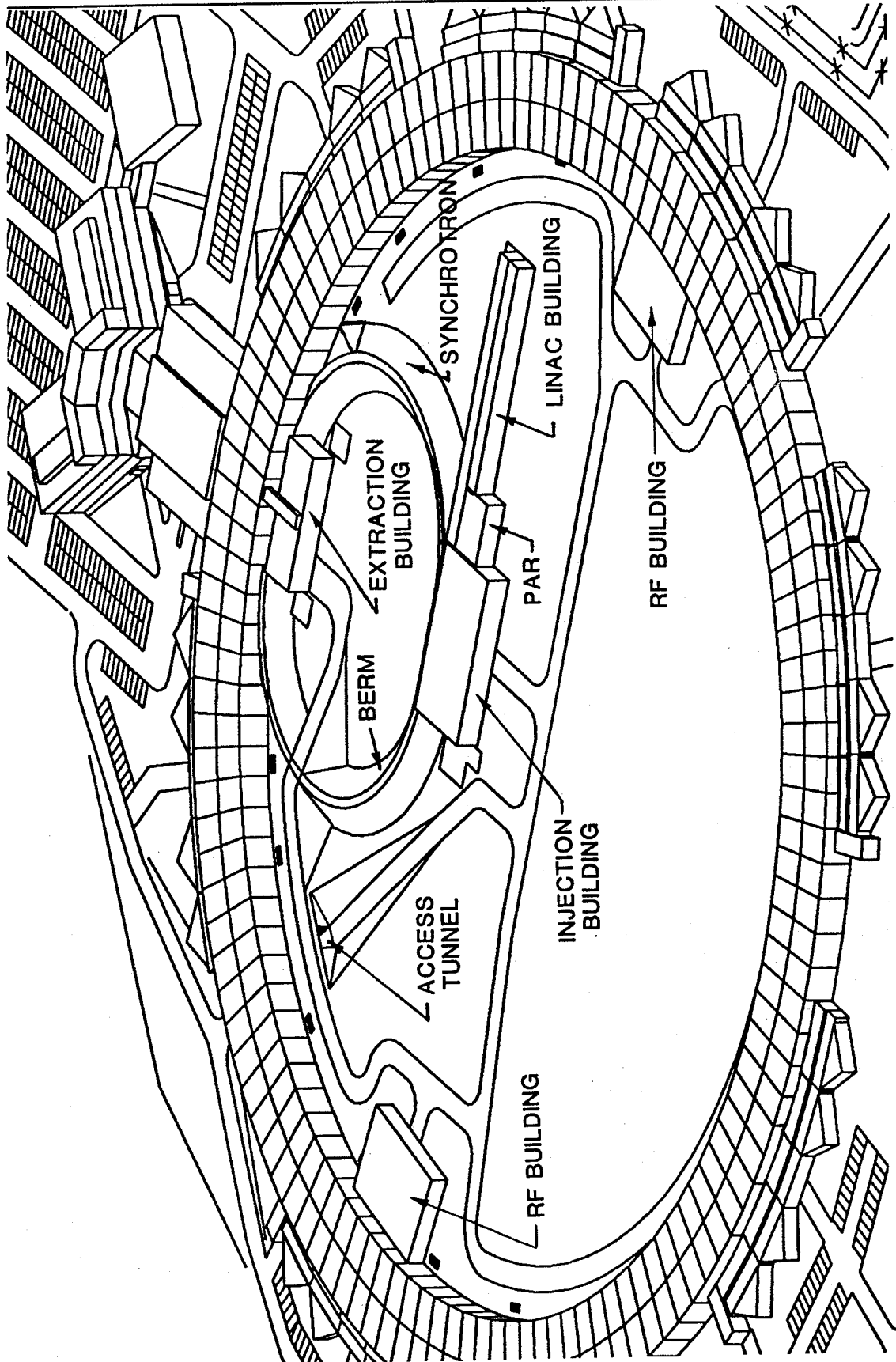


Figure IV.3.1-1
Infield isometric projection.

III. 3. BUILDING SYSTEMS DESCRIPTION

concrete blocks to allow future test beam activities on the floor of the synchrotron injection building. The full-energy positron beam dump area has been provided with full concrete wall shielding instead of an earth berm to allow future use of this beam. Finally, the two rf/power buildings have identical dimensions to allow the installation of a fourth rf power system.

A shield wall configuration is provided to allow occupation of the synchrotron during storage-ring operation and vice versa. Initial operation may require temporary stay-clear barriers because of possible beam losses.

Radiation-safe entrances to the linac are provided by a maze in the linac gun area and a maze in the positron accumulator ring (PAR) area. Access to the synchrotron is by moving block doors from the synchrotron injection and extraction buildings and by maze to the storage-ring tunnel in the beam transfer area. Infield-side entrances to the storage ring are by mazes from each of the rf/power buildings, a maze in the beam transfer area, and a maze in the south portion of the ring. Access to the storage ring from the experiment hall side are by mazes near the injection and rf straight sections. These placements of access/egress points for the storage ring result in maximum travel distances of about 400 ft, which is a fire safety requirement for this type of structure. The moving block doors giving access to the photon beam front-ends are not considered fire safety exits.

Construction staging for the two linacs, the PAR, and the synchrotron technical components occurs in the synchrotron injection building. Equipment is moved through the removable-block-shielded areas. The control tunnel is used to transport equipment from this staging area or from the central laboratory/office building to the synchrotron extraction building. Construction staging for the storage ring occurs in the experiment hall, with equipment passed through the roof hatches in the straight-section regions.

3.1.2 Linac Building [Replacement]

The one-story linac building is composed of two parts: the linac enclosure and the klystron gallery, which are parallel to each other and share a common wall along their entire length. The linac enclosure houses the electron and positron linear accelerators and the PAR, while the klystron gallery encloses the associated klystrons and other equipment. At its west end, the linac building is connected to the synchrotron injection building.

The rectangular klystron gallery is 286 ft long by 20 ft wide and 19 ft high. At the east end near the PAR, the gallery widens to 45 ft to cover the PAR enclosure, for a gross klystron-gallery area of 6555 ft². The interior of the 286-ft-long linac enclosure is 9 ft wide by 9 ft high, except in the PAR area where it widens to 40 ft, for a gross linac-enclosure area of 6596 ft². This space is surrounded by radiation protection material -- 6.5 ft (2 m) of concrete on the klystron-gallery side and 3.25-ft-thick (1-m-thick) concrete roof and wall, with earth berm on the roof and opposite side, respectively. The

III. 3. BUILDING SYSTEMS DESCRIPTION

PAR area is enclosed with 4.3-ft-thick (1.3-m-thick) concrete walls and 4.9-ft-thick (1.5-m-thick) concrete roof, the west end being composed of removable concrete blocks 4.9 ft (1.5 m) thick to form an entrance maze. Figure IV.3.1-2 shows plan and section views of this building. The low-energy (east) end shielding enclosure is 2 m thick and is made of removable concrete blocks.

3.1.2.1 Architecture [Replacement]

The interior of the klystron gallery is open to accommodate technical component equipment along the length of the linac enclosure. The klystron gallery is entered from the synchrotron injection building and has an emergency exit at the opposite end.

There are no interior partitions or doors in the linac building except for those forming the linac and PAR enclosures. The radiation protection afforded by the 6.5-ft-thick (2-m-thick) concrete shielding is augmented by 1-ft-thick steel plates in the walls and roof that extend for 16 ft (5 m) in the positron target area near the middle of the building. An additional 1-ft thickness of concrete wall is provided for 33 ft (10 m) in the target area.

Conduit, piping, and ductwork in the enclosure are exposed and unpainted. Floors are exposed, surface-hardened concrete. No furnishings are provided for this building.

The windowless exterior of the klystron gallery is clad with 4-in. insulated metal panels supported on horizontal girts. The roof of the klystron gallery is protected by a single-ply roofing membrane, board insulation, and ballast in an inverted roof membrane assembly (IRMA) system conforming to Argonne's current standard. The outer wall and roof of the linac enclosure shielding is covered with a waterproofing membrane and an earth berm.

Unistrut channels are cast into all usable linac and PAR enclosure walls and ceilings and the klystron side of the shielding wall. The channel (1-5/8 in.) is embedded in the concrete on 6-ft centers, vertically on the walls and across the width of the enclosure on the ceilings, to form a rack for mounting equipment.

3.1.2.2 Structure [Replacement]

The structural system for the klystron gallery consists of a beam and girder roof system supporting a welded metal deck with wide flange columns with spread footings. A 9-in.-thick reinforced concrete floor slab rests on 6-in.-thick compacted granular backfill.

A shielding wall separates the linear accelerator from the adjacent klystron gallery and is constructed of reinforced concrete, 6.5 ft thick. The opposite wall and the roof of the linac, also of reinforced concrete construction, are 3.25 ft thick. The walls (4.3 ft thick) and roof (4.9 ft thick) of the PAR enclosure area are of reinforced

III. 3. BUILDING SYSTEMS DESCRIPTION

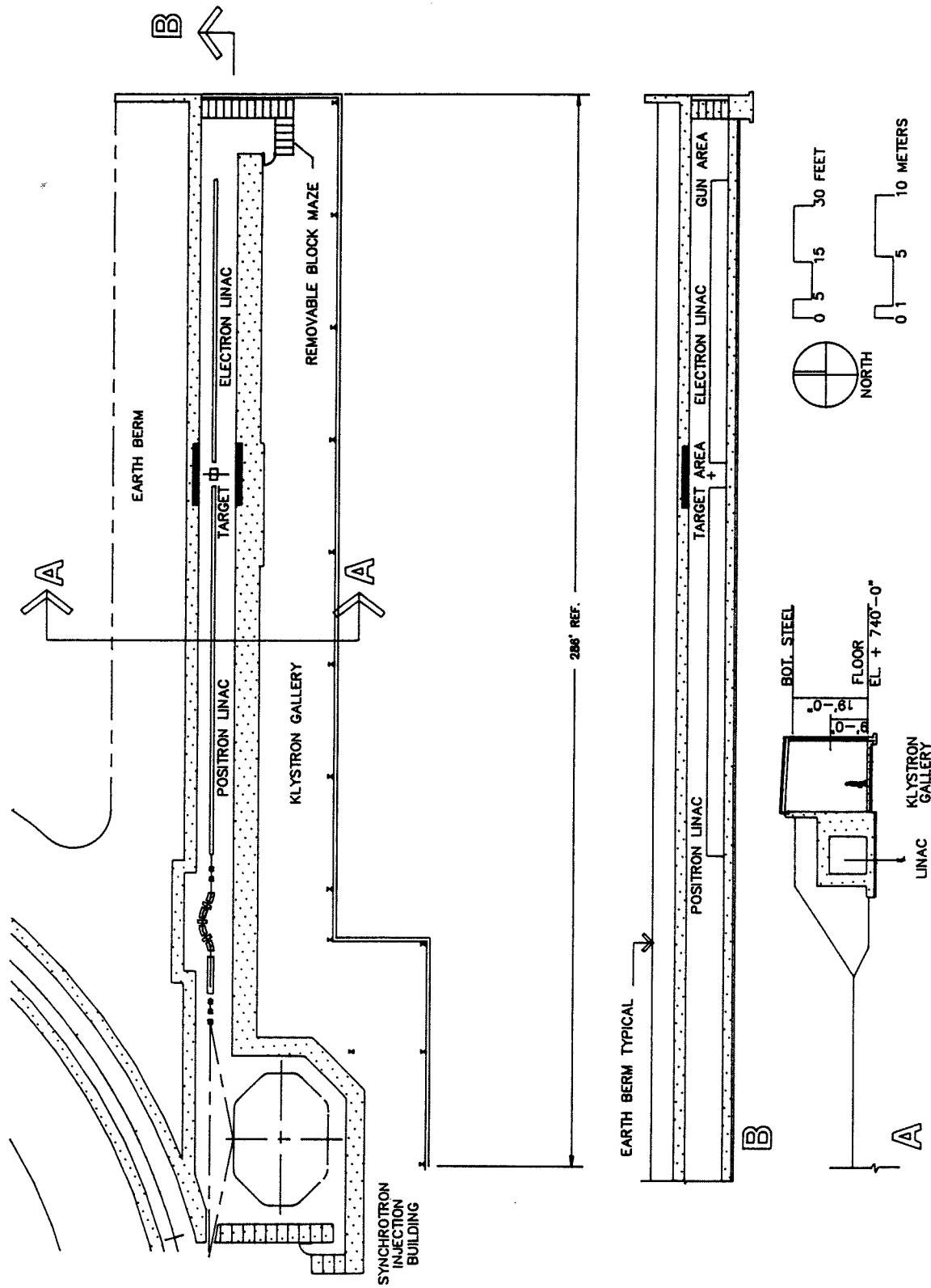


Figure IV.3.1-2
Linac building.

III. 3. BUILDING SYSTEMS DESCRIPTION

concrete. Compacted backfill placed on top of the roof and against the outer wall provides additional shielding. This shielding berm, with a slope of approximately 1 vertical in 1.5 horizontal, is protected against erosion. The slab on grade for the linac consists of a 2-ft-thick reinforced concrete slab over 6 in. of compacted granular backfill.

3.1.2.3 Heating, Ventilation, and Air-Conditioning (HVAC) [Replacement]

The klystron gallery of the linac building, although not air-conditioned, is ventilated with outside air to limit the maximum space temperature to 10°F above the outside ambient temperature during the summer. For this purpose, three $4000\text{-ft}^3/\text{min}$ supply fans with steam coils and exhaust fans are provided. In winter, six unit heaters with steam coils and integral thermostats operate to maintain the space temperature above 60°F when process equipment is not operating. No space humidification is provided.

The linac and PAR enclosures are air-conditioned to maintain a space temperature of $75^{\circ}\text{F} \pm 2^{\circ}\text{F}$ year-round. Two 100% outside air units at $1300\text{ ft}^3/\text{min}$ each with steam and chilled water coils supply conditioned air to each end of the enclosure. Two fans exhaust air from the middle of the enclosure, and three fan coil units with integral thermostats located along the inside of the enclosure provide cooling, heating, and dehumidification. No space humidification is provided. Chilled water and steam are supplied from a connection through the control tunnel to the utility loop above the storage ring. A direct digital controller (DDC) in this building controls the HVAC equipment.

3.1.2.5 Electrical Power [Replacement]

Electrical power is distributed to the linac building at 480Y/277 V from a substation located in the synchrotron injection building.

The klystron gallery is lighted with high-bay, high-pressure sodium fixtures to an average of 30 footcandles of illumination. Lighting in the linac and PAR enclosures consists of two-lamp, wall-mounted fluorescent fixtures mounted on 8-ft centers, switched from lighting panels.

An equipment grounding system is provided from connections on each piece of equipment to grounding conductors running with all power feeders. Lightning protection is provided by copper rods mounted around the perimeter of the roof. These rods are connected by copper cables Cadwelded to the building structural steel. A building ground system uses bare copper cable Cadwelded to the building structural steel, which is connected to ground rods spaced around the building. In addition, all computers and related equipment are provided with a separate quiet grounding system that is isolated

III. 3. BUILDING SYSTEMS DESCRIPTION

from the other grounding systems and is connected to a separate counterpoise and ground rod system.

The fire alarm system consists of manual-pull stations located at the building exits and flow and tamper switches in the sprinkler system. Smoke detectors are installed throughout the building and in the HVAC system. The alarm system is annunciated at the Argonne fire station and at the APS security point in the main control room.

Telephone communications are a branch from the private branch exchange (PBX) in the central laboratory/office building, with a telephone terminal cabinet in the klystron gallery.

3.1.3 Synchrotron Injection Building [Replacement]

The synchrotron injection building is located between the linac building and the synchrotron enclosure. The building houses the beam transfer area, where the beam of positrons from the PAR is injected into the synchrotron. Included within the building are the synchrotron power supplies, linac test beam areas, and injection facility control room. The synchrotron injection building also serves as the southern terminus of the control tunnel.

The building incorporates portions of the synchrotron and PAR enclosures, in addition to the concrete enclosure for the beam transfer area, as shown on Fig. IV.3.1-3. Removable blocks in the sidewall of the beam transfer enclosure allow redirection of the linac beam to targets in the building for test purposes.

This one-story rectangular building is 82 ft by 164 ft with a footprint of 13,138 ft² and a gross floor area of 14,605 ft², including a 1467-ft² mezzanine. The beam transfer area occupies 470 ft², and 3190 ft² is used for enclosed laboratory, electronic, control, and toilet/locker areas. Refer to Fig. IV.3.1-3 for plan and section views of this building.

3.1.3.1 Architecture [Replacement]

The interior of the building is open except for several small rooms in the southeast corner. The building may be entered from four directions: from grade along the south wall, from the klystron gallery on the east, through a block door from the synchrotron enclosure, and from the control tunnel to the synchrotron extraction building and central laboratory/office building. Access to the control tunnel from the main floor level is provided by a stairway and an elevator located at the southeast corner. Emergency exits are provided at several locations along the exterior building walls.

Interior partitions are of gypsum drywall construction with a painted finish. In the open areas, the roof structure is left exposed and unpainted; conduit, piping, and ductwork are also exposed and unpainted. In the small rooms in the southeast corner of the building, acoustical tile ceilings with recessed lighting and HVAC diffusers are

III. 3. BUILDING SYSTEMS DESCRIPTION

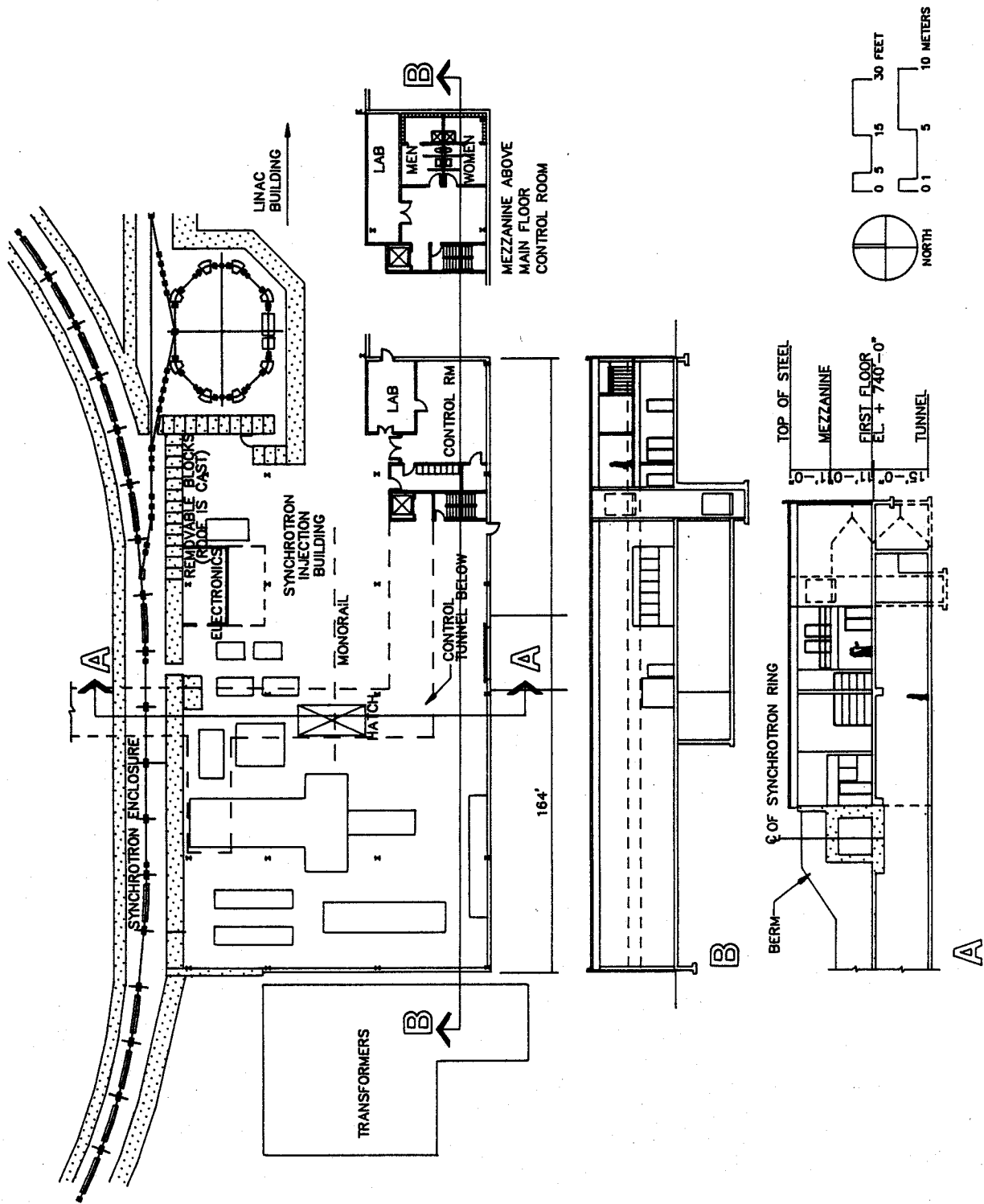


Figure IV.3.1-3
Synchrotron injection building.

III. 3. BUILDING SYSTEMS DESCRIPTION

suspended from the structure, with the electrical and mechanical distribution systems concealed in the ceiling space. The floors in the open area are exposed, surface-hardened concrete. In the small rooms, floors are covered with vinyl tile.

The windowless exterior of the building is clad with 4-in.-thick insulated metal panels supported on horizontal girts. A 14-ft rolling steel door accessible from the roadway on the south provides drive-in access for equipment deliveries. The roof of the building is protected by a single-ply roofing membrane, board insulation, and ballast in an inverted (IRMA) system conforming to Argonne's current standard.

Furnishings to be provided include desks, chairs, bookcases, and filing cabinets in the control room, and cabinets and counters along the long walls of the laboratories.

Unistrut channels are cast into the exposed wall of the beam transfer area and synchrotron enclosures. The channels (1-5/8 in.) are embedded vertically, 6 ft on center, to form a rack for the mounting of equipment.

3.1.3.5 Electrical Power [Replacement]

Electrical power is delivered to the synchrotron injection building from the 13.2-kV switchboard in the utility building via a 15-kV loop feeder to a 3750-kVA, 13.2-kV to 2400V, pad-mounted power transformer and a 2000 kVA, 13.2-kV to 480Y/277 V pad-mounted distribution transformer located adjacent to the building. The 480Y/277 V power is then distributed to the linac building, the synchrotron enclosure, and the synchrotron extraction building from the substation in the synchrotron injection building.

An equipment grounding system is provided from connections on each piece of equipment to grounding conductors running with all power feeders. Lightning protection is provided by copper rods mounted around the perimeter of the roof. These rods are connected by copper cables Cadwelded to the building structural steel. A building ground system uses bare copper cable Cadwelded to the building structural steel, which is connected to ground rods spaced around the building. In addition, all computers and related equipment are provided with a separate quiet grounding system that is isolated from the other grounding systems and is connected to a separate counterpoise and ground rod system.

The building is lighted by high-bay, high-pressure sodium fixtures for an average illumination of 30 footcandles. Lighting in the control room, laboratory, and electronics room is provided by 2-ft by 4-ft lay-in fluorescent fixtures, wall-switched in two levels.

The fire alarm system consists of manual-pull stations located at the building exits and flow and tamper switches in the sprinkler system. Smoke detectors are installed throughout the building and in the HVAC system. The alarm system is annunciated at the Argonne fire station and at the APS security point in the main control room.

III. 3. BUILDING SYSTEMS DESCRIPTION

Telephone communications are a branch from the PBX in the central laboratory/office building, with a telephone terminal cabinet in this building. Telephone outlets are provided in the electronics room and control room.

3.1.4 Synchrotron Enclosure [Replacement]

The synchrotron building is located between the synchrotron injection and synchrotron extraction buildings. The building houses the annular synchrotron in a rectangular concrete tube, which is partially buried and partially bermed with earth to provide radiation shielding.

The interior of the enclosure is 9 ft wide by 9 ft high, with 12 in. concrete ceiling and curved walls. Walls adjacent to the extraction and injection buildings are straight sections 4.9 ft thick. The enclosure forms an oval, 1210 ft in circumference, measuring 420 ft in the east-west direction and 330 ft in the north-south direction at the beam centerlines.

3.1.4.1 Architecture [Replacement]

The interior of the building is completely open. Entry to the usually uninhabited enclosure is through radiation-proof block doors in the synchrotron injection and synchrotron extraction buildings and through a maze from the storage-ring enclosure. Because strict operational procedures prevent access during operational periods when the doors are closed, no additional emergency exits are provided. The building is clad with membrane waterproofing and completely earth-covered.

To provide a mounting rack for technical equipment, Unistrut channels are cast into the walls and ceilings of the enclosure, as well as the surface on the outside of the enclosure adjacent to usable spaces. The channels (1-5/8 in.) are embedded every 6 ft on center, vertically on the walls and across the width of the enclosure on the ceilings. Conduit, piping, and ductwork in the enclosure are exposed and unpainted. The floors are surface-hardened concrete.

3.1.5 Synchrotron Extraction Building

Figure IV.3.1-4 (cited in Sec. IV.3.1.5 of CDR-87) is revised.

3.1.5.1 Architecture [Replacement]

The interior of the building is open except for the portion of the synchrotron enclosure that passes through the building, the shielded beam transfer area, and the stairway, elevator, toilet, and electronics room at the center of the south wall.

III. 3. BUILDING SYSTEMS DESCRIPTION

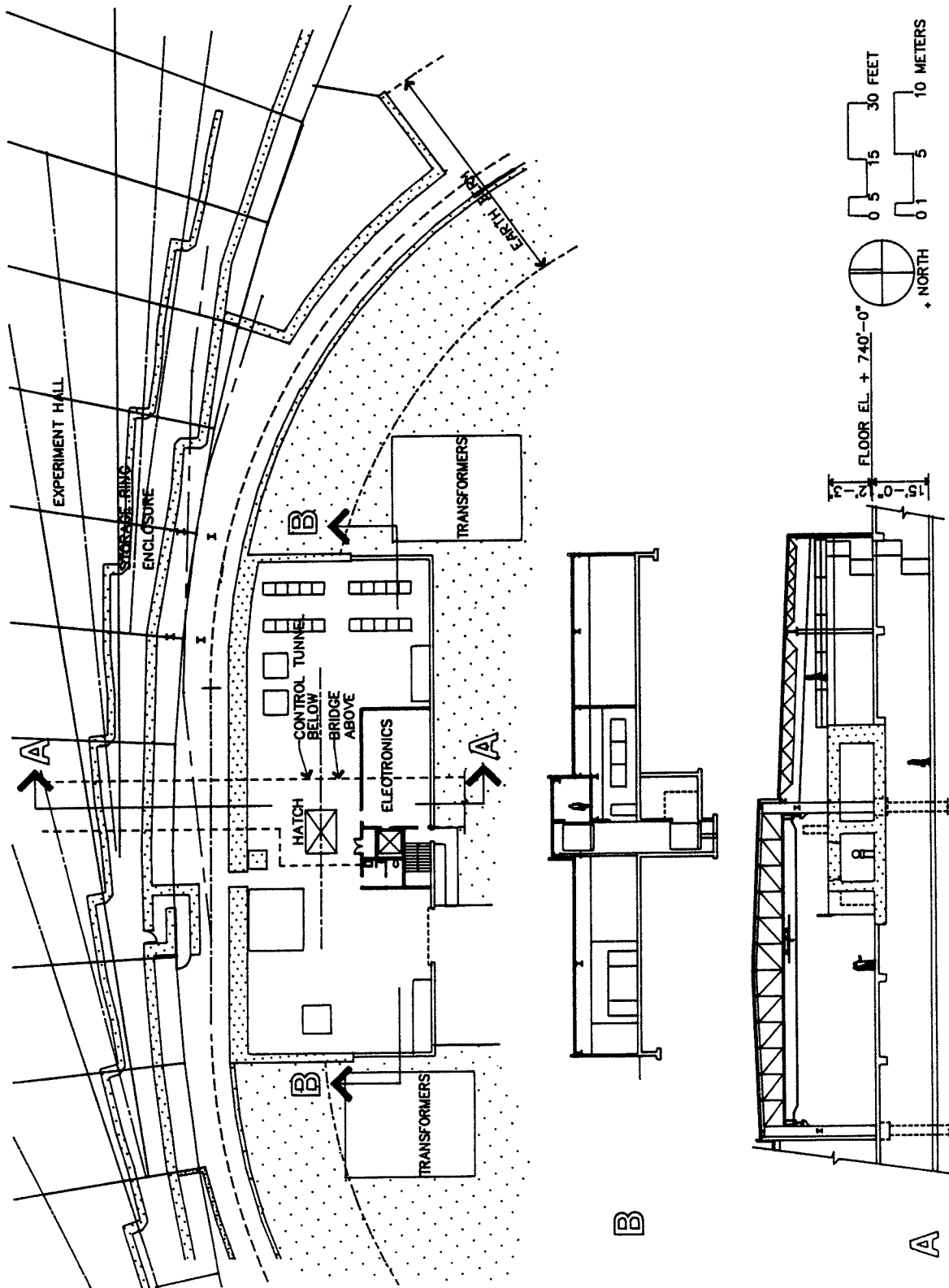


Figure IV.3.1-4
Synchrotron extraction building.

III. 3. BUILDING SYSTEMS DESCRIPTION

The building is entered from the control tunnel, through a block door from the synchrotron enclosure, or from the top of the storage-ring enclosure. Emergency exits are provided along the exterior wall. Access between the three floor levels is provided by a stairway and an elevator located at the southern edge of the building. Partitions are of concrete masonry construction with a painted finish.

Conduit, piping, ductwork, and the exposed underside of roof deck in the open areas are unpainted. In the electronics room, acoustical tile ceilings with recessed lighting and HVAC diffusers are suspended from the structure, concealing electrical and mechanical distribution systems in the ceiling space. The floors are generally exposed, surface-hardened concrete, except the floors in the electronics room, which are covered with vinyl tile. No furnishings are provided for this building.

The windowless exterior of the building is clad with 4-in.-thick insulated metal panels supported on horizontal girts. The roof of the building is protected by a single-ply roofing membrane, board insulation, and ballast in an inverted (IRMA) system conforming to Argonne's current standard.

Unistrut channels are cast into the exposed walls of the beam transfer area and synchrotron enclosures. The channels (1-5/8 in.) are embedded vertically 6 ft on center to form a mounting rack for technical equipment.

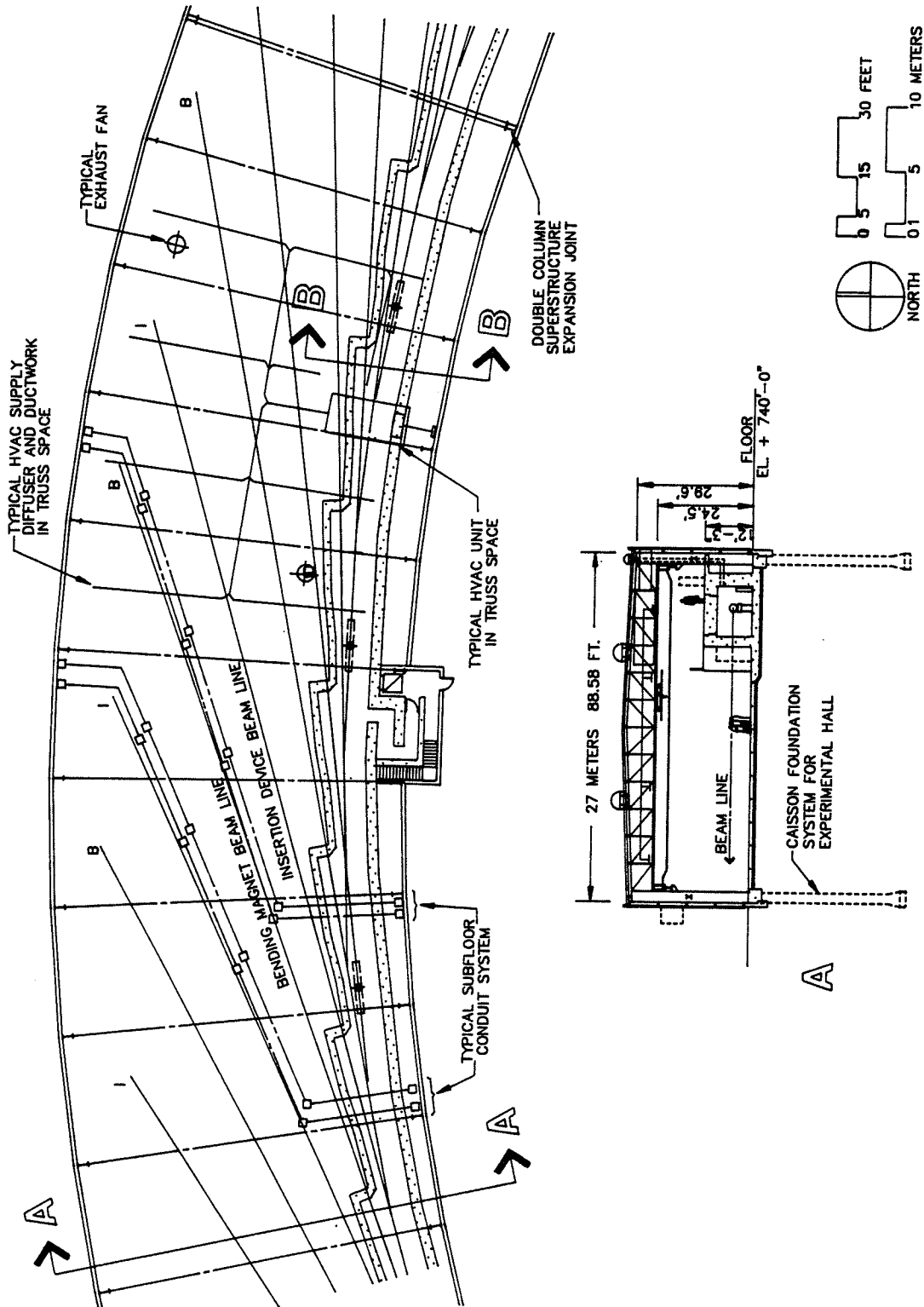
3.1.6 Storage-Ring Enclosure [Replacement]

The normally uninhabited storage-ring enclosure is located inside the inner perimeter wall of the experiment hall. The concrete tunnel-like enclosure, which is 3478 ft (1060 m) long, houses the storage-ring technical components. The primary purpose of the enclosure is to provide radiation shielding with its use of 2.6-ft-thick (0.8-m-thick) normal concrete for the inner wall, 1.8-ft-thick (0.56-m-thick) heavy concrete for the outer wall, and 3.25-ft-thick (1.0-m-thick) normal concrete for the roof. The enclosure is basically circular in plan, although the outer perimeter wall is composed of numerous "L"-shaped sections resulting in a ratchet-like configuration, as illustrated in Figs. IV.3.1-5 and IV.3.1-6. The short portions of the ratchet wall (normal to the photon beam line) are 2.6 ft (0.8 m) thick, and also of reinforced heavy concrete. The size and spacing of the sections are determined by the exit points of the photon beam lines. The resulting interior cross section of the enclosure varies from 11.6 ft to 18.9 ft wide, at a constant ceiling height of 9 ft clear inside. A detailed cross section through the enclosure is shown in Fig. IV.3.1-7.

3.1.6.1 Architecture [Replacement]

The interior of the storage-ring enclosure is open, with no intervening partitions. Entry from the experiment floor is provided by any one of three concrete mazes located near the injection and two rf regions, and by any one of 32 6.5-ft-long by 6.5-ft-high

III. 3. BUILDING SYSTEMS DESCRIPTION



SECTION A IS ALSO SHOWN ON FIGURE IV.3.2-1

SECTION B IS SHOWN ON FIGURE IV.3.1-7

Figure IV.3.1-5
Experiment hall segment.

III. 3. BUILDING SYSTEMS DESCRIPTION

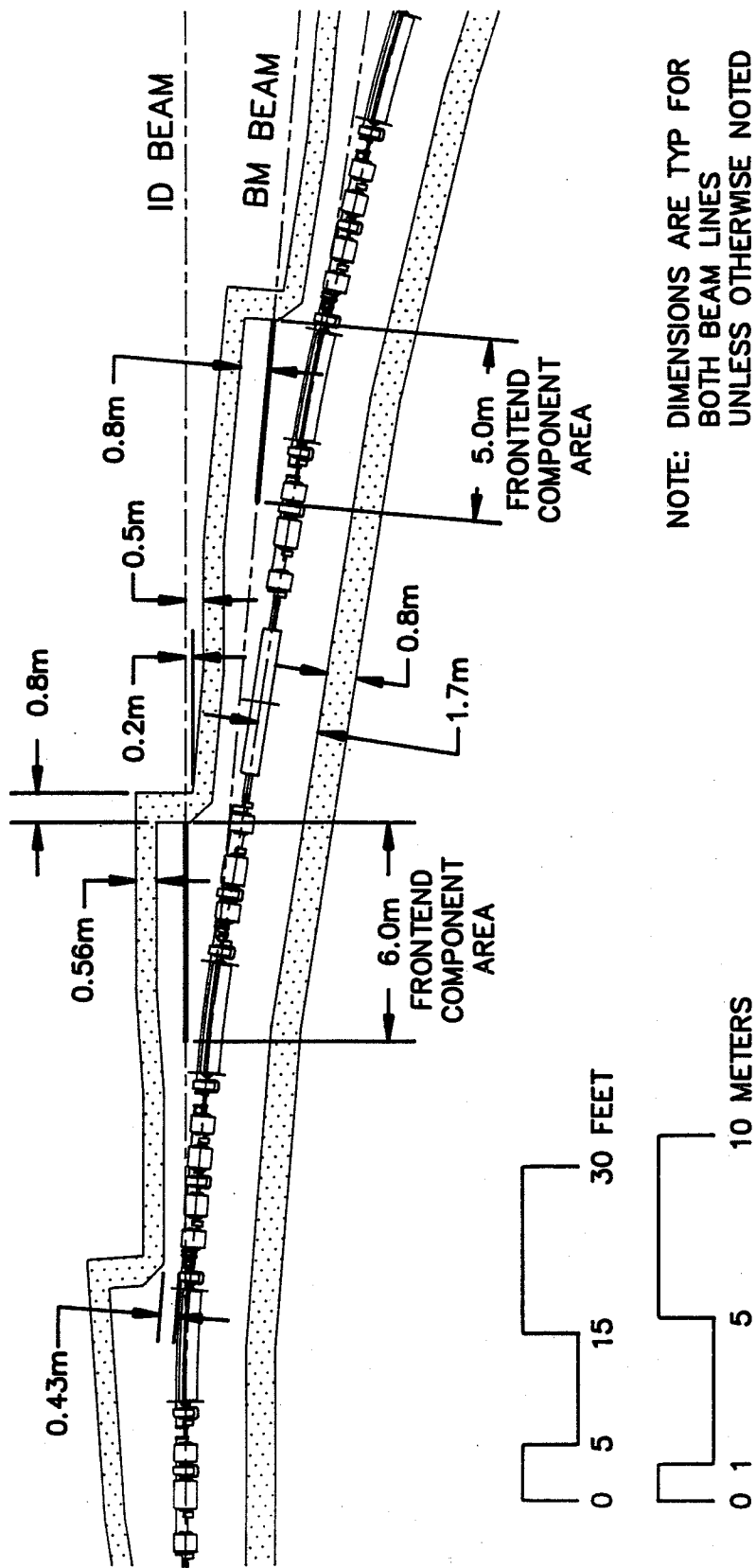
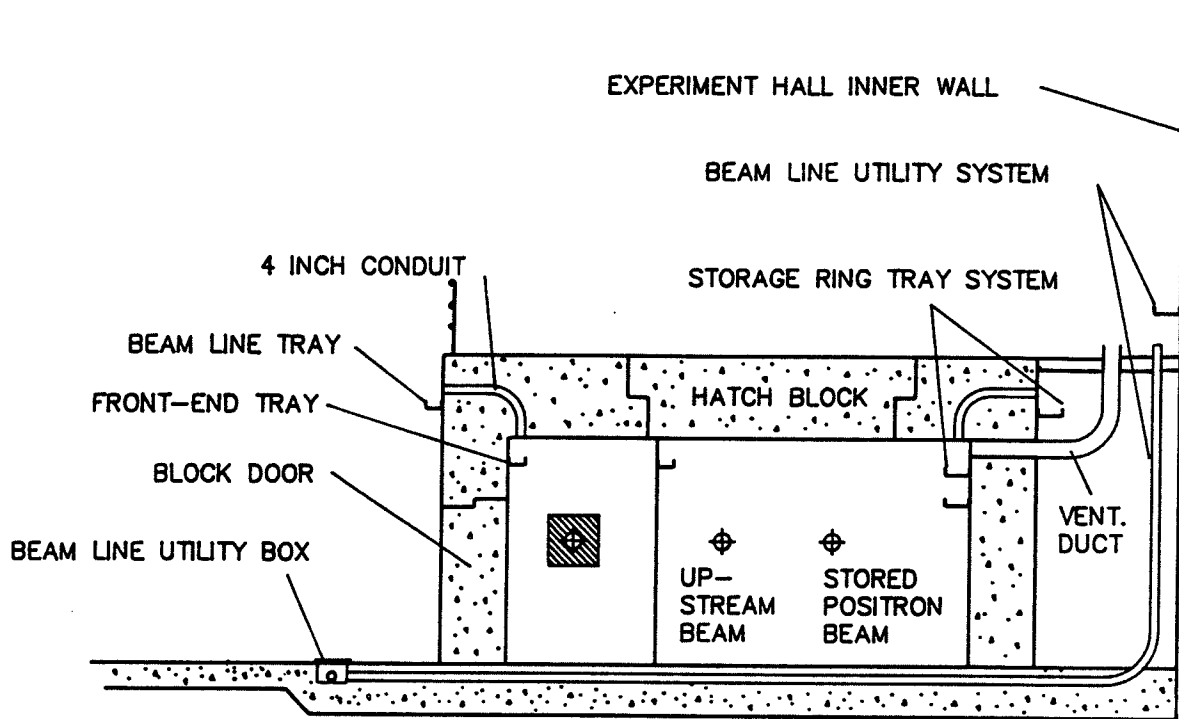


Figure IV.3.1-6
Ratchet-wall dimension details.

III. 3. BUILDING SYSTEMS DESCRIPTION



(SECTION B FROM FIGURE IV.3.1-5)

Figure IV.3.1-7
Cross section through storage-ring enclosure.

III. 3. BUILDING SYSTEMS DESCRIPTION

movable concrete doors that are located adjacent to each bending-magnet beam-line enclosure exit point. Entry from the infield side is provided by any one of four concrete mazes -- one each in the two rf/power buildings, the synchrotron injection building, and at the south end of the ring. Electronic and procedural controls ensure that alternative exit routes are available when the enclosure is open, and that no personnel are inside when the enclosure is sealed for normal operation.

Access between the roof of the enclosure and the main experiment floor level is provided by permanent stairways to the experiment floor near the rf/power and synchrotron injection buildings and to the infield area at the maze locations. In addition, an equipment lift is provided at each of the entrance mazes, except in the synchrotron injection building, where an elevator to the main floor and control tunnel is available.

Access to the storage-ring technical component may be attained by means of 40 large openings in the roof of the enclosure, one above each straight section. During beam operation, these openings are sealed by 3.25-ft-thick (1-m-thick) shielding cover blocks, which are removed and replaced as required using the experiment hall radial bridge crane.

Conduit, piping, and ductwork within the enclosure are exposed and unpainted. Unistrut channels are embedded into the concrete walls and ceiling at 6-ft intervals to provide support for the extensive utility loops that are needed. The same channel spacing is used on the outside of the outer perimeter wall of the enclosure, where it forms the ratchet wall of the experiment floor area. The interior floor and the technical equipment area atop the shield both have a surface-hardened finish.

3.1.6.2 Structure [Replacement]

The storage-ring enclosure is constructed with inner walls of 2.6-ft-thick normal concrete, outer walls of 1.8-ft-thick heavy concrete, and a roof of 3.25-ft-thick normal concrete, all of reinforced concrete construction. A 2-ft-thick reinforced concrete slab is set on 6 in. of compacted granular backfill. The base slab of the beam enclosure is separated from the experiment hall structure by expansion joints. Reinforced concrete cover blocks provide a roof access opening 3.25 ft thick, 8.2 ft wide, and 32.8 ft long. Steel framing along the block edges maintains true linear alignment, and inserts on top of the blocks facilitate removal and placement of the blocks by the overhead crane.

3.1.7 RF/Power Buildings (East and West) [Replacement]

The two rf/power buildings are each connected to the inner perimeter walls of both the storage-ring enclosure and the experiment hall, directly across the infield from each other at the "four o'clock" and "ten o'clock" positions, "twelve o'clock" being due north. These buildings house the rf klystrons for the storage ring and emergency power generators for the entire facility. In addition, one of the rf/power buildings houses the

III. 3. BUILDING SYSTEMS DESCRIPTION

dipole magnet power supply for the storage ring. Each provides a maze access point into the storage-ring enclosure from the inner perimeter side.

Each one-story rectangular building is 90 ft by 120 ft with a footprint and gross floor area of 10,800 ft², of which 600 ft² is devoted to the enclosed electronics area and sanitary facilities. A plan and a section through a typical rf/power building are illustrated in Fig. IV.3.1-8.

3.2 Experiment Support

3.2.1 Introduction [Replacement]

This section describes the buildings and facilities that support the experimental program and the general administration of the Advanced Photon Source. The most prominent feature is the experiment hall, and this structure determines the geometry and placement of most other buildings. Because of the large size of this building and the fact that it has a controlled environment, its size was the subject of much optimization effort. The radial width is determined by the storage-ring cross section and shield wall thickness plus the floor area needed for photon beam lines. The maximum beam-line length accommodated within the building is 80 m measured from the radiation source point. The addition of a 3-m equipment circle and a 1.5-m outer aisle space results in a building width of 27 m. The height of the building is determined by the necessary roof truss depth, crane depths, and the hook clearance of 21 ft (6.4 m). The hook clearance will allow 10-foot-high structures to be moved over each other. The crane clearance over the storage-ring roof is 8.75 ft and is sufficient for equipment racks and the removal of the 1-m-thick roof access-hatch blocks. The resulting building height is 32 ft (9.75 m).

Hatches with overlapping concrete cover blocks are provided in the storage-ring tunnel roof at each insertion-device location (including the injection and rf areas) to facilitate the installation of machine, insertion device (ID), and beam-line front-end components. The clear opening provided is 10 m by 2.5 m.

The length of beam line occurring outside the shield wall is determined by the lattice geometry, the shield wall thickness, and the beam-centerline-to-wall clearances. For the clearances shown in Fig. IV.3.1-6, the resulting ID beam-line length inside the shield is 29.2 m. For a bending-magnet beam line, this length is 26.7 m. The resulting beam-line length available outside the shield is 50 m for the ID beam and 52.5 m for the bending-magnet beam.

Access to the beam-line front-ends is provided by three maze entrances located near the injection and rf straight sections and by 32 movable block doors located at each bending-magnet front-end. Stairway access to the ring roof is provided at each maze and ladder access at each block door.

III. 3. BUILDING SYSTEMS DESCRIPTION

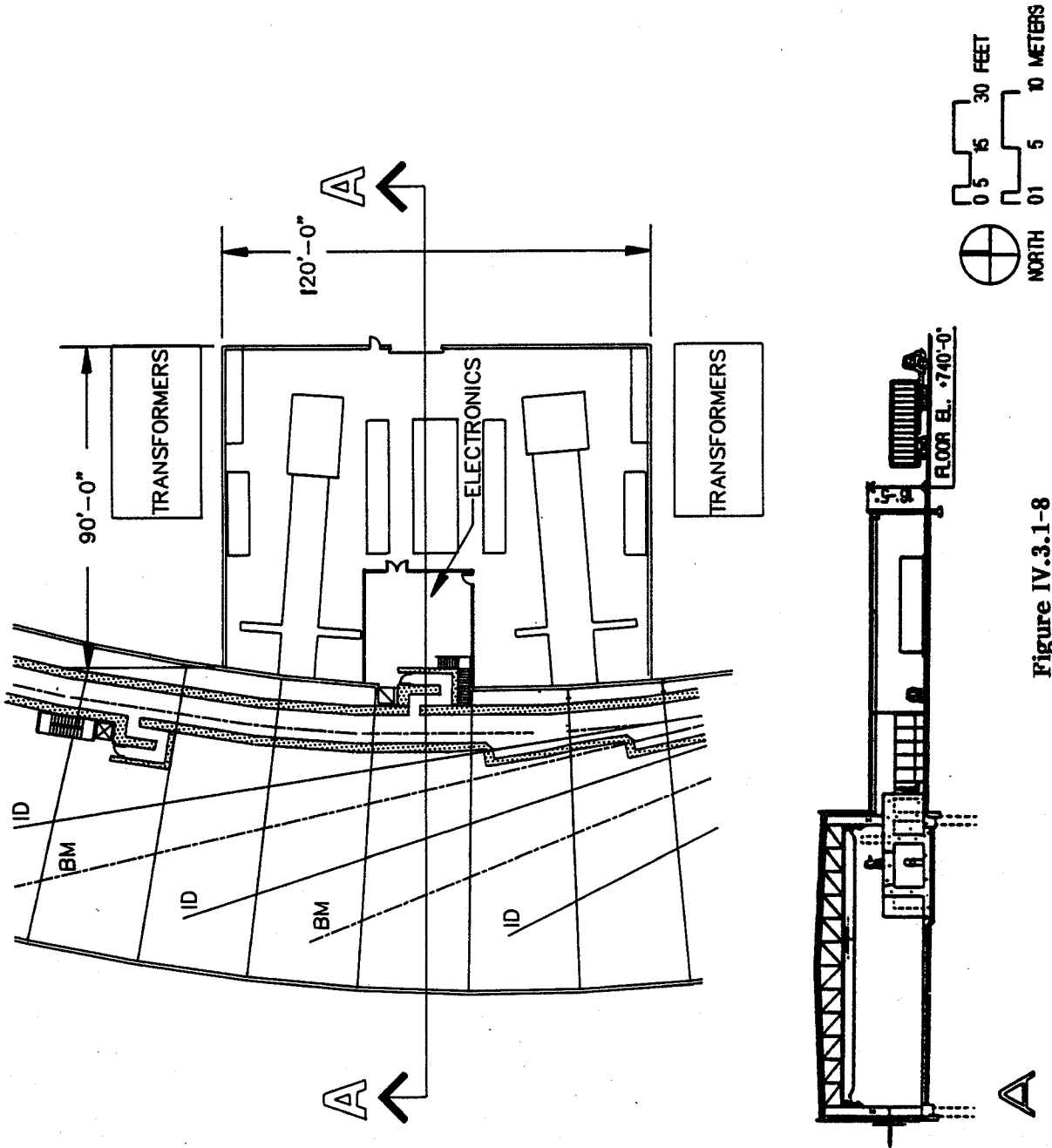


Figure IV.3.1-8
A section through a typical rf/power building.

III. 3. BUILDING SYSTEMS DESCRIPTION

Utility distribution to the beam-line front-end within the ring shield is from distribution centers located above the ring shield along the inner wall of the experiment hall. Utility distribution to the floor portion of the beam line is from these same distribution centers via an underfloor conduit system parallel to each beam line. Cooling water is routed through a dedicated conduit for use along the beam line. All conduits extend to the building outer wall to provide the capability of distributing computer network, communication, and special-purpose wiring.

The four laboratory/office modules provide laboratories, offices, meeting rooms, small shops, toilet/locker rooms, and kitchen and break areas in close proximity to the experimental stations. Modules can be equipped with either clean-room support facilities or a floor-level truck air lock and entrance to facilitate delivery and crane access for large equipment, while maintaining the building temperature and cleanliness.

The central laboratory/office building houses the administrative staff of the APS, operations and control staff, user liaison staff, Argonne-based research and development staff, central clean room, and shop facilities. It will also act as the central interaction point for all research activities. As such, this building has been given considerable design effort and some amenities and appearance features that will help define its role as the "front door" of the project. At the same time, construction efficiency and expansibility have been built in to allow nearly all of the building functions to be expanded in the future.

The support wing of this building, comprising the high-bay area, shops, clean room, and large assembly laboratories, will be constructed initially and will be used during technical component construction and assembly. The Class 1000 clean room can accommodate the long vacuum chamber sections common to the storage ring and insertion devices. The office wing, comprising the control and computer rooms, the lab and office sections, and the meeting facility, will be constructed later. The office wing contains space for a library and conference rooms for project activities.

The control room and the data analysis computer facilities are located in this building. High-performance computer networks link the data analysis computer system to the laboratory/office modules and beam lines. The data network can be extended to the proposed user housing facility, allowing high-performance terminal or workstation interaction with experimental equipment.

3.2.2 Experiment Hall [Replacement]

The single-story experiment hall is an annular structure housing both the storage-ring enclosure and the experiment floor, where the experiments are conducted.

The building is 91 ft wide by 3472 ft (1060 m) in circumference at the storage ring's centerline, for a gross area of 334,836 ft². Of that total, 52,000 ft² is occupied by the storage-ring enclosure, 19,200 ft² is reserved for the utility corridor between the

III. 3. BUILDING SYSTEMS DESCRIPTION

inner perimeter wall and the storage-ring enclosure, and 263,636 ft² is available for experiments. The clear height from the experiment floor to the underside of the trusses is 24.5 ft. See Fig. IV.3.1-5, Experiment Hall Segment, and Fig. IV.3.2-1, Experiment Hall Cross Section.

A system of underfloor conduits with access boxes on 33-ft centers provides a means of supplying process or chilled water, electrical power, and telemetry services to the beam-line experiments. These conduits parallel every experiment beam line.

3.2.2.1 Architecture [Replacement]

Except for the enclosed areas around the storage ring and the utility corridor at the inner perimeter, the experiment floor is a continuous open space.

Primary entry to the building is from the laboratory/office modules and the central laboratory/office building. Secondary entries are from the rf/power buildings, the synchrotron extraction building, and the maze entry at the south end of the infield. Emergency exits are provided at the outer perimeter end of every insertion-device beam-line position wherever a laboratory/office module is not covering the outer wall at that point. Passage between the experiment floor and the top of the storage-ring enclosure is provided by permanent stairways near the rf/power and synchrotron extraction buildings. Access to the interior of the storage-ring enclosure is provided by hydraulically-movable block doors, 6.5 ft high, 6.5 ft wide, and 1.8 ft thick, adjacent to each bending-magnet beam-line front-end.

Conduit, piping, ductwork, and the exposed underside of the roof deck are unpainted. The floors are exposed, surface-hardened concrete. Two radial 10-ton bridge cranes run on concentric tracks around the building to provide full crane coverage for the placement of experiment equipment and for the moving of shielding blocks on top of the storage-ring enclosure. No furnishings are provided in the experiment hall.

The windowless exterior of the building is clad with 4-in. insulated metal panels supported on 12-in.-wide horizontal girts. The roof of the building is protected by a single-ply roofing membrane, board insulation, and ballast in an IRMA system conforming to Argonne's current standard.

3.2.2.2 Structure [Replacement]

Trusses spanning 83 ft carry purlins and a welded metal deck. The trusses are spaced on 30.5-ft centers at the building center line, and frame into 33-in.-deep, wide-flange perimeter columns, to create a column-free interior in this annular building. A steel beam track directly below the truss system supports two 10-ton cranes, which span the experiment hall area. The trusses are arrayed in a radial configuration; purlins, girts, truss bracings, crane support beams, and bracing members located in the

III. 3. BUILDING SYSTEMS DESCRIPTION

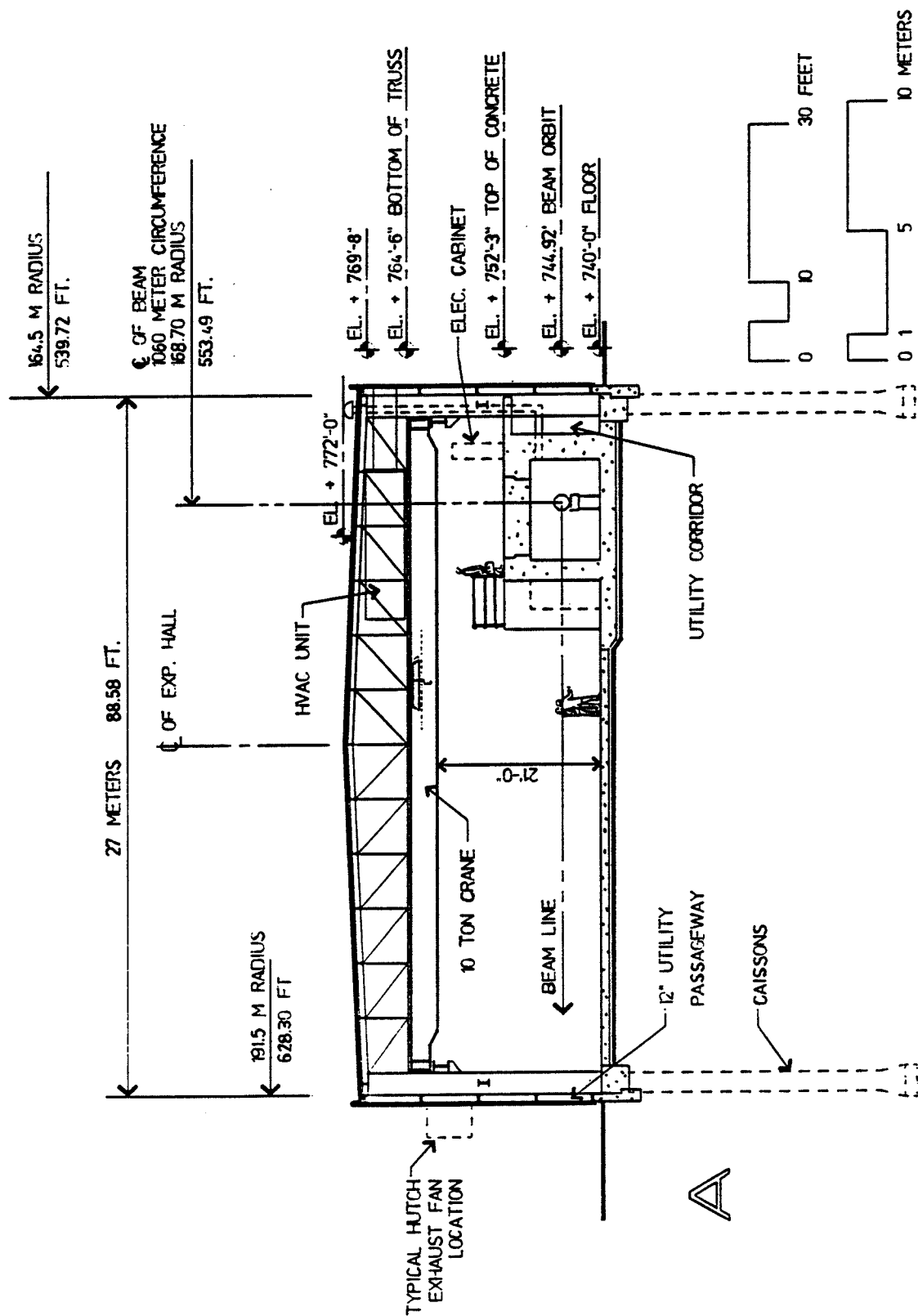


Figure IV.3.2-1
Experiment hall cross section.

III. 3. BUILDING SYSTEMS DESCRIPTION

exterior walls are installed on chords. The building is divided into ten segments, with expansion joints between them. A double set of trusses and columns, supported on single sets of caissons, occurs at each expansion joint. Reinforced concrete foundation members have the following dimensions:

<u>Component</u>	<u>Dimensions</u>
Caissons	2 ft, 6 in. diameter
Caisson bells	4 ft, 0 in. diameter, 40 ft below finished grade
Caisson caps	4 ft, 6 in. wide x 4 ft, 6 in. high x 2 ft, 6 in. deep
Grade beams	1 ft, 6 in. wide x 4 ft, 0 in. deep
Exp. hall slab	1 ft, 0 in. thick, on 6 in. compacted granular backfill
Storage-ring slab	2 ft, 0 in. thick, on 6 in. compacted granular backfill

In both the injector facilities and the storage ring, the guiding and focusing magnets around the beam tube are mounted on pedestals that are approximately 4 ft high and rest on reinforced concrete slabs. The magnets have adjustment capabilities at the pedestals to correct for vertical and lateral movements due to creep and soil settlements.

In order to minimize vibration transfer by isolating the source from the receiving system, the following provisions are included:

- Expansion joints are provided at the outer edges of the slab-on-grade of the experiment hall and storage ring, separating them from the other foundation members, to minimize vibration transfer from the structure to the machine foundation and experiment hall slab.
- Elastomeric bearing pads are provided beneath the base plates of the columns, to dampen vibrations generated by wind loads on the building exterior, by mechanical equipment supported from the trusses, and by movement of the two column-supported 10-ton cranes.

In order to minimize the vibration induced into the accelerators and storage ring, machines with moving parts are centrifugal rather than reciprocating, and these machines are installed with proper base-isolation devices. To limit the creation of additional cultural vibration, the moving of heavy loads across the building floor during beam-line operation is to be avoided.

3.2.2.4 Plumbing/Process Piping/Fire Protection [Replacement]

Plumbing systems in the experiment hall are limited to system loops of 4-in. domestic water, 3-in. laboratory service water, and process system loops of 3-in.

III. 3. BUILDING SYSTEMS DESCRIPTION

compressed air and 3-in. natural gas. These loops are routed around the inside of the utility corridor concentric with the storage-ring enclosure, with valved service adjacent to the starting point of each beam line's underfloor conduit system. Drainage systems include the sanitary waste system, with a floor drain located near the center of the building between alternate beam lines.

The 90°F equipment process water cooling loop (one megohm deionized) is located around the inner perimeter above the storage ring. Both the 40°F loop and the 90°F loop contain one valve per bay, at approximately 30-ft intervals around the inner perimeter of the ring. These valves are 2-in. connections to link to the technical component cooling equipment located in the storage ring.

A wet-pipe automatic sprinkler system is provided for fire protection. The experiment hall is divided into ten equal segments, with each segment a complete fire zone with individual water supply, control and drain valves, and alarm functions. Experiment hatches requiring internal fire protection are linked to the experiment hall sprinkler system. Automatic sprinkler systems are based on the requirements of NFPA 13, "Ordinary Hazard - Group 1," with protection provided by 1/2-in.-orifice sprinkler heads as approved by Factory Mutual for this occupancy. Hand-operated fire extinguishers are distributed in accordance with FM and NFPA requirements.

3.2.3 Laboratory/Office Modules [Replacement Section]

The four laboratory/office module buildings are connected to the outer perimeter wall of the experiment hall. The modules provide office, laboratory, and support facilities for researchers working with the beam lines in the immediate vicinity. The building design and complement of spaces is intended to provide each beam line with one laboratory and four office spaces in such a way that individual layouts can be made and special needs met. The common facilities located in the middle of the module provide shop space, toilet/locker rooms, a kitchen and break area, a meeting room, and a controlled-access entry point, all convenient to the offices, laboratories, and experiment hall.

There are 32 office spaces along the exterior walls and eight laboratories adjacent to the experiment hall in each module. Two of the modules have one of their laboratories configured as a Class 1000 clean room, with the blower and filter equipment located in an adjacent lab support room. The remaining modules use this additional room as a floor-level truck air lock to facilitate deliveries to the experiment hall. Additional facilities in each module include corridors and mechanical spaces. Each of the one-story buildings has a floor area of 19,000 ft². A floor plan of a typical module (equipped with a clean room and biology laboratory instead of a truck air lock) is shown in Fig. IV.3.2-2.

III. 3. BUILDING SYSTEMS DESCRIPTION

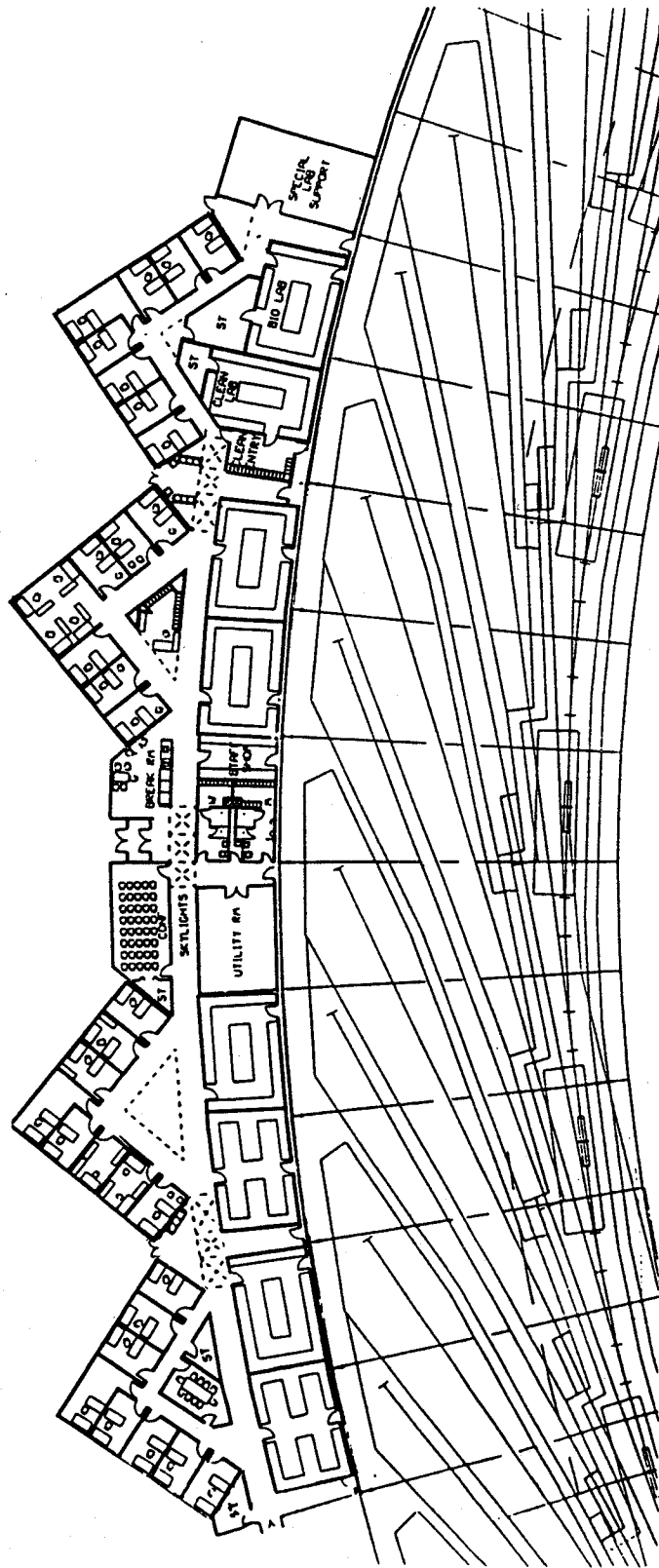


Figure IV.3.2-2
Typical laboratory/office module.

III. 3. BUILDING SYSTEMS DESCRIPTION

3.2.3.1 Architecture [Replacement]

The interior of each module is organized by a longitudinal corridor that provides access to laboratories, offices, common facilities, and entry points. Entry to the building is from the adjacent parking areas or from the interior of the experiment hall. Emergency exits are provided at several locations around the building.

Partitions are of gypsum drywall construction with a painted finish, except in the clean room laboratory (where provided), where special wall finishes are required. Acoustical tile ceilings with recessed lighting and HVAC diffusers are suspended from the structure, concealing the electrical and mechanical distribution systems in the ceiling space. Skylights over the longitudinal corridor at intersections with the three radial corridors provide outside awareness in interior spaces. Floors are covered with vinyl tile, except in the mechanical-equipment areas and in the truck air lock, where the floors are exposed, surface-hardened concrete.

The exterior of the building is clad with 4-in.-thick insulated metal panels. Energy-efficient thermal-break aluminum window frames with 1-in. insulating glass form a continuous band around the building exterior, except in the windowless truck air lock or lab support room. The roof of the building is protected by a single-ply roofing membrane, board insulation, and ballast in an IRMA system conforming to the current Argonne site standard.

Furnishings to be provided include desks, chairs, bookcases, and filing cabinets in the offices, and cabinets and counters along the walls of the laboratories.

3.2.3.3 Heating, Ventilation, and Air-Conditioning [Replacement]

The office area of each module will be maintained at a space temperature of $75^{\circ}\text{F} \pm 2^{\circ}\text{F}$ year-round and a relative humidity of 50% maximum in summer and 25% minimum in winter. A variable-volume air-conditioning unit sized at 25 tons, with a return fan, is located in the mechanical-equipment room of each module, and each office has a variable-volume terminal box to adjust space temperature to local conditions. A hot-water-baseboard heating system is provided in perimeter offices.

The laboratory area of each module is kept at a space temperature of $75^{\circ}\text{F} \pm 2^{\circ}\text{F}$ year-round and relative humidity of 50% maximum in summer and 25% minimum in winter. Two constant-volume air-conditioning units with a return fan located in the mechanical-equipment room are provided for air circulation. The temperature in each laboratory is individually controlled with a reheat coil at the supply air duct.

The clean room (where provided) is designed to meet Class 1000 standards. Equipment for this space maintains a temperature of $72^{\circ}\text{F} \pm 1^{\circ}\text{F}$ and relative humidity of $40\% \pm 5\%$ year-round. One $6000\text{-ft}^3/\text{min}$ air-handling unit (and one standby unit) supply air at a rate of $15\text{ ft}^3/\text{min}$ per ft^2 of floor area. Air is returned through an underfloor

III. 3. BUILDING SYSTEMS DESCRIPTION

plenum and vertical air shaft. Makeup air to this air-handling unit is supplied from the laboratory air-conditioning unit, to provide space dehumidification and pressurization.

Hot water is converted from steam in the mechanical-equipment room. Chilled water and steam are supplied from a connection to the utility loop above the storage ring. A direct digital controller in this building controls the HVAC equipment.

3.2.4 Central Laboratory/Office Building — Support Wing [Replacement]

As shown in Fig. IV.1.2-1, the project site plan, the support wing of the central laboratory/office building is located between the office wing of the same building and the north end of the experiment hall. The support wing houses the large-equipment assembly areas, oversize laboratories, clean room, and machine shops. It is of special importance during the machine assembly period as the technical components are prepared for installation.

As shown in the floor plan in Figs. IV.3.2-3 and IV.3.2-4, the building includes an 80-ft by 140-ft high-bay assembly area with full bridge-crane coverage, delivery truck air lock, Class-1000 clean room, five oversize laboratories, machine shops, offices, employee break area, and an observation area for visitors on the second-floor (mechanical-equipment) level.

The basically rectangular one-story support wing has a footprint of 27,000 ft² and a gross floor area of 34,500 ft², including a 7,500-ft² mechanical-equipment room above the clean room and lab areas along the east side of the building. The high-bay assembly area has a clear height of 27 ft.

3.2.4.1 Architecture [Replacement]

The interior of the building is organized around the central high-bay assembly area, with all shops and labs having direct access to it, as illustrated by the cross sections in Fig. IV.3.2-5. The support wing is entered through corridors on the main and mechanical-equipment levels from the office wing, through doors from the experiment hall, and through a truck air lock in the northwest corner. A stairway and elevator located in the southeast corner of the building provide movement between the main floor, the control tunnel that runs beneath the south portion of the assembly bay, and the upper-level mechanical-equipment room. A floor hatch allows direct crane access from the high-bay assembly area to the control tunnel.

Partitions are concrete masonry construction with a paint finish, except in the clean rooms, where special wall finishes are required. Steel overhead roll-up doors provide access between the high-bay area and the laboratories and shop areas. In the high-bay assembly and mechanical-equipment areas, conduit, piping, ductwork, and the exposed structure are unpainted. In the laboratories, offices, toilets, locker, and break

III. 3. BUILDING SYSTEMS DESCRIPTION

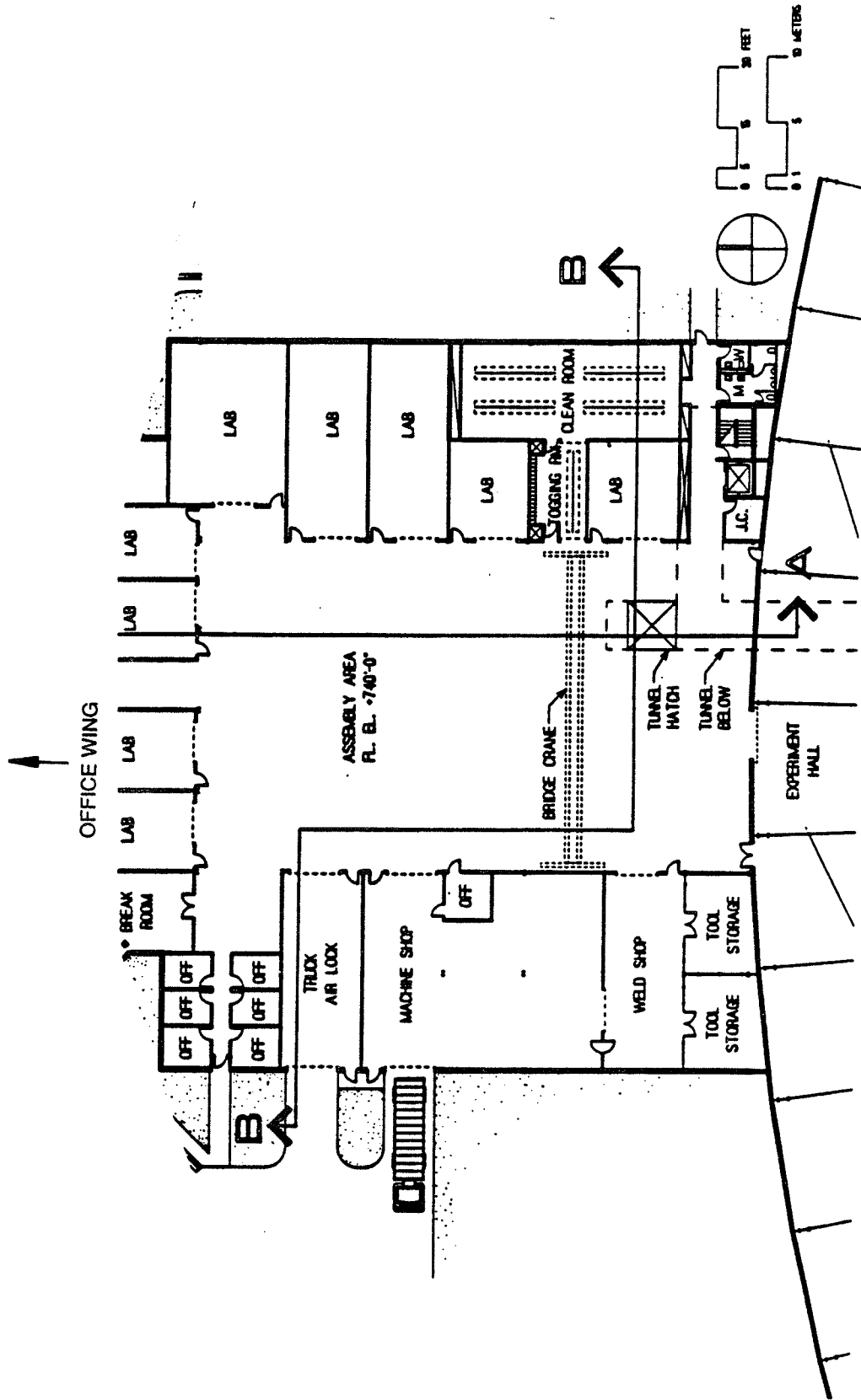


Figure IV.3.2-3
Support wing, central laboratory/office building ground floor plan.

III. 3. BUILDING SYSTEMS DESCRIPTION

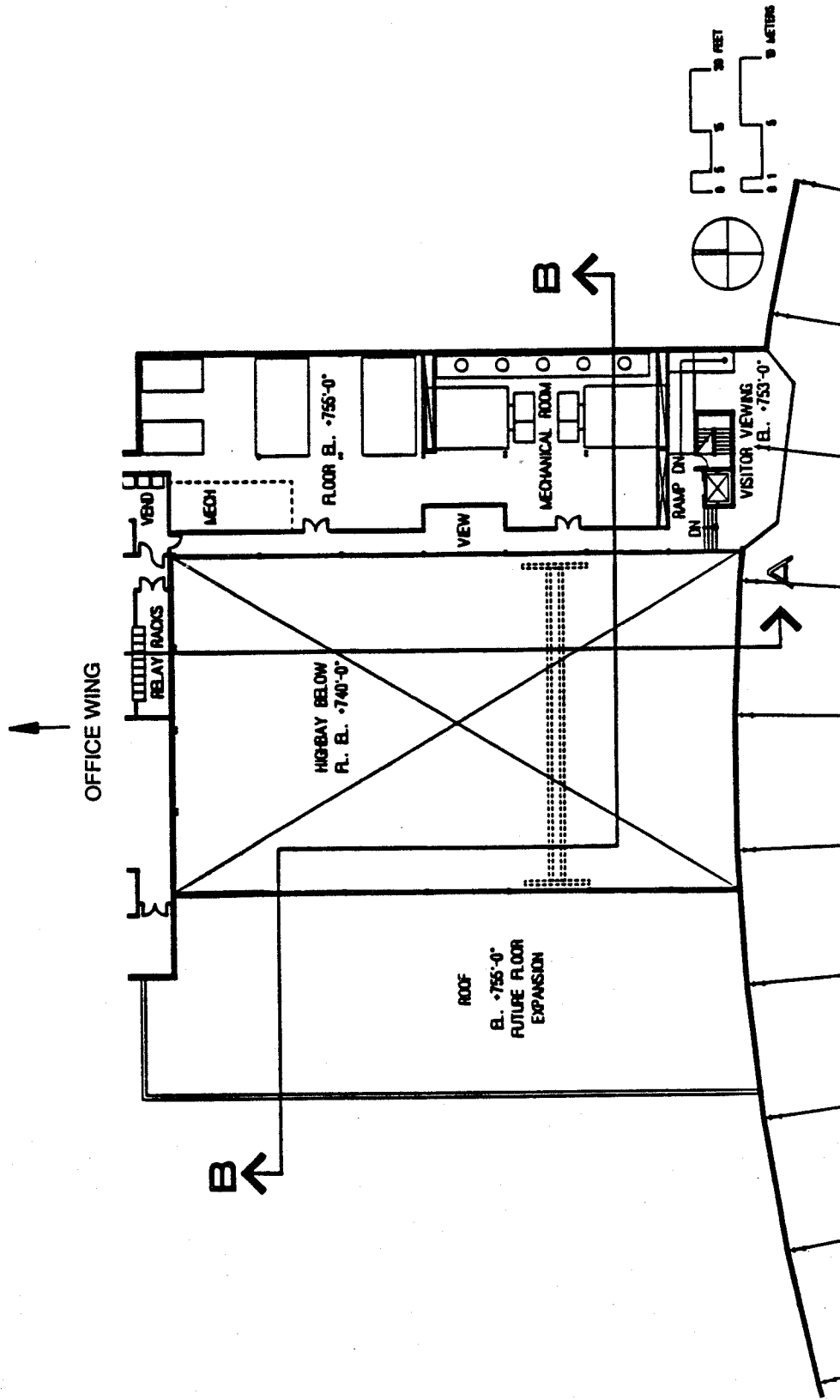


Figure IV.3.2-4
Support wing, central laboratory/office building mechanical-equipment penthouse plan.

III. 3. BUILDING SYSTEMS DESCRIPTION

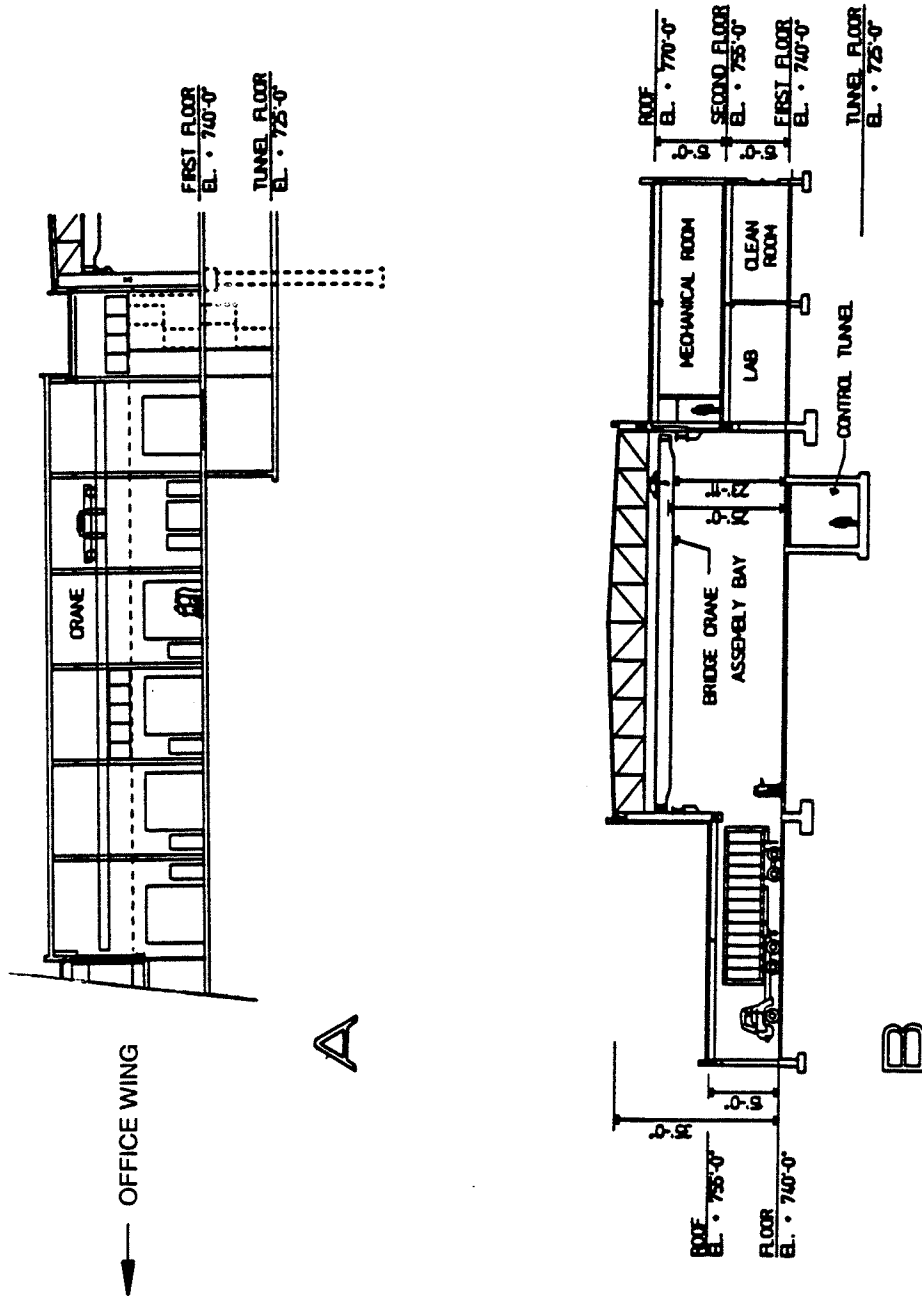


Figure IV.3.2-5
Support wing, central laboratory/office building sections.

III. 3. BUILDING SYSTEMS DESCRIPTION

areas, acoustical tile ceilings with recessed lighting and HVAC diffusers are suspended from the structure. Electrical and mechanical distribution systems are concealed in the ceiling space. The clean room uses special HEPA filter (high-efficiency particulate air filter) integrated ceiling systems.

Floors are covered with vinyl tile in the labs, offices, and lounge areas. Toilet rooms have ceramic tile floors and walls. In all other areas, the floors are exposed, surface-hardened concrete.

The exterior of the building is clad with 4-in.-thick insulated metal panels supported on horizontal girts. Energy-efficient thermal-break aluminum window frames with 1-in. solar insulating glass are provided in the shop and break areas. The roof of the building is protected by a single-ply roofing membrane, board insulation, and ballast in an IRMA system conforming to Argonne standards. Skylights provide natural light to the high-bay and shop areas.

Furnishings to be provided include desks, chairs, bookcases, and filing cabinets in the offices, and cabinets and counters along the long walls of the laboratories.

3.2.4.3 Heating, Ventilation, and Air-Conditioning [Replacement]

The laboratories are maintained at a space temperature of $75^{\circ}\text{F} \pm 2^{\circ}\text{F}$ year-round, with relative humidity of 50% maximum in summer and 25% minimum in winter. Three constant-volume air-conditioning units with three return fans are located in the upper-level mechanical-equipment room, a plan of which is shown in Fig. IV.3.2-4. Each laboratory is provided with a reheat coil at the supply air duct for space temperature control.

The Class 1000 clean room is supplied with air at $15\text{ ft}^3/\text{min}$ per ft^2 . The clean room is served by two air-handling units. Air is returned through an underfloor plenum and a vertical air shaft. A make-up air-handling unit supplies conditioned outside air to the three air-conditioning units for dehumidification and pressurization of the clean room.

The upper-level mechanical-equipment room is ventilated in summer and heated in winter to maintain a space temperature of 60°F . Hot water is converted from steam in the mechanical-equipment room. Chilled water and steam are supplied from a connection to the utility loop above the storage ring. A direct digital controller in this building controls the HVAC equipment.

3.2.5 Central Laboratory/Office Building - Office Wing [Replacement]

The office wing houses the APS main reception area, laboratories, and offices for the APS operating staff, as well as the main computer and control rooms. A short corridor on the east side links the office wing to the meeting facility and the

III. 3. BUILDING SYSTEMS DESCRIPTION

exhibition/lounge area. The office wing of the central laboratory/office building is connected to the support wing of the same building by a common wall, penetrated by two corridors and the control tunnel.

The building includes 46 three laboratories, two laboratory-size shops, 132 offices, 10 conference rooms, a three-laboratory space for a library, and various associated support spaces. Entry, reception, display spaces, and a visitor's viewing area on the fourth floor provide a front door for the facility. The large computer and control rooms serve as the APS nerve center.

The "Y"-shaped, four-story building has a footprint of 35,320 ft². The gross floor area of 131,700 ft² includes a lower service level, in addition to the main floor level and the two upper floors of lab and office space and top-floor visitor viewing area. The ground floor plan is shown in Fig. IV.3.2-6. Figure IV.3.2-7 shows the layout of stockroom, maintenance, toilet/locker rooms, storage, and mechanical-equipment spaces on the service level.

3.2.5.1 Architecture [Replacement]

The main entry to the building is from the north, into a skylighted single-story section that provides space for the public entry and reception areas and the main computer and control rooms. From there, two corridors on the right and left loop around two cores of windowless laboratories and other building support areas in multistoried sections. Offices ring the outer perimeters of each loop. Alternative entry points are near the ends of each office block and through corridors from the support wing to the south.

The computer and control rooms each have raised-floor cable-way and air-plenum systems.

Personnel movement between the five floor levels is provided by stairways at each exit location, by a passenger elevator located next to the main building entry and reception area, and by two freight elevators. The central laboratory/office building sections are shown in Fig. IV.3.2-8, and the fourth-floor plan with its visitor's viewing area, conference rooms, and fan rooms is shown in Fig. IV.3.2-9.

Wall partitions are of gypsum drywall construction with painted finish. Hollow metal doors and frames are 8 ft high for all lab spaces. Acoustical tile ceilings with recessed lighting and HVAC diffusers are suspended from the structure, concealing the electrical and mechanical distribution systems in the ceiling space. Vinyl tile is the typical floor finish, except in the mechanical-equipment areas, where the floors are exposed, surface-hardened concrete.

The exterior of the building is clad with an aluminum panel and glass curtain wall system. Energy-efficient thermal-break aluminum framing, insulated panels, and 1-in.

III. 3. BUILDING SYSTEMS DESCRIPTION

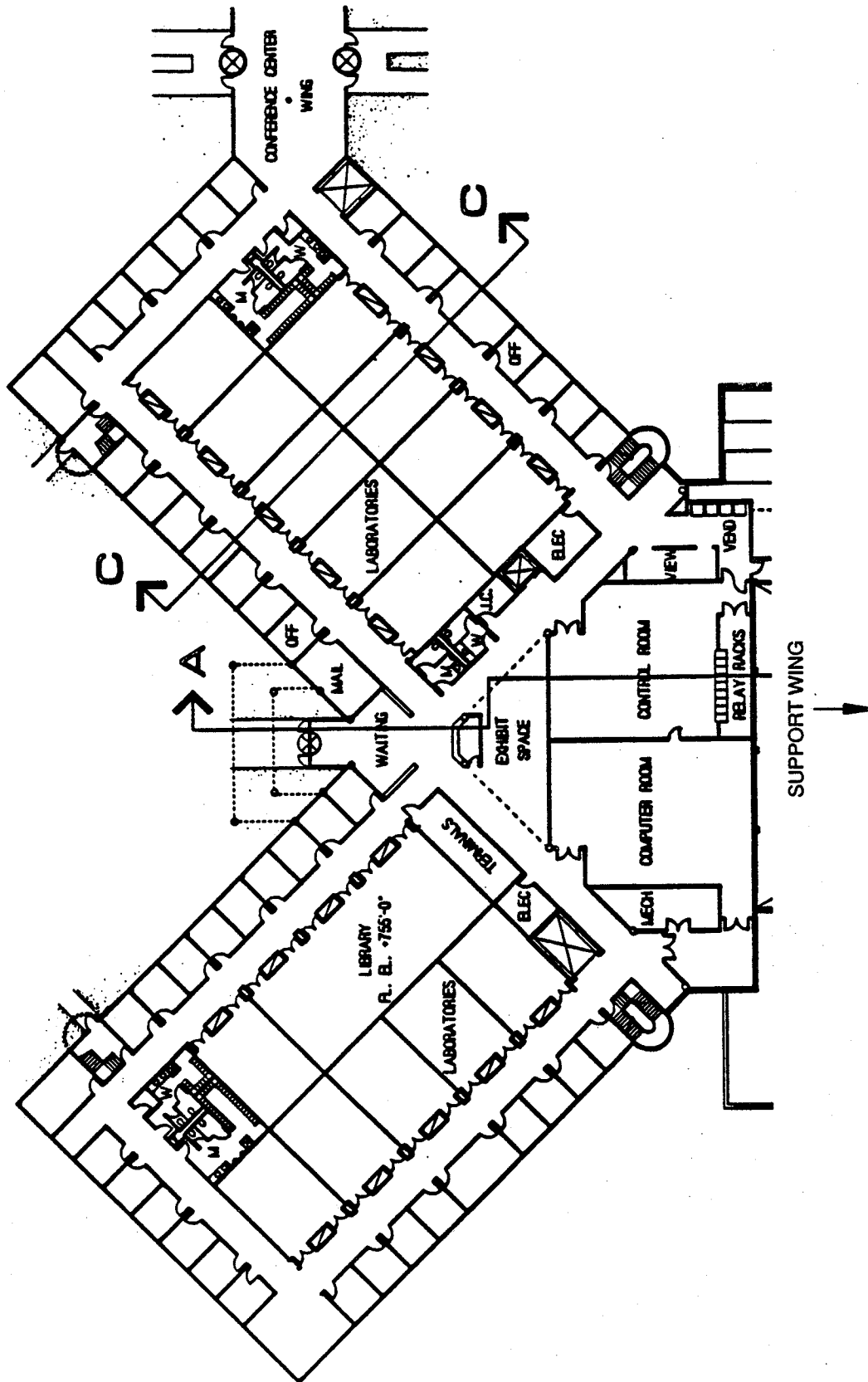


Figure IV.3.2-6
Office wing, central laboratory/office building ground floor plan.

III. 3. BUILDING SYSTEMS DESCRIPTION

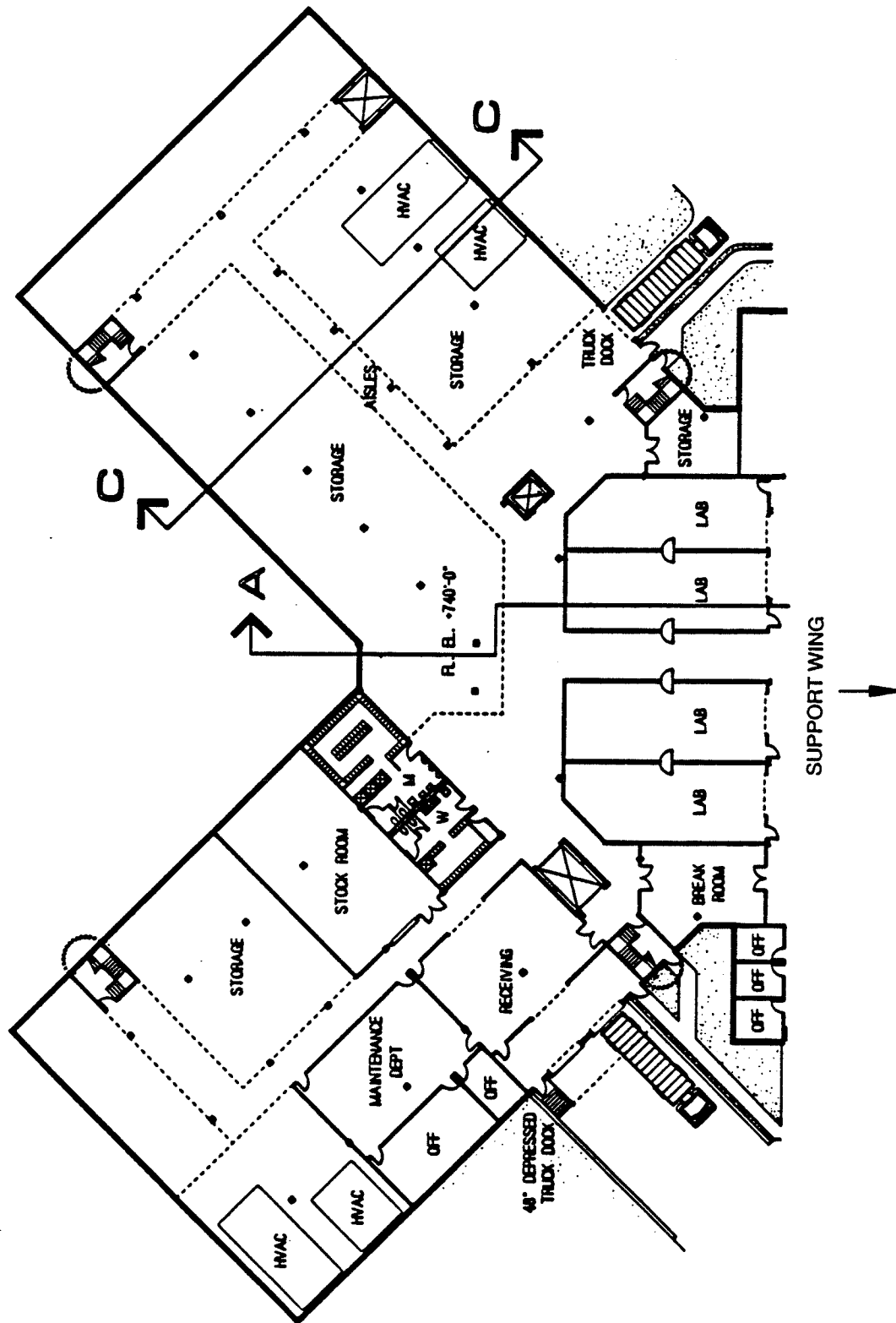


Figure IV.3.2-7
Office wing, central laboratory/office building service level plan.

III. 3. BUILDING SYSTEMS DESCRIPTION

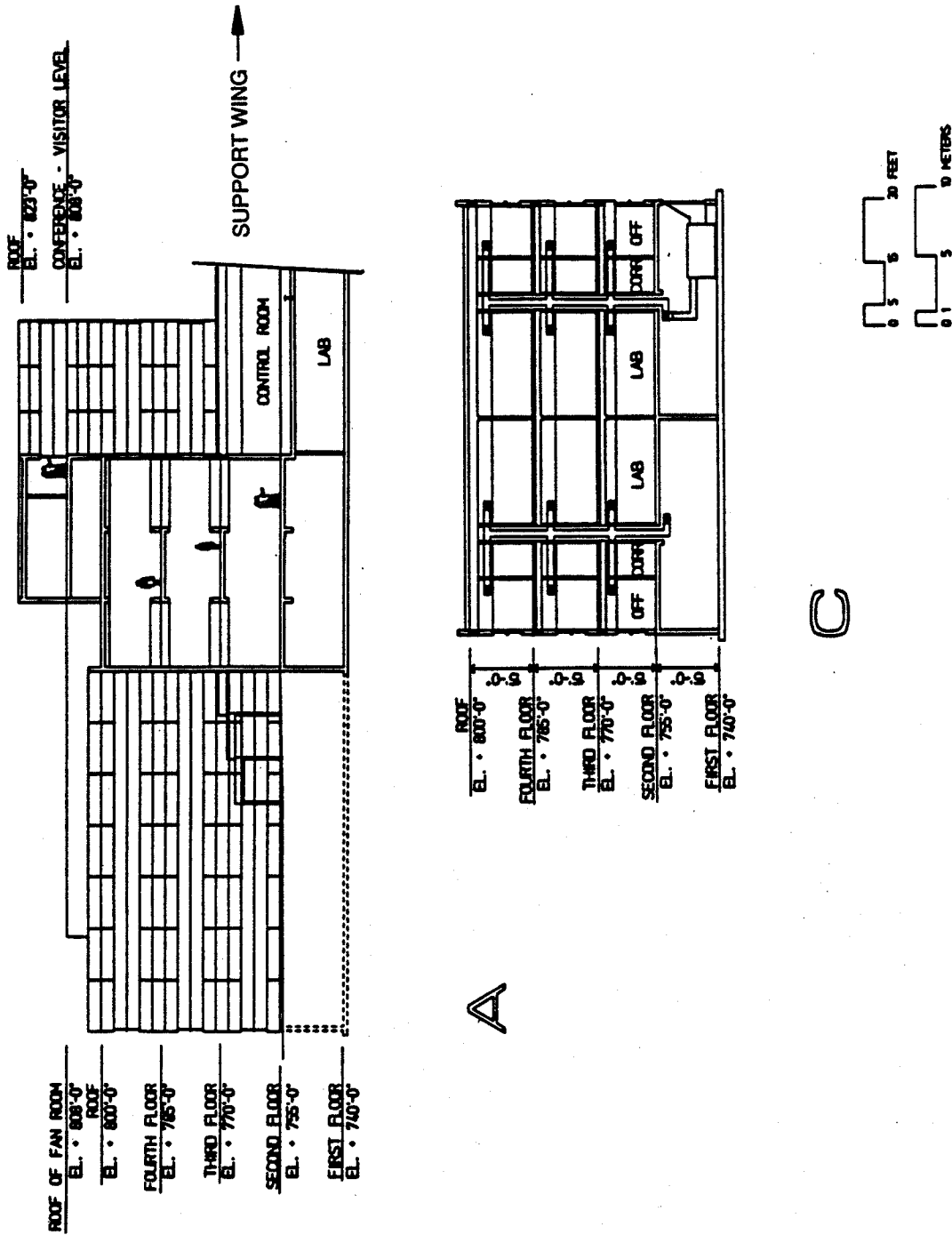


Figure IV.3.2-8
Office wing, central laboratory/office building sections.

III. 3. BUILDING SYSTEMS DESCRIPTION

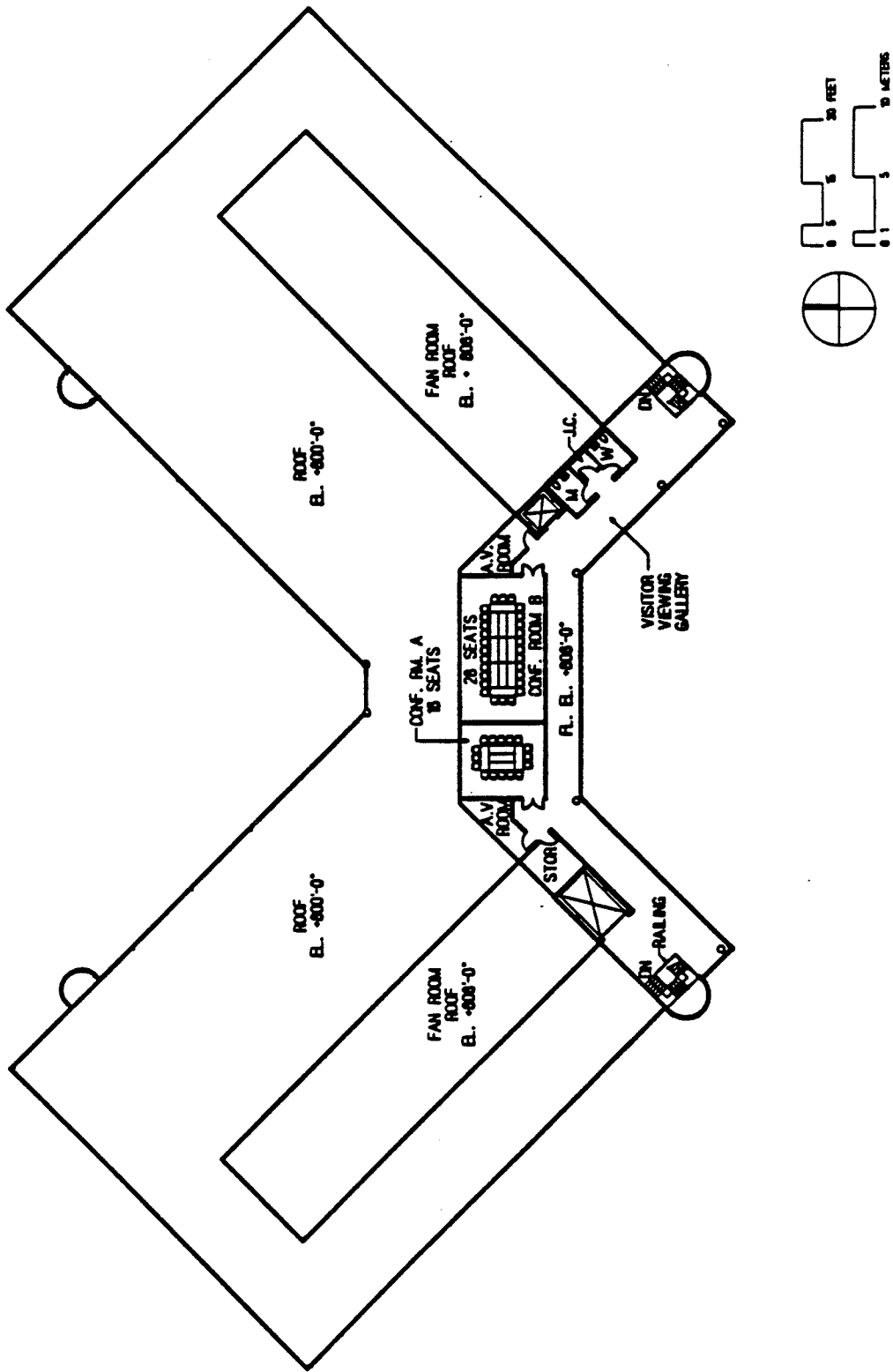


Figure IV.3.2-9
Office wing, central laboratory/office building fourth-floor plan.

III. 3. BUILDING SYSTEMS DESCRIPTION

solar insulating glass are provided to minimize energy loss through the building skin. A light shelf is incorporated into the exterior wall design to reflect daylight farther into the office areas, thereby reducing the need for artificial lighting and, thus, conserving energy. The roof of the building is protected by a single-ply roofing membrane, board insulation, and ballast in an IRMA system conforming to Argonne standards.

Furnishings to be provided include a reception desk and seats in the reception area; tables and chairs in conference rooms; desks, chairs, bookcases, and filing cabinets in the offices; and cabinets and counters along the long walls of the laboratories.

3.2.6 Central Laboratory/Office Building — Multi-Function Meeting Facility Wing [Replacement]

The meeting facility wing is located just east of the office wing. The central, 80-ft by 80-ft column-free area can be used as a single, 600-seat auditorium and can be divided with movable partitions into several areas of various sizes. These areas can be used for a variety of APS-related functions, such as meetings of various sizes, tutorials, poster sessions, catered dinners, and social gatherings. The meeting facility is attached to the office wing by an enclosed entry corridor. It is adjacent to the APS main parking area and is separated from the central laboratory/office building, so that visitors may enter the meeting facility without disturbing the operations of the central laboratory/office or the experiment hall. The square building is 110 ft on each side, with a footprint of 12,100 ft². Figure IV.3.2-10 shows plans and cross sections of the meeting facility wing.

3.2.6.1 Architecture [Replacement]

The 80-ft by 80-ft multi-function space is laid out in the east corner of the 110-ft by 110-ft building. This space can be subdivided in half (by means of acoustic-barrier, movable walls) in either direction to create two 40-ft by 80-ft spaces and in quarters to create four 40-ft by 40-ft spaces. The northwest half can also be divided (with ordinary divider walls) into eighths to create four 20-ft by 40-ft spaces. All movable walls and movable seating are stored in closets when not in use. At the north and south ends of the lobby/exhibit area are rest rooms and storage, and at the south end there is a small kitchen for the preparation of coffee and snacks. A registration desk is located at the west corner near the entrances and connection to the central laboratory/office building. Located above the west corner coat and storage areas is a projection booth, and above the restroom areas are two mechanical-equipment rooms.

Inside the building, the wall partitions are of gypsum drywall construction with vinyl wall covering in most areas, with ceramic tile used in the rest rooms. Ceilings with recessed lighting and HVAC diffusers are suspended from the structure, concealing electrical and mechanical distribution systems in the ceiling space. Acoustic ceiling

III. 3. BUILDING SYSTEMS DESCRIPTION

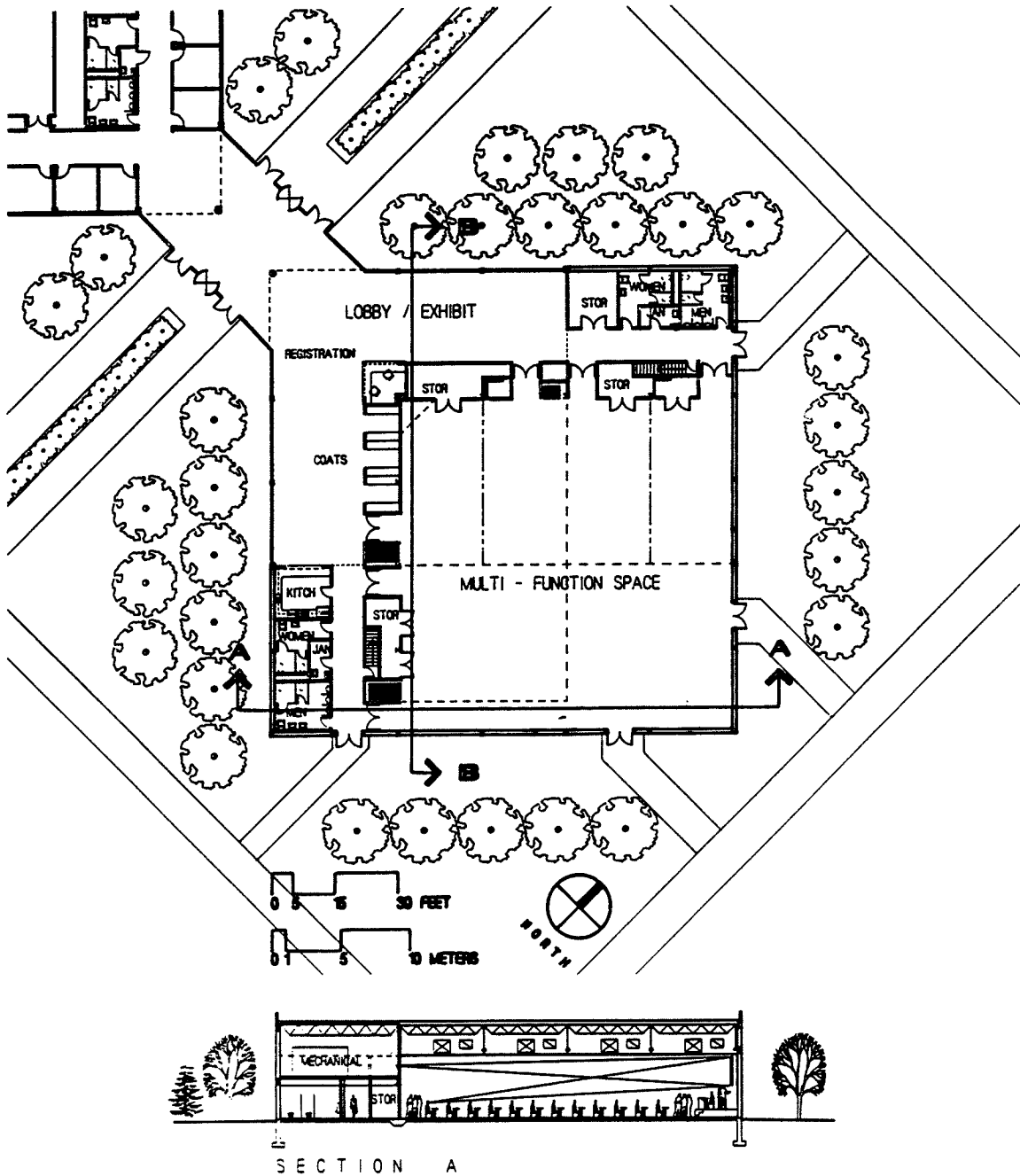


Figure IV.3.2-10
Multi-function meeting facility wing, central laboratory/office building.

III. 3. BUILDING SYSTEMS DESCRIPTION

material is used in all areas. Special acoustic baffles are located above the multi-function space to control sound transmission between divided spaces. Carpeting is used in the lobby/exhibit and multi-function spaces, and ceramic tile is used in the restrooms.

The exterior of the building is clad with an aluminum panel and glass curtain-wall system matching that used for the office wing. Energy-efficient thermal-break aluminum framing, insulated panels, and 1-in. solar insulating glass are provided to minimize energy loss through the building skin. The roof of the building is protected by a single-ply roofing membrane, board insulation, and ballast in an IRMA system conforming to Argonne standards.

Furnishings include movable seating, movable wall systems, kitchen equipment, coat racks, and counters.

3.2.6.2 Structure [Replacement]

The meeting facility consists of deep long-span steel joists, girders, and columns supporting a welded metal deck roof, with structural steel bracing in the exterior wall for resistance against lateral loads. Foundations are conventional spread footings. The floor is a 6-in. reinforced concrete slab on-grade over six inches of compacted granular backfill.

3.2.6.3 Heating, Ventilation, and Air-Conditioning [Replacement]

Three variable-volume air-handling units located in the mechanical-equipment spaces above the rest-room areas maintain a space temperature of $75^{\circ}\text{F} \pm 2^{\circ}\text{F}$ year-round, with 45% maximum relative humidity in summer and 25% minimum in winter in the auditorium and the exhibit/lounge space. One unit serves the lobby/exhibit area, and the other two each serve one half of the multi-function space. These units can operate independently to conserve energy if half of the facility is not in use. Hot-water baseboard and fin-tube radiators at the perimeter walls maintain the space temperature in winter. Units are on local direct-digital control.

3.2.6.5 Electrical Power [Replacement]

Electrical power is distributed to the auditorium at 480Y/277 V from the central laboratory/office building.

An equipment grounding system is provided from connections on each piece of equipment to grounding conductors running with all power feeders. Lightning protection is provided by copper rods mounted around the perimeter of the roof, which are connected by copper cables Cadwelded to the building structural steel. A building ground

III. 3. BUILDING SYSTEMS DESCRIPTION

system uses bare copper cable Cadwelded to the building structural steel, which is connected to ground rods spaced around the building.

General illumination for the multi-function space is provided by metal halide downlights, arranged in patterns corresponding to the subdivided floor plan and controlled from a master dimming system with local controls in the projection room and provisions for remote control from the various spaces.

Speakers, amplifiers, and input jacks located in the various spaces and in the projection room make up the multi-channel sound system.

Three lighting systems -- fluorescent fixtures, track lighting, and downlights -- serve the lighting needs of the exhibit/lounge area. Each lighting system is switched separately. Floor receptacles are installed in a grid pattern throughout the exhibit/lounge space to accommodate various display configurations.

The fire alarm system, a separate zone of the central laboratory/office building, consists of manual-pull stations at the exits, flow and tamper switches in the sprinkler system, and smoke detectors throughout the building and in the HVAC system.

3.3 Utilities and Sitework

Figure IV.3.3-1 (cited in Sec. IV.3.3.1 of CDR-87) is replaced.

3.3.5.2 Control Tunnel [Replacement]

The control tunnel runs from beneath the southeast corner of the support wing of the central laboratory/office building beneath the main control room, beneath the support wing and experiment hall to the synchrotron extraction and synchrotron injection buildings. The tunnel carries control wiring, utilities, and rf waveguides, in addition to providing direct, all-weather access for APS operations staff and equipment to the primary technical components. The tunnel interior is 13 ft wide and 13 ft high, but only a 9-ft by 9-ft cross section is available for pedestrians; the rest is reserved for wiring, piping, and ductwork.

Access to the tunnel is provided by stairways and elevators at the southeast corner of the support wing, in the synchrotron extraction building, and in the synchrotron injection building. In addition, floor hatches provide crane access to the tunnel from the high-bay assembly area and the synchrotron injection and extraction buildings.

The tunnel is constructed of reinforced concrete, protected from water penetration by membrane waterproofing and perimeter drains.

The conduit, cable trays, piping, and ductwork are exposed and unpainted. Unistrut channels are cast into the walls and ceilings. The 1-5/8-in. channel is embedded

III. 3. BUILDING SYSTEMS DESCRIPTION

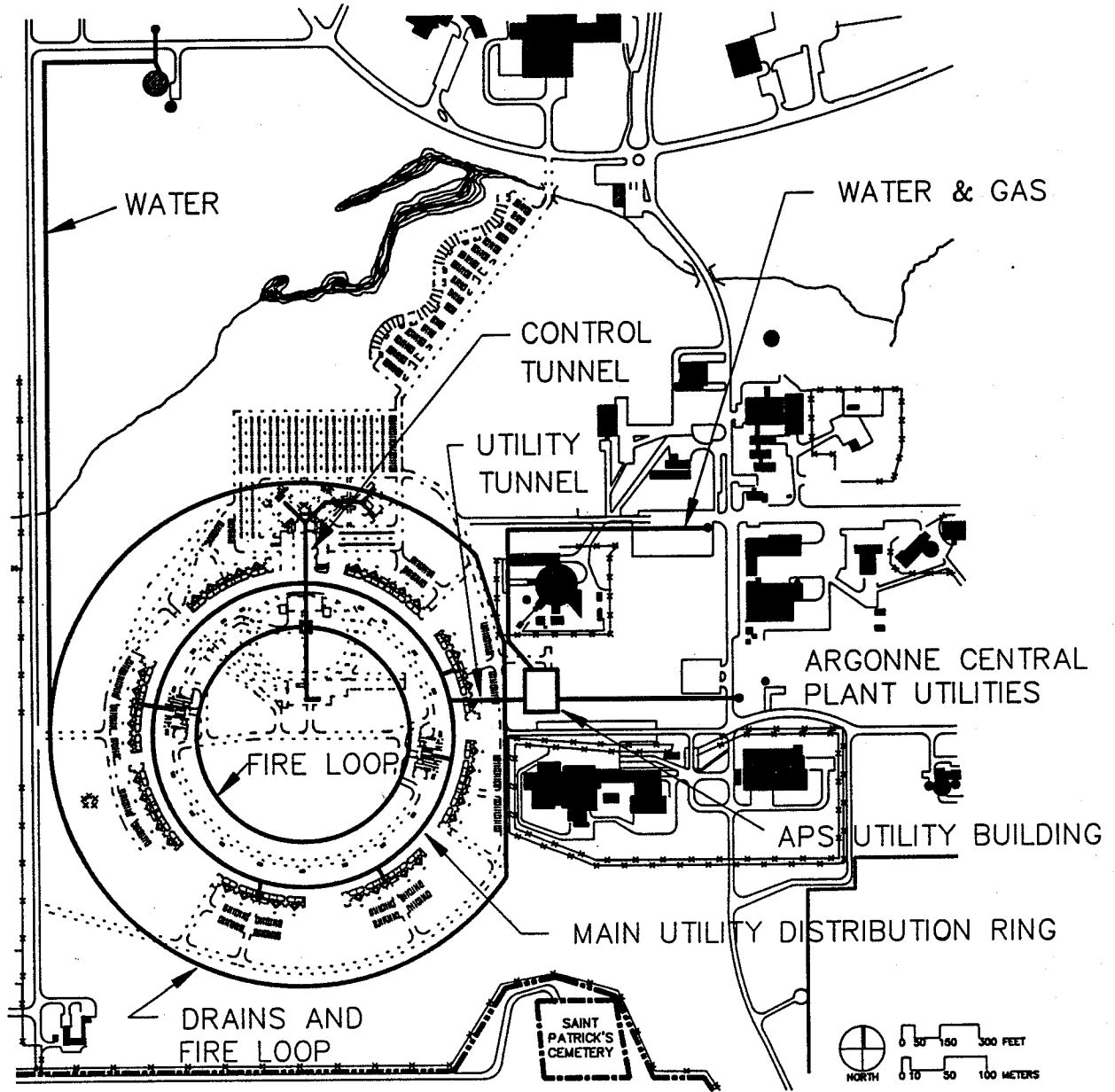


Figure IV.3.3-1
Utility area plan.

III. 3. BUILDING SYSTEMS DESCRIPTION

on 6-ft centers, vertically on the walls, and across the width of the tunnel on the ceilings.

Packaged air-handling units with chilled-water coils provide the necessary air changes and dehumidification.

A wet-pipe automatic sprinkler system provides fire protection. Hand-operated Halon 1211 fire extinguishers are located at intervals along the tunnel.

The tunnel is lighted by two-lamp, 4-ft-long, wall-mounted fluorescent fixtures mounted on 8-ft centers on one side of the tunnel. They are switched from lighting panels. Duplex receptacles are mounted on 50-ft centers, 3 ft above the floor on one wall.

The fire alarm system consists of manual-pull stations located at the tunnel exits, flow and tamper switches in the sprinkler system, and smoke detectors throughout the tunnel and in the HVAC system.

III. 3. BUILDING SYSTEMS DESCRIPTION

Distribution for ANL-87-15 Annex

Internal:

Associate Laboratory Director for the
Advanced Photon Source (ALD/APS) (661)
ANL Patent Dept.

ANL Contract File
ANL Libraries
TIS Files (3)

External:

DOE-TIC, for distribution per UC-400 (25)

DOE Chicago Operations Office:

Manager

University of Chicago Board of Governors for Argonne National Laboratory, Committee
to Advise the Laboratory Director on APS Construction (7)